USF UNIVERSITY OF SOUTH FLORIDA

Department of Civil and Environmental Engineering

EVALUATING THE EFFECT OF TEMPORARY CASING ON DRILLED SHAFT ROCK SOCKET FRICTION

BDV25 TWO977-18

FINAL REPORT

Gray Mullins, Ph.D., P.E., Principal Investigator

and

Researchers

Lucas Caliari, Ph.D.,

Kelly Costello, E.I., Ph.D. Candidate

Tristen Mee, Research Assistant

April 2018

Disclaimer

The opinions, findings, and conclusions expressed in this publication are those of the authors and not necessarily those of the State of Florida Department of Transportation.

APPROXIMATE CONVERSIONS TO SI UNITS

SYMBOL	WHEN YOU KNOW	MULTIPLY BY	TO FIND	SYMBOL
				LENGTH
in	inches	25.4	millimeters	mm
ft	feet	0.305	meters	m
yd	yards	0.914	meters	m
mi	miles	1.61	kilometers	km

SYMBOL	WHEN YOU KNOW	MULTIPLY BY	TO FIND	SYMBOL
				AREA
in^2	square inches	645.2	square millimeters	mm^2
ft^2	square feet	0.093	square meters	m^2
yd^2	square yard	0.836	square meters	m^2
ac	acres	0.405	hectares	ha
mi^2	square miles	2.59	square kilometers	km^2

SYMBOL	WHEN YOU KNOW	MULTIPLY BY	TO FIND	SYMBOL
				VOLUME
fl oz	fluid ounces	29.57	milliliters	mL
gal	gallons	3.785	liters	L
ft^3	cubic feet	0.028	cubic meters	m^3
yd^3	cubic yards	0.765	cubic meters	m^3
			NOTE: volumes greater than 1000 L shall be shown in	m^3

SYMBOL	WHEN YOU KNOW	MULTIPLY BY	TO FIND	SYMBOL
				MASS
oz	ounces	28.35	grams	g
lb	pounds	0.454	kilograms	kg
T	short tons (2000 lb)	0.907	gagrams (or "metric ton")	Mg (or "t")

SYMBOL	WHEN YOU KNOW	MULTIPLY BY	TO FIND	SYMBOL
				TEMPERATURE (exact degrees)
^{o}F	Fahrenheit	5 (F-32)/9 or (F-32)/1.8	Celsius	^{o}C

SYMBOL	WHEN YOU KNOW	MULTIPLY BY	TO FIND	SYMBOL
				ILLUMINATION
fc	foot-candles	10.76	lux	lx
fL	foot-Lamberts	3.426	candela/m^2	cd/m^2

SYMBOL	WHEN YOU KNOW	MULTIPLY BY	TO FIND	SYMBOL
				FORCE and PRESSURE or STRESS
lbf	poundforce	4.45	newtons	N
lbf/in^2	undforce per square inch	6.89	kilopascals	kPa
kip	kilopound	4.45	kilonewtons	kN

APPROXIMATE CONVERSIONS TO SI UNITS

SYMBOL	WHEN YOU KNOW	MULTIPLY BY	TO FIND	SYMBOL
				LENGTH
mm	millimeters	0.039	inches	in
m	meters	3.28	feet	ft
m	meters	1.09	yards	yd
km	kilometers	0.621	miles	mi

SYMBOL	WHEN YOU KNOW	MULTIPLY BY	TO FIND	SYMBOL
				AREA
mm^2	square millimeters	0.0016	square inches	in^2
m^2	square meters	10.764	square feet	ft^2
m^2	square meters	1.195	square yards	yd^2
ha	hectares	2.47	acres	ac
km^2	square kilometers	0.386	square miles	mi^2

SYMBOL	WHEN YOU KNOW	MULTIPLY BY	TO FIND	SYMBOL
				VOLUME
mL	milliliters	0.034	fluid ounces	fl oz
L	liters	0.264	gallons	gal
m^3	cubic meters	35.314	cubic feet	ft^3
m^3	cubic meters	1.307	cubic yards	yd^3

SYMBOL	WHEN YOU KNOW	MULTIPLY BY	TO FIND	SYMBOL
				MASS
g	grams	0.035	ounces	oz
kg	kilograms	2.202	pounds	lb
Mg (or "t")	gagrams (or "metric ton")	1.103	short tons (2000 lb)	T

SYMBOL	WHEN YOU KNOW	MULTIPLY BY	TO FIND	SYMBOL
				TEMPERATURE (exact degrees)
^oC	Celsius	1.8C+32	Fahrenheit	^oF

SYMBOL	WHEN YOU KNOW	MULTIPLY BY	TO FIND	SYMBOL
				ILLUMINATION
lx	lux	0.0929	foot-candles	fc
cd/m^2	$candela/m^2$	0.2919	foot-Lamberts	fl

SYMBOL	WHEN YOU KNOW	MULTIPLY BY	TO FIND	SYMBOL
				FORCE and PRESSURE or STRESS
N	newtons	0.225	poundforce	lbf
kPa	kilopascals	0.145	ındforce per square inch	lbf/in^2
kN	kilonewtons	0.225	kilopound	kip

*SI is the symbol for the International System of Units. Appropriate rounding should be made to comply with Section 4 of ASTM E380.

Technical Report Documentation Page

1. Report No.	2. Government Accession No.	3. Recipient's Catalog No.
4. Title and Subtitle EVALUATING THE EFFECT OF TEMPORARY CASING ON DRILLED SHAFT ROCK SOCKET FRICTION		5. Report Date January 2018 6. Performing Organization Code
7. Author(s) G. Mullins and L. Caliari		8. Performing Organization Report No.
9. Performing Organization Name and Address University of South Florida Department of Civil and Environmental Engineering 4202 E. Fowler Avenue, ENB 118s Tampa, FL 33620		10. Work Unit No. (TRAIS) 11. Contract or Grant No. BDV25 TWO 977-18
12. Sponsoring Agency Name and Address Florida Department of Transportation 605 Suwannee Street, MS 30 Tallahassee, FL 32399		13. Type of Report and Period Covered Final Report 04/15-03/18 14. Sponsoring Agency Code
15. Supplementary Notes FDOT Project Manager: Larry Jones		

16. Abstract

Installation of large diameter steel pipes, called casing, is a common means of stabilizing open excavations needed for drilled shaft construction. While methods vary in both the installation and sequencing of their installation, an expected depth of casing embedment based on boring logs can vary from that which actually is observed in the field. When the casing is terminated in limestone formations deeper than anticipated there is concern that the resulting concrete bond with the limestone outside the casing may be diminished once the casing is extracted and the fresh still fluid concrete is permitted to make contact with the limestone.

The primary objective of this study was to quantify the effects on side shear from the use of temporary casing in regions where the casing is embedded into the limestone. Both small and large scale field evaluations of rock socketed shafts were performed

Small scale field tests involved casting 29, 1/10th scale shafts constructed with three different casing installation / extraction methods including driven casing, and two different rotated casing cutting heads. Pullout test results of the small scale rock sockets showed the temporary cased shaft could have as low as 60% of the capacity of the uncased controls used for comparison.

Full scale field testing entailed casting s side-by-side pair of 2ft diameter rock socketed shafts in limestone where the SPT blow counts were on the order of 50-60. This strength of limestone is sufficient in strength to seat a casing, but is also weak enough to allow for a casing to be embedded well within or even pass through. The results of the full scale tests showed the temporary cased shaft exhibited 83% of the uncased control.

While often not necessary, the casing can be driven through extremely hard material which was tested in the small scale testing with a wide range of limestone strengths; the full scale tests could not practically test the same range of strengths. To this end, the large scale tests targeted what was thought to be the most likely scenario ($N \leq 60$). Small scale tests showed a higher reduction in side shear relative to the unconfined compression strength for stronger parent limestone (Figure 5.2). This is thought to be a by-product of larger voids / higher roughness in the weaker material that promotes better bond even when debris from outside the casing is present.

The evaluation of temporary casing used in rock socketed drilled shafts in simulated limestone showed construction procedures can lead to different side shear and hence an adjusted resistance factors could be considered. Based on the results of this study, the present FDOT specification requiring extending the socket depth by 50% of the unplanned additional embedment depth in Florida limestone formations is reasonable.

17. Key Word	18. Distribution Statement
Drilled shaft, temporary casing, load test	No restrictions.

19. Security Classif. (of this report)	20. Security Classif. (of this page)	21. No. of Pages	22. Price
Unclassified.	Unclassified.	106	

Form DOT F 1700.7 (8-72) Reproduction of completed page authorized

Acknowledgments

The authors would like to acknowledge the Florida Department of Transportation for funding this project, with specific thanks to Larry Jones, Juan Castellanos, Dr. David Horhota, Rodrigo Herrera, and the entire FDOT review team for their insightful contributions.

The authors would also like to thank R.W. Harris, Inc, for working so closely with the research team and making a site available for the full scale test program. Tierra, Inc. is also gratefully acknowledged for the assisting in the field exploration at the Miami test site. Finally, Hayward Baker is similarly acknowledged for offering the use of their 300ton reaction beam.

Executive Summary

Installation of large diameter steel pipes, called casing, is a common means of stabilizing open excavations needed for drilled shaft construction. While methods vary in both the installation and sequencing of their installation, an expected depth of casing embedment based on boring logs can vary from that which actually is observed in the field. When the casing is terminated in limestone formations deeper than anticipated there is concern that the resulting concrete bond with the limestone outside the casing may be diminished once the casing is extracted and the fresh still fluid concrete is permitted to make contact with the limestone.

The primary objective of this study was to quantify the effects on side shear from the use of temporary casing in regions where the casing is embedded into the limestone. Both small and large scale field evaluations of rock socketed shafts were performed

Small scale field tests involved casting 29, $1/10^{th}$ scale shafts constructed with three different casing installation / extraction methods including driven casing, and two different rotated casing cutting heads. Pullout test results of the small scale rock sockets showed the temporary cased shaft could have as low as 60% of the capacity of the uncased controls used for comparison.

Full scale field testing entailed casting a side-by-side pair of 2ft diameter rock socketed shafts in limestone where the SPT blow counts were on the order of 50-60. This strength of limestone is sufficient in strength to seat a casing, but is also weak enough to allow for a casing to be embedded well within or even pass through. The results of the full scale tests showed the temporary cased shaft exhibited 83% of the uncased control shaft capacity.

While often not necessary, the casing can be driven through extremely hard material which was tested in the small scale testing with a wide range of limestone strengths; the full scale tests could not practically test the same range of strengths. To this end, the large scale tests targeted what was thought to be the most likely scenario ($N \leq 60$). Small scale tests showed a higher reduction in side shear relative to the unconfined compression strength for stronger parent limestone (Figure 5.2). This is thought to be a by-product of larger voids / higher roughness in the weaker material that promotes better bond even when debris from outside the casing is present.

The evaluation of temporary casing used in rock socketed drilled shafts in simulated limestone showed construction procedures can lead to different side shear and hence an adjusted resistance factors could be considered. Based on the results of this study, the present FDOT specification requiring extending the socket depth by 50% of the unplanned additional embedment depth in Florida limestone formations is reasonable.

Table of Contents

Disclaimer ii
Conversion Factors iii
Technical Report Documentation vi
Acknowledgments vii
Executive Summary viii
List of Tables xii
List of Figures xiii

Chapter One: Introduction 1

1.1 Background 1

1.2 Organization of the Report 3

Chapter Two: Literature Review 4

2.1 Background 4

2.2 Construction Effects 6

2.2.1 Slurry 7

2.2.2 Concrete and Cage Spacing 8

2.2.3 Casing 9

2.3 Mechanical Stabilization of Drilled Shafts with Temporary Casing 12

2.4 Rock-Sockets 18

2.4.1 Calculations of Ultimate Side Shear of Rock Sockets 19

2.5 Construction of Rock Sockets 25

2.6 States Specifications for Drilled Shafts Constructed with Temporary Casing 28

2.7 Construction Effects on Side Resistance of Rock Sockets – Case Studies 30

2.7.1 Case Study: Influence of Side Walls Roughness (O'Neill, 2001) 30

2.7.2 Case Study: Effect of Bond between Limestone Side Walls and Concrete (Law, 2002) 32

2.7.3 Case Study: Comparison between Temporary Casing, Bentonite and Polymer Slurries (Brown, 2002) 37
2.7.4 Case Study: Comparison between Cased and Uncased Zones in the Florida's Limestone (Castelli and Fan, 2002) 39
2.7.5 Case Study: IGM Calculated Ultimate Side Shear versus Measured using Temporary Casing (Hossain et al., 2007) 43
2.7.6 Case Study: Effects of Stress Relaxation on Granular IGM (Seavey and Ashford, 2004) 46
2.8 Brief Introduction to Limestones 47
2.8.1 Florida Limestones 48
2.9 Chapter Summary 58

Chapter Three: Small Scale Testing 59
3.1 Overview 59
3.2 Simulated Limestone Material 59
3.3 Shafts Construction 61
3.3.1 Rock Socket Excavation 64
3.3.2 Concrete Placement 67
3.4 Pull-Out Load Tests 70
3.5 Test Results 71
3.6 Chapter Summary 78

Chapter Four: Full Scale Testing 79
4.1 Site Selection 79
4.2 Site Exploration 80
4.3 Estimated Rock Socket Capacity 83
4.4 Construction Preparations 83
4.5 Shaft Construction 86

4.6 Load Testing 91
4.7 Chapter Summary 96
Chapter Five: Discussions and Conclusion 97
5.1 Overview 97
5.2 Small Scale Testing 97
5.3 Large Scale Testing 99
5.4 Conclusions 100
References 103

List of Tables

Table 2.1 Friction angles between foundation materials and soil or rock (adapted Bowles 1996). 7
Table 2.2 φ factors for cohesive IGM (O'Neill and Reese, 1999). 20
Table 2.3 U.S. States that do not provide specifications for drilled shafts for primary structures. 28
Table 2.4 U.S. States that provide general specifications for drilled shafts, but not specific recommendations for the use of temporary casings. 28
Table 2.5 U.S. States that provide similar specifications for construction of drilled shafts using temporary casings, with no further details. 29
Table 2.6 U.S. States that provide more detailed specifications for construction of rock sockets using temporary casings. 29
Table 2.7 Design side shear used for the limestone (Castelli and Fan, 2002). 40
Table 2.8 Summary of measured side friction in Limestone, from the load tests data (Castelli and Fan, 2002). 42
Table 2.9 Calculated versus measured side shear (Reese et al., 1985), from Seavey and Ashford (2004). 47
Table 2.10 Variation of UCS with SPT-N (Terzaghi and Peck 1967). 53
Table 2.11 Extrapolated values of SPT-N vs Su (psi) (Djoenaidi 1985; Kulhawy 1986; Schmertmann 1975). 54
Table 2.12 Typical relationships in Miami and Fort Thompson Limestone (Frizzi and Meyer 2000). 55
Table 2.13 Table 3.4. Lab and field tests setup (data from McVay et al. 1992). 56
Table 2.14 Summary of UCS vs SPT-N Values (data from McVay et al. 1992). 56
Table 3.1 Types of construction used on the rock socket specimens. 62
Table 3.2 Measured dimensions of the extracted sockets. 72
Table 3.3 Maximum load for all sockets. 74
Table 3.4 Displacement at peak load for all sockets. 74
Table 3.5 Maximum side shear strength for all sockets. 77
Table 3.6 Maximum normalized side shear. 77
Table 3.7 Side shear ratios between temporary and respective control casings. 77
Table 4.1 Possible testable shaft dimensions based on a 500kip limit. 79
Table 4.2 Estimated pullout capacity. 83
Table 5.1 Small and full scale stress ratios 101

List of Figures

Figure 1.1 Surface texture from rotating casing during extraction (left, FHWA 2010); smooth surface from vibratory extraction (right). 1
Figure 2.1 Unit side shear values for various driven pile types. 4
Figure 2.2 Lateral pressure distribution resulting from fully fluid concrete pressure. 6
Figure 2.3 Concrete level differential (inside vs outside cage) with respect to cage tightness. 8
Figure 2.4 Unit side shear versus slump loss at the time of casing extraction. 9
Figure 2.5 Conceptual process during casing extraction where a water-filled void around the casing is filled by denser, higher pressure fluid concrete resulting in trapped water inside casing or shaft volume (Sliwinski et al., 1984). 10
Figure 2.6 Example case where concrete / water exchange was detected by field integrity test; this a problem which can be a by-product of temporary casing. 11
Figure 2.7 Construction using casing through slurry-filled starter hole: (a) drill with slurry; (b) set casing and bail slurry; (c) complete and clean excavation, set reinforcing; (d) place concrete to head greater than external water pressure; (e) pull casing 13
Figure 2.8 Construction using casing advanced ahead of excavation: (a) drive casing into bearing stratum; (b) drill through casing; (c) complete and clean hole, set reinforcing; (d) place concrete to head greater than external water pressure; (e) pull casing while maintaining sufficient concrete head. 13
Figure 2.9 Oscillator rig used to advance segmental casing ahead of the excavation (FHWA, 2010). 14
Figure 2.10 Use of a vibro-hammer (left) and twister bar (right) to advance casing (FHWA, 2010). 14
Figure 2.11 Cutting Teeth on the Casing to Assist Penetration into the Bearing Stratum (FHWA, 2010). 15
Figure 2.12 Example of rotator machine (Malcolm, 2016). 16
Figure 2.13 Telescoping Casing, most likely permanent (FHWA, 2010). 17
Figure 2.14 Casing extraction using vibratory hammer (FHWA, 2010). 18
Figure 2.15 α factor for cohesive IGM material (O'Neill and Reese, 1999). 20
Figure 2.16 Summary of stress states at rock-shaft interface (McVay et al., 1992). 23
Figure 2.17 Modeled strength envelope for Florida limestone (McVay et al., 1992). 23
Figure 2.18 Examples of rock augers (FHWA, 2010). 26
Figure 2.19 Examples of single wall core barrels (FHWA, 2010). 27
Figure 2.20 Examples of double wall core barrels (FHWA, 2010). 27
Figure 2.21 Sinusoidal roughness pattern, with potential smear zone at concrete-soft rock (IGM) interface (O'Neill, 2001, after Hassan and O'Neill, 1997). 31
Figure 2.22 Predicted side resistance versus displacement relationships for rock sockets with different interface conditions (O'Neill and Hassan, 1994, O'Neill, 2001). 32
Figure 2.23 Schematic section of Test Shaft 1 (Law, 2002). 34

Figure 2.24 Schematic section of Test Shaft 2 (Law, 2002). 35
Figure 2.25 Load-displacement at top for test shaft 1. (Law, 2002) 36
Figure 2.26 Load-displacement at top for test shaft 2 (Law, 2002). 36
Figure 2.27 Load versus deflection results from load tests performed on the four cased shafts (Brown, 2002). 38
Figure 2.28 Measured side shear on the shafts constructed with different methods (Brown, 2002). 39
Figure 2.29 Subsurface profile at St. Johns River crossing (Castelli and Fan, 2002). 40
Figure 2.30 Details and Subsurface Conditions for Test Shaft 1 (Castelli and Fan, 2002). 41
Figure 2.31 Details and Subsurface Conditions for Test Shaft 2 (Castelli and Fan, 2002). 42
Figure 2.32 Generalized subsurface soil profile at the Clinical Research Center facility, Bethesda, Maryland Hossain et al. (2007). 44
Figure 2.33 Scheme of the test shaft instrumented at CRC facility project (Hossain et al., 2007). 45
Figure 2.34 O-cell load – displacement curves from CRC facility project (Hossain et al., 2007). 45
Figure 2.35 Detail of an oolitic limestone, where ooids have been dissolved out; millimetric scale, Permian, N. E., England (Tucker 2003). 48
Figure 2.36 Geology of Florida, cross Section A-A' (Scott et. al, 2001). 49
Figure 2.37 Geology of Florida, cross Section B-B' (Scott et. al, 2001). 49
Figure 2.38 Porous oolitic limestone (Prieto-Portar 1982). 50
Figure 2.39 Fort Thompson limestone (Prieto-Portar 1982) 51
Figure 2.40 UCS vs porosity of southern Florida limestone (data from Saxena 1982; Frizzi and Meyer 2000). 52
Figure 2.41 Elastic modulus vs dry density of southern Florida limestone (data from Saxena 1982). 53
Figure 2.42 Relationships between SPT-N and Su (data from Djoenaidi 1985). 54
Figure 2.43 Different limestone surface textures (Sarno et al. 2010). 57
Figure 2.44 Figure 3.5. Limestone adhered to piles extracted from Gandy Bridge / Friendship Trail over Tampa Bay. 58
Figure 3.1 Field retrieved limestone cores (left); core from simulated limestone bed and simulated limestone cylinder specimen (right). 59
Figure 3.2 Casting of simulated limestone bed. 60
Figure 3.3 Debonding plastic disks (left) and centering rods (right). 61
Figure 3.4 Preparation of cylinders from limestone bed material. 61
Figure 3.5 Rock socket construction layout on each simulated limestone bed. 62
Figure 3.6 Casing cutting tips, drive shoe, casing extensions and drill rod couplers. 63
Figure 3.7 Fine-tooth (left), coarse-tooth (center) and driving shoe (right). 63
Figure 3.8 Top of simulated limestone beds flooded with water and being pre-cored. 64
Figure 3.9 Pre-drilling (left) and driving the casing (right). 65

Figure 3.10 Airlift vacuum used to clean up fragments from inside the installed casings. 65
Figure 3.11 Rotatory casing installation (left) and drill bit (right). 66
Figure 3.12 Cuttings replacement on the outer perimeter of the casings. 67
Figure 3.13 Example of high-resolution pictures taken on the control holes. 67
Figure 3.14 Filling tremie and hopper while casting rock sockets. 68
Figure 3.15 Anchor rod placed in tremie before concreting. 69
Figure 3.16 Debonding plastic sleeves on top 8in of the sockets. 69
Figure 3.17 Rock socket specimens after concreting (left), ready for load testing (right). 70
Figure 3.18 Pull-out load test in progress. 70
Figure 3.19 Extracted sockets from bed 5 (left), bed 1 (center) and bed 4 (right). 71
Figure 3.20 Load vs displacement for all sockets. 73
Figure 3.21 Side shear resistance vs displacement for all sockets. 75
Figure 3.22 Normalized side shear resistance (by bed UCS) vs displacement. 76
Figure 3.23 Temporary / control side shear ratio vs displacement. 78
Figure 4.1 Locator map for the Miami test site. 80
Figure 4.2 Plan view of R.W. Harris yard in Northeast Miami, Hialeah area. 81
Figure 4.3 Soil profile from the NW and NE borings (Tierra, 2017). 82
Figure 4.4 Soil profile from the SW and SE borings (Tierra, 2017). 82
Figure 4.5 Reinforcing cage layout for pull out cages. 84
Figure 4.6 Base plates (left) and upper spacer plates (right) being cut out. 84
Figure 4.7 Cage components. 85
Figure 4.8 Cage assembly. 86
Figure 4.9 Rock auger and casing used to excavate both shafts. 87
Figure 4.10 Both shafts after excavation and casing advancement. 87
Figure 4.11 Casing extraction and clean out of uncased control shaft. 88
Figure 4.12 Cage installation: control shaft (left) and temporary cased shaft (right). 89
Figure 4.13 Concreting: control shaft (left) and temporary cased shaft (right). 89
Figure 4.14 Concreting: over-pouring control shaft (top left); filling temporary casing with extra concrete (top right and bottom left) and after casing extraction (bottom right). 90
Figure 4.15 Two 18in x 24in x 2in thick plates match drilled as top load transfer beam. 91
Figure 4.16 All load testing equipment loaded out for Miami test site. 92
Figure 4.17 Load test setup. 93
Figure 4.18 Completed loading system with reference beam. 94
Figure 4.19 Load trace showing uniform loads for the two shaft specimens. 94
Figure 4.20 Comparative load test results for temporarily cased and uncased conditions. 95
Figure 4.21 Displacement rate vs load. 96
Figure 5.1 Rock socketed specimens being prepared for pull-out tests 98
Figure 5.2 Design and measured side shear / UCS ratio vs simulated limestone beds UCS 98
Figure 5.3 Resistance bias factor based on four design methods 99
Figure 5.4 Strength ratio of temporary cased to uncased shaft capacities 100

Intentionally Left Blank

Chapter One: Introduction

Construction methods affect drilled shaft side shear resistance but are not fully addressed by design equations. However, the design methodologies do stem from the performance of previously tested shafts constructed with a variety of methods with different slurry types, excavation tools, and range of shaft sizes and therefore was thought to, in part, account for these effects (i.e. O'Neill's beta method). The effects from full length or partial length temporary casing can present the same concern. The primary objective of this study is to quantify the effects of temporary casing installation and extraction on the resulting side shear in the portions of the rock sockets used to embed and seal the casing.

1.1 Background

Casing installation/extraction equipment varies most notably in the methodology used. Typical approaches include vibratory, drilled/screwed in, oscillated, etc., but even the casing thickness and/or design (i.e. outer ribs or stiffeners) can add the list of variables, all of which have an effect on the side shear resistance. Figure 1.1 shows the resultant surface from oscillating and rotating the casing during extraction (left); using vibratory/straight vertical extraction results in a polished smooth surface (right).

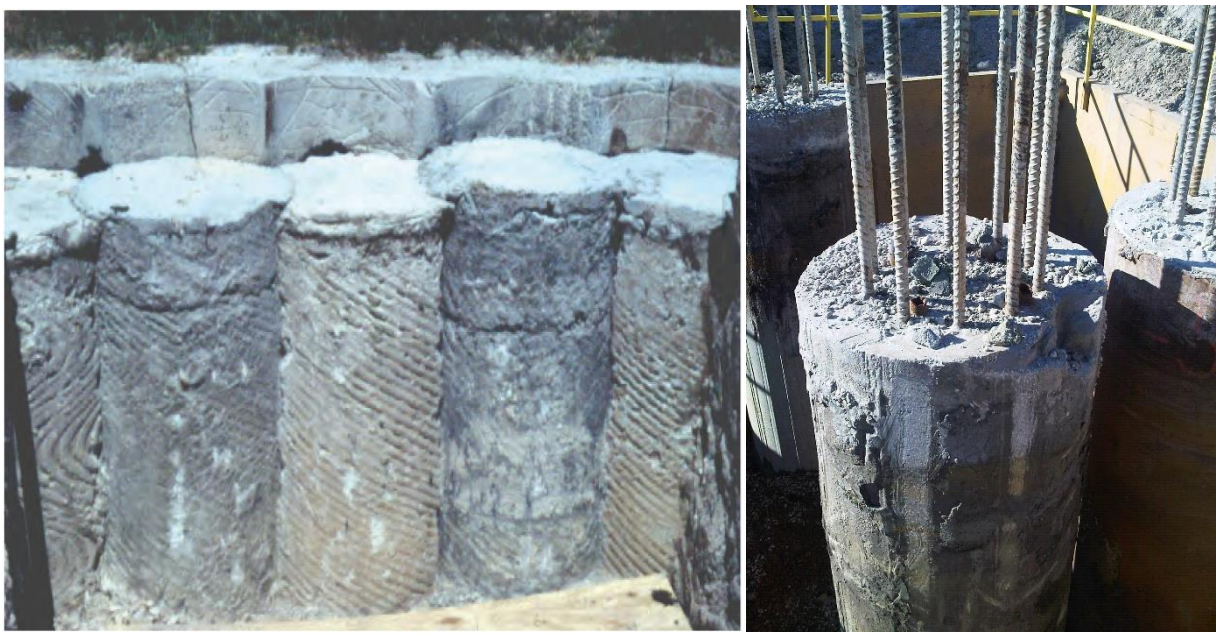

Figure 1.1 Surface texture from rotating casing during extraction (left, FHWA 2010); smooth surface from vibratory extraction (right).

For rock-socketed shafts, the use of casing can have similarly unpredictable consequences. The process of vibrating a temporary casing into the upper portions of a rock socket (and thereby stabilize the upper soils during excavation) pulverizes and crumbles the rock around the casing. In some cases, a suitable seal is formed isolating the excavation from the ground water; in other cases, the crumbled stone fragments around the casing embedment region freely allow water to flow into the excavation. If water can flow freely in and out of the excavation then "slurry" level is difficult to maintain above the ground water elevation and unwanted cave-ins from around the casing can result ("slurry" is usually water in these cases). In any event, the region around the embedded casing has unknown properties. Upon casing extraction, concrete may bond well to the surrounding fragments and rock stratum or it may not.

At present the FDOT 2014 455-15.7 specification restricts the available capacity of the casing embedment region when more than the anticipated embedment is needed to provide a good seal. Recall, the designer usually disregards or degrades capacity from strata above the rock socket and the casing embedment length is not considered as part of the rock socket. If the contractor needs to use some of the anticipated rock socket length to form a sufficient seal, either the rock was not as good as expected or that portion of the rock socket now used to seal the casing may not perform as expected by the designer. To this end, a quick field fix to this possible occurrence is specified without the need for designer intervention or recalculation of the as-built circumstances (FDOT, 2014):

455-15.7 Casings. Ensure casings are metal . . .
. . . . If temporary casing is advanced deeper than the minimum top of rock socket elevation shown in the Plans or actual top of rock elevation if deeper, withdraw the casing from the rock socket and overream the shaft. If the temporary casing cannot be withdrawn from the rock socket before final cleaning, extend the length of rock socket below the authorized tip elevation one-half of the distance between the minimum top of rock socket elevation or actual elevation if deeper, and the temporary casing tip elevation.

The primary motivation for this specification stems from the unknown conditions in the casing embedment zone of the rock socket.

While virtually all aspects of construction techniques are presently vacant from design specifications, it is the focus of this research study to identify the magnitude of side shear reduction that accompanies the crumbling of the rock material around the casing and the effectiveness (or ineffectiveness) of the concrete to bond with the surrounding rock strata.

For the past 20 years, researchers at the University of South Florida have been striving to bridge the gap between research and practice and to speed the process by which academic findings are implemented by the foundations industry. Their aim is and has been to solve on-going construction problems, enhance usable capacity, and assure quality foundation elements (Mullins, 2013).

1.2 Organization of the Report

This report contains four ensuing chapters: Chapter 2 provides a review of literature dealing with cased shaft construction and design, Chapter 3 describes an in depth small scale evaluation of rock sockets capacity in simulated limestone, Chapter 4 extends the small scale work into the field where large scale shafts were constructed and tested, and Chapter 5 provides conclusions.

Chapter Two: Literature Review

2.1 Background

Foundations for tall buildings, bridges or other heavy structures often use deep foundations to ensure adequate load carrying capacity can be developed. These can be comprised of a single or group of structural elements that extend down to firm bearing strata and may be hundreds of feet deep. The elements can be timber, steel or concrete pipes, H-piles, square, round, hexagonal, octagonal, or rectangular concrete sections and may be cast-in-place or precast.

Most design methods recognize a strong distinction between driven piles and bored piles. Driven pile design also takes note of pile material / surface texture and whether or not it introduces additional passive lateral pressure that often is accompanied by higher side shear resistance (e.g. displacement or non-displacement piles). In this way a large range of side shear (or end bearing) might develop (Figure 2.1).

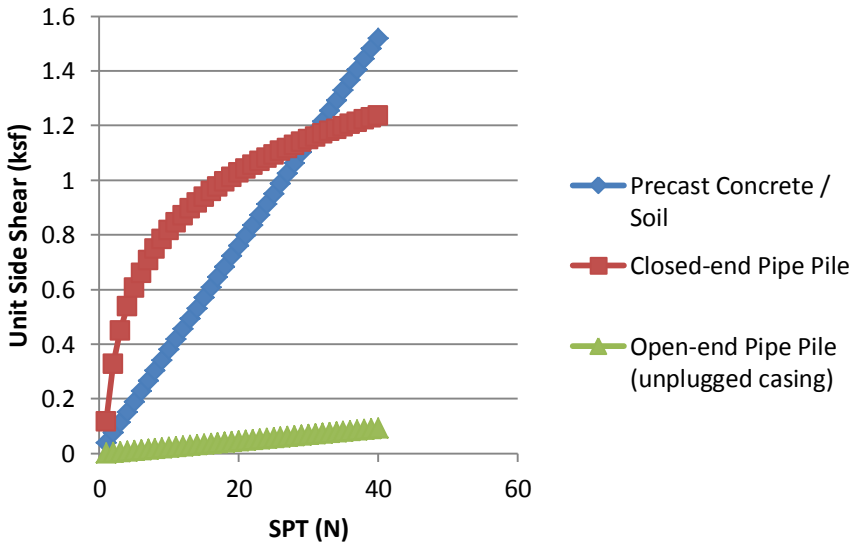

Figure 2.1 Unit side shear values for various driven pile types in sand.

Bored piles are also sub-divided into augercast piles or cast-in-drilled-hole piles (more commonly called drilled shafts in the U.S.) which are also significantly different in the manner by which they are constructed. Depending on the equipment used, augercast piles may be considered full displacement piles if over pumped or laterally displaced by an increasing auger stem diameter (e.g. omega pile or Bauer displacement pile). But, if not pumped to more than 100% of the theoretical auger diameter/volume then the soil can be left in a lower active lateral

pressure state which drastically reduces the resulting capacity. As this study addresses drilled shafts, the factors affecting augercast capacity are not discussed further.

Focusing on drilled shafts, the same lateral pressure considerations can be extended to open excavations that are either supported by casing or slurry. For instance, full or partial length temporary casing is a widely accepted means to stabilize lateral soil movement and prevent collapse during shaft construction. In the driven pile arena, the casing would be considered a non-displacement pile that has little to no effect on the at-rest lateral pressure state. Given the procedures that might be used to construct a shaft (excavate, place steel, pour concrete, and remove casing if applicable), the final lateral pressure state of the soil may be: (1) fully active where the concrete did not flow quickly and hold back the soil upon casing removal, (2) passive to the level and equaling the hydrostatic pressure of completely fluid concrete head, or (3) somewhere in between. Use of slurry (polymer or mineral) may remove some uncertainty as to the final pressure state where the soil pressure would be at least at the level of the slurry pressure head and the presence of concrete pressure would only increase that value. This assumes the concrete was fluid enough to make contact with the soil upon initial placement. Figure 2.2 shows the active soil pressure distribution in an 80ft deep excavation with water table at 10ft. If concrete is placed under fully fluid conditions (sufficient slump), the resulting pressure becomes passive at almost 5 times the active state. This commonly occurs during slurry concrete placement, but may not when casing is used and if the concrete slump falls making it unable to adequately flow through the reinforcing cage.

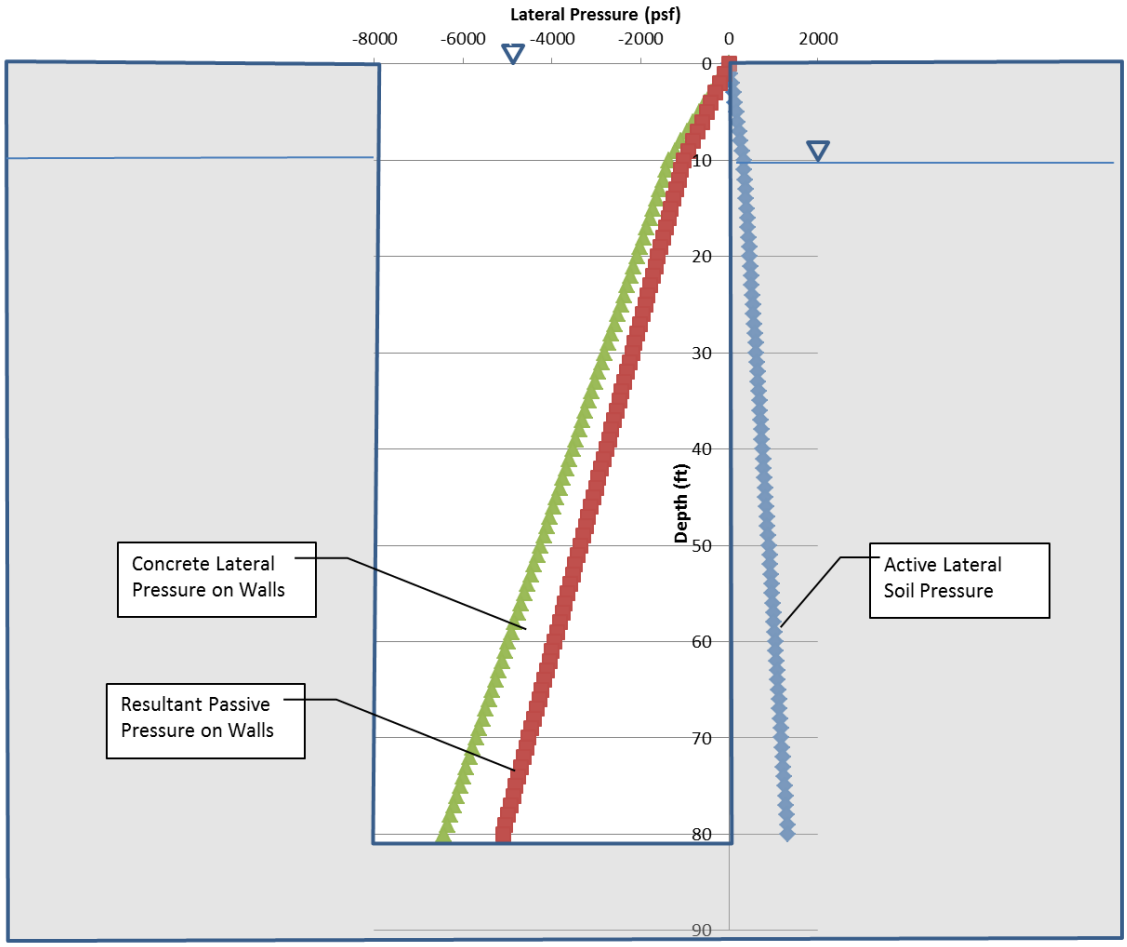

Figure 2.2 Lateral pressure distribution resulting from fully fluid concrete pressure.

In general, all shaft construction techniques have an effect on the resulting side shear (and/or end bearing) and as such should be addressed in design. This study addresses a specific condition involving the unknown surface condition that arises in the areas where casing is socketed into limestone and then removed after concreting.

2.2 Construction Effects

While design methods vary, it is well understood that the shear interface that develops between steel and soil is different (usually lower strength) than precast concrete and soil (discussed above). Concrete cast-in-place directly against a rough soil surface forms an even more intimate interface whereby the concrete/soil interface shear exceeds the soil to soil interface directly adjacent the concrete/soil interface. Bowles (1996) assigned recommended values of friction angles, δ, for various foundation materials and soil conditions (Table 2.1).

Table 2.1 Friction angles between foundation materials and soil or rock (adapted Bowles 1996).

Interface Materials	Friction angle, δ,
Cast-in-place concrete on sound rock	ϕ
Cast-in-place concrete on gravel, gravel/sand, coarse sand	ϕ
Cast-in-place concrete on fine to medium sand	ϕ
Cast-in-place concrete on sand silty or clayey fine sand	ϕ
Cast-in-place concrete on sandy silt, nonplastic silt	ϕ
Cast-in-place concrete on very stiff or preconsolidated clay	ϕ
Cast-in-place concrete on medium stiff clay or silty clay	ϕ
Steel sheet piles against clean gravel, gravel/sand, well-graded rock fill	22
Steel sheet piles against clean sand, silty sand, poorly graded rock fill	17
Steel sheet piles against silty sand, gravel or sand mixed with silt or	14
Steel sheet piles against fine sandy silt, nonplastic silt	11
Precast concrete against clean gravel, gravel-sand mixtures, well graded	22-26
Precast concrete against clean sand, silty sand-gravel mixtures, poorly	17-22
Precast concrete against silty sand, gravel, sand mixed with silt or clay	17
Precast concrete against find sandy silt, nonplastic silt	14

Many of the side shear conditions discussed above are addressed at the design phase, but the effects of construction practices have significant effects on the shaft side shear performance and at present are not explicitly included in the latest design manuals (e.g. FHWA 2010 or AASHTO 2012). These variables include but are not limited to: construction equipment (auger or grabs), cased or slurry stabilized, vibrated or oscillated casing installation, slurry type, time of slurry exposure, etc. Side shear capacity is simply computed based on parameters such as soil type, density, depth, intactness of recovered samples, unconfined compression strength and/or SPT blow counts (e.g. O'Neill beta method, clay alpha method, McVay limestone method, FHWA effective stress method). Therein, these methods employ theoretical, empirical, or semi-empirical correlations. The O'Neill beta method, however, is based on the performance of as-constructed shafts which in part accounts for construction variability. It is unclear at present, what percentage of shafts was constructed with a given construction technique. O'Neill identified, but made no attempt to separate these effects in his final form of the equations used.

2.2.1 Slurry

The effect of slurry type has been investigated in silt, silty sand and sand whereby the recurring conclusion shows polymer slurries produce a slightly higher side shear in pervious soils when compared to mineral type slurries (Mullins et al. 2014; Camp et al. 2002; Brown and Drew 2000). In contrast, the slurry viscosity has shown to have no discernible effect on side shear but some concerns still exist with regards to long-term durability from higher viscosity slurries. A companion study is presently investigating these effects which is outside the scope of this project.

2.2.2 Concrete and Cage Spacing

Concrete properties have been shown to affect side shear capacity and flow-ability through the cage. Some state and federal specifications recommend minimum clear cage spacing or spacing to max aggregate diameter ratio (CSD) to ensure concrete presses unrestricted against the side wall of the excavation. Figure 2.3 shows the results of concrete flow tests performed on a wide range of CSD ratios (Mullins and Ashmawy, 2005). The study findings showed that tighter cage spacing (small CSD) caused the concrete level inside the cage to rise before squeezing out into the annular concrete cover region. Higher concrete placement / flow rates had a similar effect.

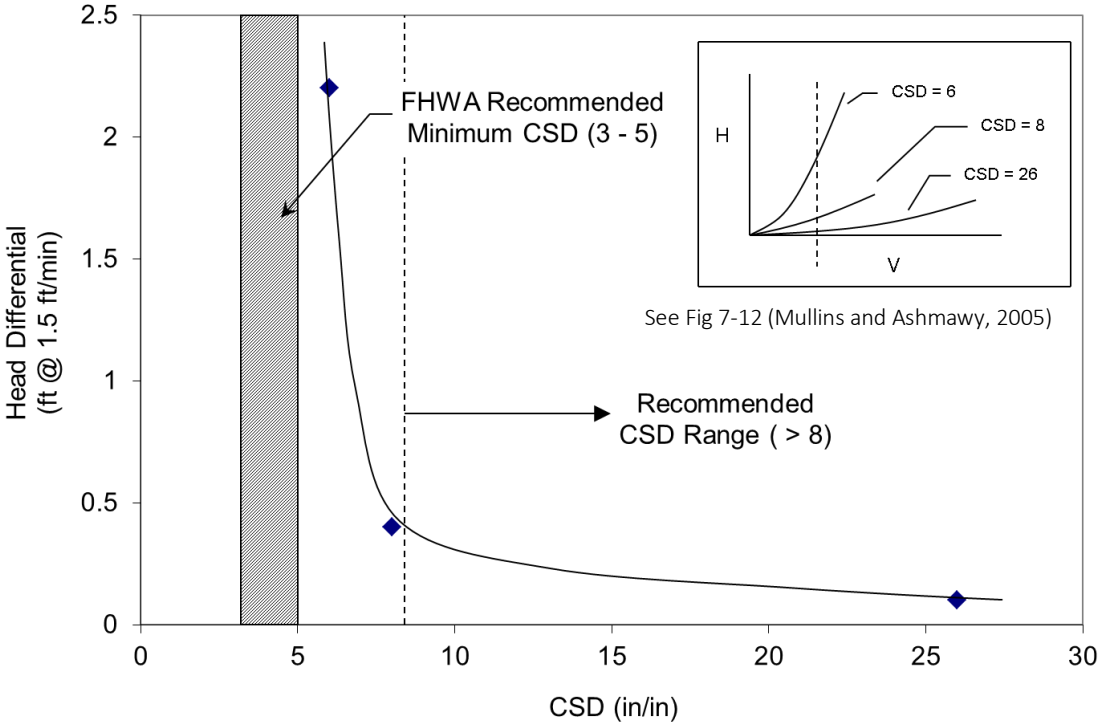

Figure 2.3 Concrete level differential (inside vs outside cage) with respect to cage tightness.

In an effort to further minimize adverse effects from concrete properties during placement, many specifications restrict the concrete slump at the time of pour (e.g. 7 to 10in) and the slump loss that can be tolerated over the duration of concrete placement. The latter is particularly important when full length temporary casing is used to stabilize the excavation or when full length tremies are used to pour long shafts.

Previous studies showed that the hypothetical scenario (poorly flowing concrete) outlined above had real consequences when slump reduced before casing was extracted (Figure 2.4). In that study, model shafts were constructed with slumps within specified limits and then intentionally waited too long before casing extraction to cause the slump to fall below specified casting limits. When casing was extracted at the preferred casting limits (e.g. slump between 7 and 10in), side shear values were relatively unaffected. But as slump fell below 7in markedly reduced side shear

resulted. At slump values approaching 3in it is likely the casing will become stuck and be forced to become permanent (constructability limit shown).

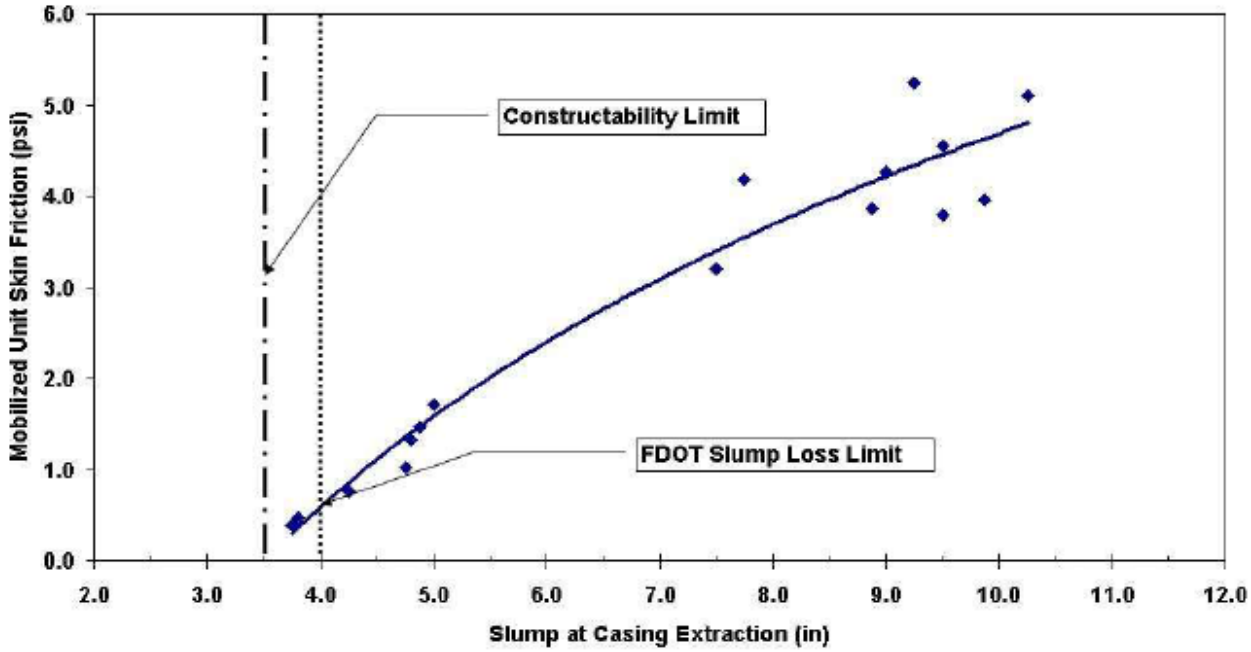

Figure 2.4 Unit side shear versus slump loss at the time of casing extraction.

Note: at the time of the original study the slump loss limit was 4in; the latest 455-17.2 specification now in part reflects these findings with a value of 5in.

The net effect is the casing slip-forms lower slump concrete as it is extracted and reduced contact pressure is achieved between the concrete and the soil. In the case of full length tremies extracted after prolonged placement times, the surrounding concrete is older, stiffer and easily pushes bleed water into the more-fluid, fresh concrete left in the tremie position. This manifests in a column of aggregate with poor cementation and might show at the top of shaft as depression with the diameter of the tremie. A central tremie hole is of little concern to shaft performance (structurally or geotechnically), but may be flagged by integrity assessments and warrant further review.

2.2.3 Casing

The mere act of installing casing changes the soil properties; in most cases these changes are for the better making loose or medium dense sand more dense. When loose deposits underlie rock layers or clays, vibration from casing installation collapses the soil resulting in a void in the upper portion of the layer over the now higher relative density sand; if below the water table, this void is the result of an exchange of loose soil volume with ground water. When a temporary casing is extracted up and through this voided region, the cover concrete will flow out first to fill

the void and some exchange of water and concrete occurs. This was described by Sliwinski et al. (1984) and shown in Figure 2.5.

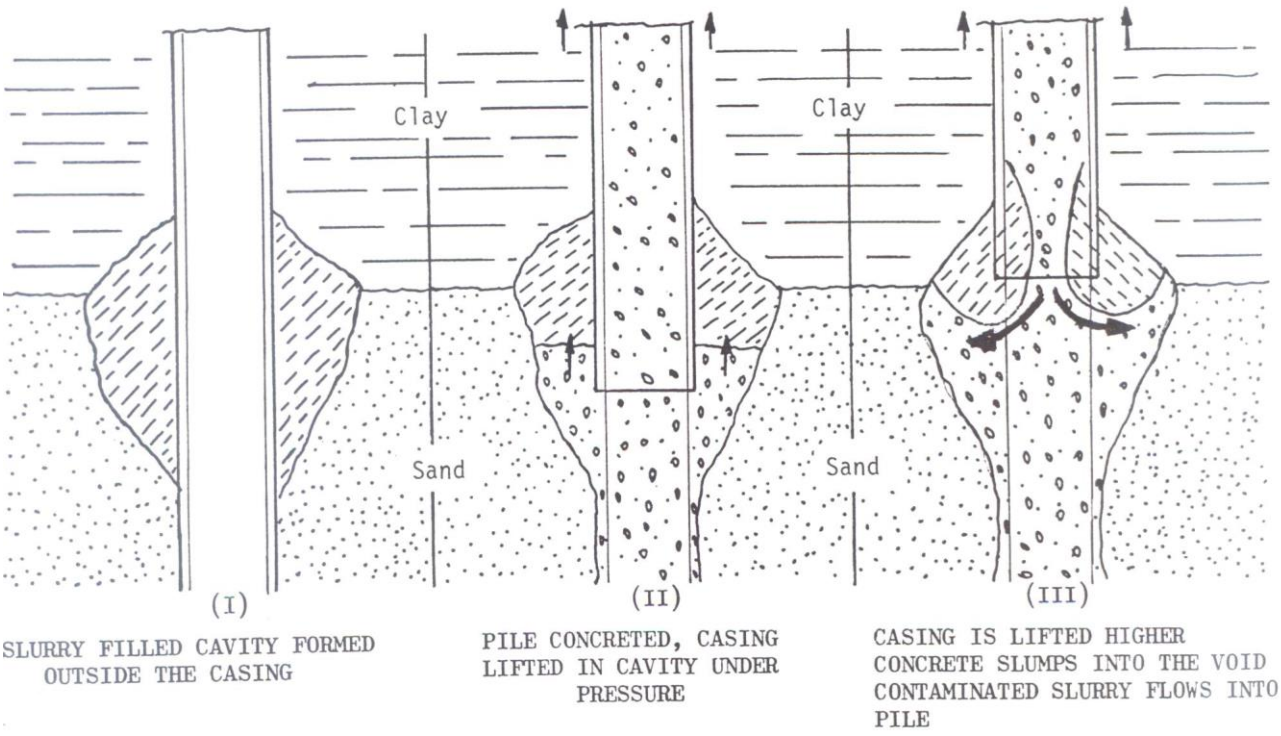

Figure 2.5 Conceptual process during casing extraction where a water-filled void around the casing is filled by denser, higher pressure fluid concrete resulting in trapped water inside casing or shaft volume (Sliwinski et al., 1984).

In a local case in south Florida, the scenario described by Sliwinski was observed where a significant drop in concrete level inside the temporary casing occurred during casing extraction. Figure 2.6 shows the predicted shaft radius from thermal profiling which indicated concrete within the permanent casing region (above 30ft depth) was less than that of the casing and below the cap rock the shaft was oversized (design radius was 30in).

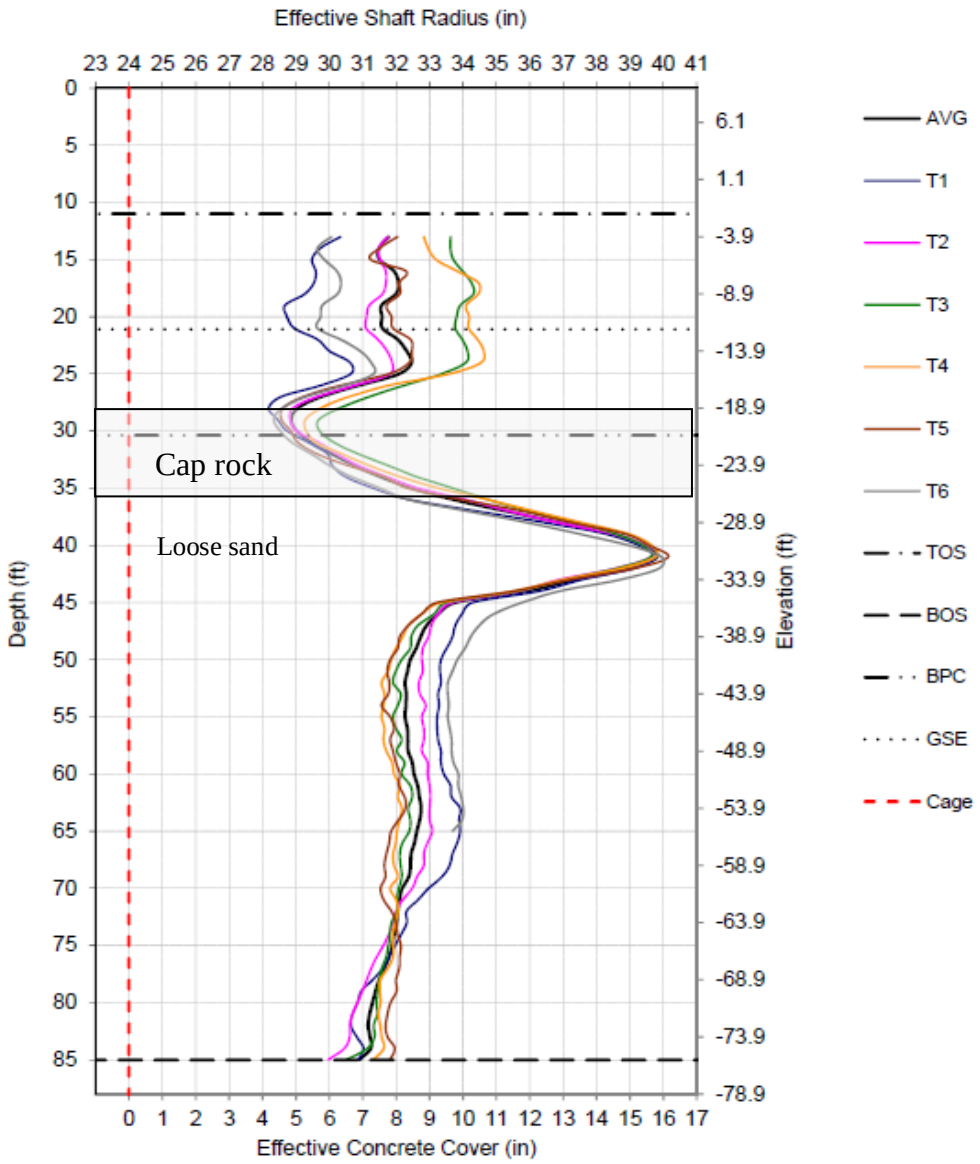

Figure 2.6 Example case where concrete / water exchange was detected by field integrity test; this a problem which can be a by-product of temporary casing.

In the case shown by Figure 2.6 the concrete was sufficiently fluid to flow into the surrounding void, and where no alternate exit for the incompressible water in the void was available. It should also be noted that the core concrete level falls much slower due to the cage obstruction making the cover region more prone to water intrusion/fluid exchange. Unfortunately, the concrete level measurement was performed inside the cage and not outside the cage, making the true severity of the drop appear less drastic than actual. The FHWA (2010) Drilled Shaft Manual talks of providing an exit and use of telescoping casings with a progressive casing extraction technique. Unfortunately, most of these conditions go undetected during construction and the designer could not have predicted the effects of the contractor's approach on the final soil conditions or

shaft integrity. In essence, the as-built soil strata may not even come close to reflecting the boring log conditions used for design.
As this study is focused primarily on the use of temporary casing in rock sockets, the ensuing sections will discuss construction and design methods as they may pertain to casing applications.

2.3 Mechanical Stabilization of Drilled Shafts with Temporary Casing

According to O'Neill and Reese (1999), the casing method is applicable to sites where soil conditions are such that caving or excessive soil or rock deformation can occur when a borehole is excavated. A notable example of a scenario in which casing could be used, which is quite common in Florida, is a clean sand below the water table underlain by a layer of impermeable limestone into which the drilled shaft will penetrate. In this case, since the overlying sand is water bearing, it is necessary to seal the bottom of the casing into the limestone to prevent flow of water into the borehole. Florida's limestone may be extremely variable in geotechnical properties, and sometimes the temporary casing penetrates layers of weak limestone, to then be sealed into a more competent layer.

As described in FHWA (2010), three types of construction of drilled shafts using temporary casings are most commonly used:

Excavate an oversized hole using the dry method, then place the casing into the hole. This method is suitable only for construction in soils that are generally dry or have slow seepage, and that will remain stable for the period of time required to advance the hole to the more stable bearing stratum. In this scenario the casing cannot preserve the soil structure and strength but rather only prevents total collapse if the side walls become unstable.

Excavate an oversized hole through the shallow permeable strata using a drilling fluid, then place and advance the casing into the bearing stratum. After the casing is sealed into the underlying more stable stratum, the drilling fluid can be removed from inside the casing and the hole advanced to the final tip elevation in the dry. A schematic diagram of this approach is provided in Figure 2.7.

Advance the casing through the shallow permeable strata and into the bearing formation ahead of the shaft excavation, and then excavate within the casing in the dry. With this approach, casing may be driven using impact or vibratory hammers or using a casing oscillator or rotator with sufficient torque and downward force to advance the casing through the soil ahead of the excavation. Even larger upward force may be required to pull the casing during concrete placement. A schematic diagram of this approach is provided in Figure 2.8.

There are different methods for installing and extracting temporary casings during the construction of drilled shafts, each one may have a different effect on the side shear. Temporary

casing can be placed through a pre-drilled hole to seat the casing into an underlying formation of more stable material, or advanced ahead of the excavation in cases where the hole will not stand open for short periods or where slurry drilling techniques are considered less attractive from a cost or performance standpoint. There are two primary methods used to advance casing ahead of the excavation. The contractor may drive the casing in advance using a vibratory hammer, or using oscillator/rotator equipment (FHWA, 2010).

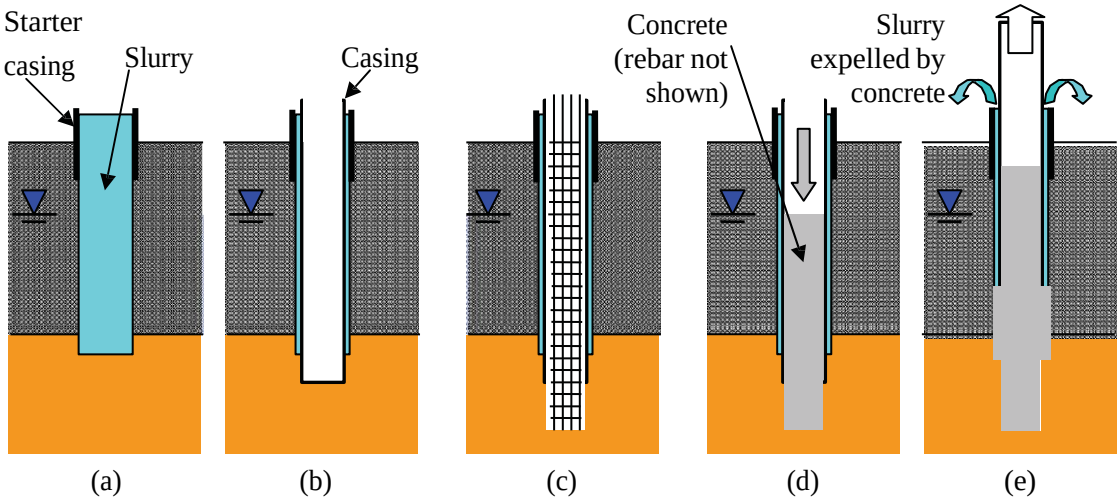

Figure 2.7 Construction using casing through slurry-filled starter hole: (a) drill with slurry; (b) set casing and bail slurry; (c) complete and clean excavation, set reinforcing; (d) place concrete to head greater than external water pressure; (e) pull casing

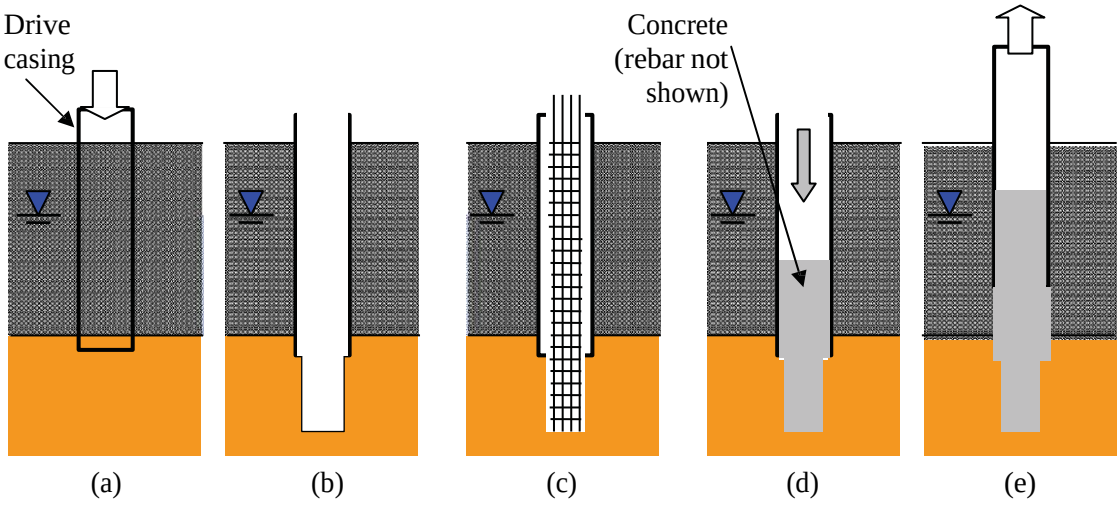

Figure 2.8 Construction using casing advanced ahead of excavation: (a) drive casing into bearing stratum; (b) drill through casing; (c) complete and clean hole, set reinforcing; (d) place concrete to head greater than external water pressure; (e) pull casing while maintaining sufficient concrete head.

In most cases, the shaft excavation will be advanced below the base of the casing for some distance into the bearing formation of soil or rock, and it is necessary that the casing achieve a seal into this bearing formation in order to control caving or seepage around the bottom of the casing. The most common equipment for casing installation today are: oscillator, vibratory hammer, and twisted. Figure 2.9 shows an oscillator (with spherical grab) and Figure 2.10 shows both vibratory hammer and twister bar systems.

Oscillators are hydraulic-driven tools for advancing and extracting casing. The casing often is a segmental pipe with bolted joints. The oscillator or rotator grips the casing with powerful hydraulic-driven jaws and twists the pipe while other hydraulic cylinders apply upward or downward force. The rotation of the oscillating motion is usually less than 90deg.

Figure 2.9 Oscillator rig used to advance segmental casing ahead of the excavation (FHWA, 2010).

Figure 2.10 Use of a vibro-hammer (left) and twister bar (right) to advance casing (FHWA, 2010).

The vibratory hammer (Figure 2.10 left) is also hydraulically activated with two functions: (1) the gripping jaws which grib either side of the casing and can be adjusted to fit a wide range of casing diameters, and (2) horizontally oriented hydraulic motors with an eccentric weight; the up and down cyclic motion of the eccentric weight produces large axial forces that advance the casing with the addition of the self weight of the hammer and casing. During casing extraction the hammer is lifted via crane to offset self weight and help overcome side shear.

Where an oscillator twists back and forth, a twisted casing system can rotate the casing through a full 360° when advancing casing. An example of a rotator is shown in Figure 2.11 (FHWA, 2010). This system conveniently couples to the drill rig by attaching a twister bar (Figure 2.10, right) so that the rig can apply torque and crowd onto the casing. Sometimes the casing is equipped with cutting teeth or carbide bits at the bottom to penetration hard layers, as shown in Figure 2.11 (FHWA, 2010).

Figure 2.11 Cutting Teeth on the Casing to Assist Penetration into the Bearing Stratum (FHWA, 2010).

Figure 2.12 Example of rotator machine (Malcolm, 2016).

The concrete used with the casing method must have good flow characteristics in order to flow easily through the reinforcing cage to fill the space outside the casing and displace any water or slurry around the casing from the bottom up. It is critical that the concrete maintain a hydrostatic pressure greater than that of the fluid external to the casing. The concrete must also retain workability beyond the duration of the concrete placement operations until the casing is completely removed. If the concrete slump becomes low, it will not easily flow through the cage to fill the space between reinforcing and the sides of the hole, which can result in near zero side shear (Mullins et al., 2013). Arching of the concrete can also occur, and the concrete will move up with the casing, creating a gap into which slurry, groundwater, or soil can enter. Finally, The casing should be pulled slowly in order to keep the forces from the downward-moving concrete on the rebar cage at a tolerable level (FHWA, 2010).

Casing sometimes needs to be used to stabilize very deep shafts and/or into very strong soil or rock, in which casing removal may be difficult. In such instances, contractors may choose to "telescope" the casing, as illustrated in the photo of Figure 2.13. With this approach, the upper portion of the shaft is excavated and a large-diameter casing sealed into a suitable stratum. A smaller-diameter shaft will then be excavated below the bottom of the upper casing and a second casing, of smaller diameter, will be sealed into another suitable stratum at the bottom of the second-stage of excavation. The process can be repeated several times to greater and greater depths until the plan tip elevation is reached. With each step, the borehole diameter is reduced, usually by about 6 inches. The casings should be extracted starting with the innermost. (FHWA, 2010).

Figure 2.13 Telescoping Casing, most likely permanent (FHWA, 2010).

In the case of the driven casing, a vibratory hammer is almost always used for temporary casing; an impact hammer may be used to install permanent casing, but temporary casing will require a vibratory hammer for extraction since casing installed with an impact hammer may be impossible to remove. During extraction, the hammer is attached and powered, and then typically used to drive the casing downward a few inches using the weight of the casing and hammer to break the casing free of the soil. Once the casing is moved, the crane pulls it upward and leaves the fluid concrete filled hole behind. Figure 2.14 shows the start of removal of a casing after completion of concrete placement. (FHWA, 2010).

Figure 2.14 Casing extraction using vibratory hammer (FHWA, 2010).

2.4 Rock-Sockets

Rock sockets are the portion of the shaft drilled into rock (Zhang, 2004). Hudyma and Hiltunen (2014) noted that rock sockets in highly variable limestone are very common in Florida.

A common application for drilled shafts is to be socketed in a rock formation below the casing to a sufficient length to develop all the required capacity. In these cases, the side shear of softer overlying materials is disregarded due to the mismatch in the displacement required to mobilize both material types. Rock sockets require relatively small movements to develop full capacity when compared to sand or clay strata. Further, although the end bearing strength of a rock socket can be quite considerable, it is often discounted for the same reason. Alternatively, a rock socket may be designed for all end bearing instead of side shear, knowing that some side shear capacity will always be available in reserve (Mullins, 2014).

2.4.1 Calculations of Ultimate Side Shear of Rock Sockets

The side shear strength of rock-socketed drilled shafts is similar to that of clayey soils in that it is dependent on the in situ shear strength of the bearing strata. In this case, rock cores are taken from the field and tested using various methods. Specifically, mean failure stresses from two tests are commonly used: the unconfined compression test, q_u, and the splitting tensile test, q_t. Local experience and results from load tests can provide the best insight into the most appropriate approach (Mullins et al. 2014).

While the construction technologies advanced rapidly after World War II, the developments of theories for design and analytical techniques lagged behind. In the late 1950's and early 1960's, computers, analytical methods, and full-scale load-testing programs began to produce a better understanding of drilled shaft behavior. Marked differences between the behavior of driven piles and drilled shafts were noted, and the importance of proper quality control and inspection was realized (O'Neill and Reese, 1999).

2.4.1.1 O'Neill and Reese (1999) Methodology

Side resistance in rock and cohesive intermediate geo-materials (IGMs) depend upon factors other than the strength of the geomaterial. These include the roughness of the socket (portion of the drilled shaft drilled into the rock or IGM), the presence of soft seams within the geomaterial, and the angle of friction between the concrete and geomaterial. As a point of reference, cohesive IGMs have unconfined compression strength, q_u, between 5 and 50tsf, and rocks have corresponding q_u > 50tsf (O'Neill and Reese, 1999).

The first recommendation that O'Neill and Reese (1999) provided was to decide whether the socket in an IGM layer will be smooth or rough, since roughness of the borehole wall has a large effect on side resistance. It was recommended that, unless the sides of the borehole will be artificially roughened during construction, that the socket be considered smooth; however, procedures must guarantee that no smeared material remains on the sides of the borehole. For design purposes, a smooth socket contains a roughness naturally created with the drilling tool, but without leaving smeared material on the sides of the borehole wall.

For a smooth socket in cohesive IGM, to be computed at each desired layer (O'Neill and Reese, 1999):

$$f_{max} = \alpha \varphi q_u \qquad eq.2.1$$

where:
α = obtained from Figure 2.15 (note that it is not the same as for clays);
φ = joint-effect factor that accounts for the presence of open joints that either are voided or contain soft gouge. φ can be estimated from Table 2.2, limited to RQD $\geq$ 20.
q_u = unconfined compression strength of the intact IGM.

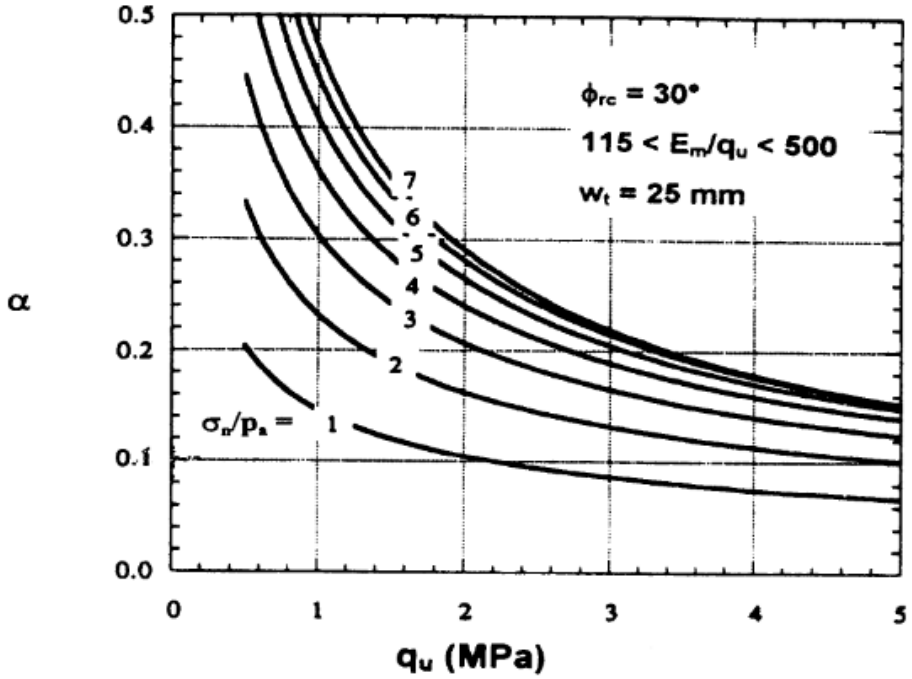

Figure 2.15 α factor for cohesive IGM material (O'Neill and Reese, 1999).

In Figure 2.15, w_t is the settlement of the socket at which α is developed; E_m is the Young's modulus of the IGM mass, and φ_{rc} is the angle of interface friction, assumed to be equal to 30 degrees. σ_n is the estimated pressure imparted by the fluid concrete at the middle of the layer being analyzed, and p_a is the atmospheric pressure. O'Neill and Reese (1999) suggest a correction for α if it is known that φ_{rc} is different than 30 degrees, and for σ_n if the slump of concrete with unit weight γ_c, is kept at or above 7in as it is placed and the concrete is placed in the borehole at the rate of 40ft per hour or faster.

Table 2.2 φ factors for cohesive IGM (O'Neill and Reese, 1999).

RQD (%)	φ	
	Closed joints	Open or gouge-filled joints
100	1.00	0.85
70	0.85	0.55
50	0.60	0.55
30	0.50	0.50
20	0.45	0.45

For smooth rock socket in a rock layer (rough surfaces in rocks or IGMs should be considered in the calculations only when specified and confirmed (O'Neill and Reese, 1999):

$$f_{max} = 0.65 p_a \sqrt{\frac{q_u}{p_a}} \qquad \leq 0.65 p_a \sqrt{\frac{f'_c}{p_a}} \qquad eq. 2.2$$

Where f'c is the 28 day compressive strength of the drilled shaft concrete (O'Neill and Reese, 1999).

2.4.1.2 AASHTO (2012) – LRFD Bridge Design Specifications

AASHTO (2012) recommends the same methods as in O'Neill and Reese (1999).

2.4.1.3 FHWA (2010) Methodology

One difference from O'Neill and Reese (1999) and FHWA (2010) regarding single drilled shafts in rocks is that FHWA does not define specific procedures for designing drilled shafts (rock sockets) in IGM. However this differentiation sometimes overlaps, IGM and sound rock are expected to behave differently. FHWA (2010) defines the maximum unit side shear similar to O'Neill and Reese (1999):

$$f_{max} = C * p_a \sqrt{\frac{q_u}{p_a}} \qquad eq. 2.3$$

C is defined as a regression coefficient used to analyze load test results. FHWA (2010) describes that C depends of the cleanliness of the excavated rock walls. If the excavation walls are clean, sound, free of smeared material, C can be assumed as 1. However, if there is some smeared material, the coefficient C reduces proportionally to 65% of the ratio between the rock mass and the sound rock Young's Modulus. This procedure approximates O'Neill and Reese (1999), even citing their proposed "φ" table (shown on Table 2.2), but how to use the reduction factor through FHWA (2010) procedure is unclear.

2.4.1.4 FDOT (2015) Methodology for Rock Sockets in Limestone

The FDOT (2015) methodology was proposed in McVay et al. (1992). The authors performed a parametric finite element study with the purpose of more closely examining the maximum skin friction at the shaft-rock interface. They considered that, since the shaft typically has the greatest stiffness, followed by the rock and then soil, failure typically initiates from the juncture of the shaft and top of rock and then migrates downward along the shaft-rock interface. A constant element stiffness was determined from a fixed Young's modulus and Poisson' s ratio, and applied to an elasto-plastic bilinear model to characterize all the rock mass. Due to the high variability of

the Florida limestones properties, the standard deviation was later included into the design approach (FDOT, 2015).

Failure of the rock was described through a Mohr-Coulomb strength envelope, established in stress space by its cohesion and friction angle. Cohesion values of 5, 10, and 15tsf, and friction angles of 30°, 40°, and 50° were investigated. Shaft embedment ratios of 5, 10, and 15 diameters were studied in this model. No special slip elements were used at the shaft-rock interface, since the authors observed, in small-scale pull out tests, that failure occurred generally within the rock. Figure 2.16 summarizes the results of this parametric study. The analysis of this plot led the authors to conclude that the Mohr circles grow toward a common failure state, and that the failure state propagates from one element to the adjacent, and as the rock elements adjacent to the shaft fail in shear, the load is transferred further down the rock-shaft interface.

McVay et al. also observed that, since the shaft/rock interface is vertical, then using the pole (also shown in Figure 2.16), it is possible to infer that the shear stress on the vertical plane is less than 10%, but usually within 5% of the rock cohesion value.

Multiple triaxial compression tests at different confining pressures could be performed to determine the cohesion more precisely. Alternatively, q_u (unconfined compression strength) could be obtained from unconfined compression tests, and, q_t (indirect tensile strength) could be obtained from splitting tensile tests, which are simpler and cheaper to be executed. Making use of trigonometric relationships and using the results provided by the numerical analysis, and based on Figure 2.17, McVay et al. derived the expression currently specified by the FDOT (2015) for calculating the ultimate side shear, f_{su}, as a function of q_u and q_t. McVay et al. (1992) assumed that the tensile strength (q_t), obtained from the splitting tensile test, was in agreement with the uniaxial tension test, which has a major principal stress of zero.

$$f_{su} = \frac{1}{2}\sqrt{q_u}\sqrt{q_t} \qquad eq.\,2.4$$

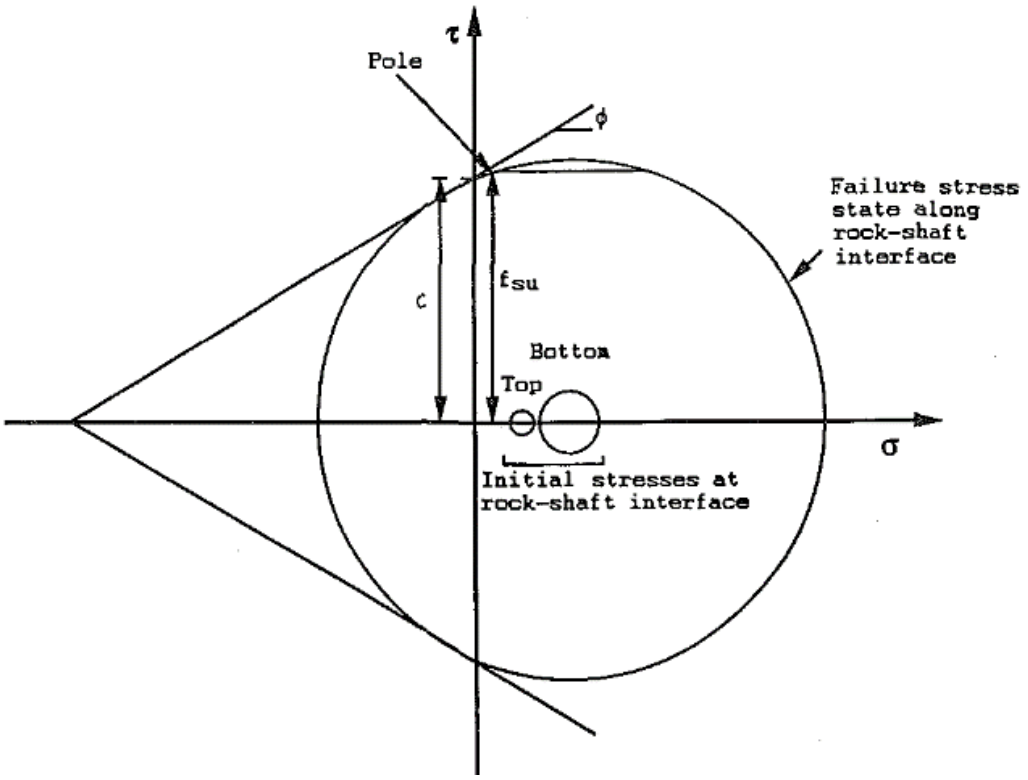

Figure 2.16 Summary of stress states at rock-shaft interface (McVay et al., 1992).

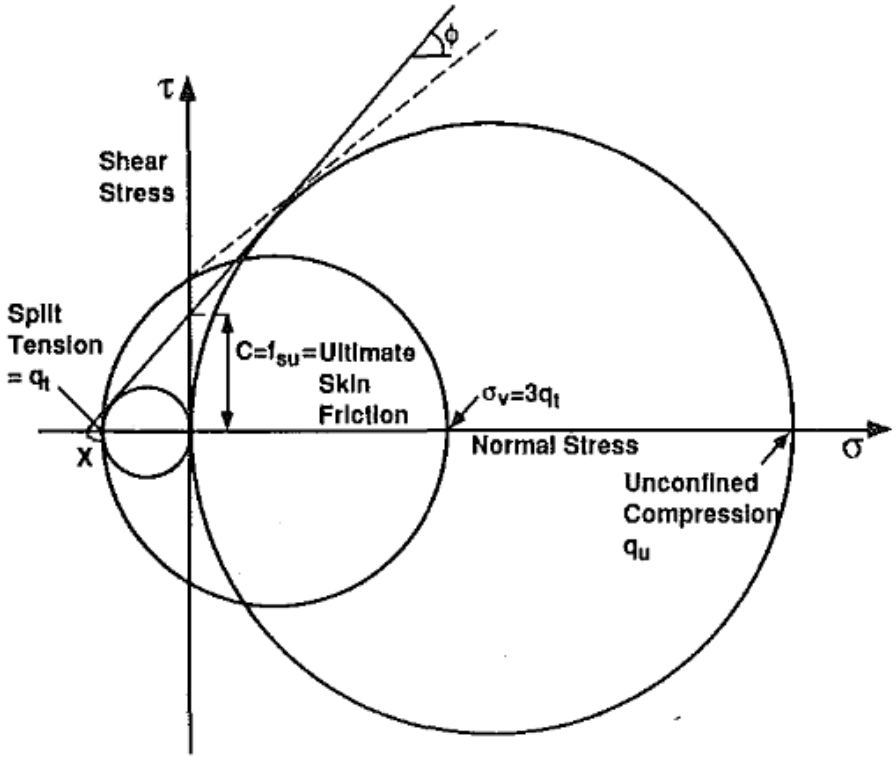

Figure 2.17 Modeled strength envelope for Florida limestone (McVay et al., 1992).

This method has been well accepted, in general, but it only accounts for the geotechnical properties of the limestone. In other words, it does not address the effects of the different types of construction and in the case of this study, effects of installation and extraction of temporary casings on the side shear.

According to the introduction of Appendix A from the Soils and Foundation Handbook 2015 (FDOT, 2015), the variability of the Florida limestone properties has always challenged engineers in deciding what should be the most representative side shear resistance. Some engineers have decided that testing the rock cores specimens is senseless due to this variability (FDOT, 2015).

FDOT (2015) proposes that, to consider the spatial variations of the rock qualities, the average REC (% recovery in decimal) is applied to the ultimate unit side shear resistance, f_{su}, and the product is used as the design side shear resistance:

$$(f_{su})_{design} = REC * f_{su} \qquad eq.2.5$$

According to FDOT (2015), this method has been used by Department engineers for several years and it has provided reasonable estimates of design side shear resistance when compared with load test data.

To reduce the uncertainties regarding the quality of the rock cores, FDOT (2015) requires a minimum core barrel size of 2.4in (61mm), yet it recommends a 4in (101.6mm) for better evaluation of the Florida limestone properties. The manual also requires a triple or double barrel as a minimum to have a better percentage recovery as well as RQD, depending on the core size. However, different exploration equipment may lead to different RQD and design side shear values.

Due to the variability of the Florida limestone formations, to obtain representative values for design side shear resistance (and other properties), FDOT (2015) recommends that one has to obtain a lot of rock core samples, and this number depends on the desired level of confidence. The following relationship identifies the amount of standard error (E) in terms of the number of laboratory specimen tested (n), the confidence level (t), and the standard deviation of strength test (σ) can be expressed as (FDOT, 2015):

$$E = \frac{t\sigma}{\sqrt{n}} \qquad eq.2.6$$

Determining whether the test results are reasonably consistent across the project site, or whether there are different approximate areas or sites within the project is the first step towards understanding the overall variability of the site (Paikowsky, 2004 from FDOT, 2015). FDOT (2015) proposes a data reduction method for obtaining the q_u, q_t and REC values to be used in design. This method is comprised of eleven steps of analyses that are applicable for each area, or

site, within the project limits. Construction methods/effects are not addressed as part of the design methodology.

2.5 Construction of Rock Sockets

The attention to detail in the construction of drilled shafts is critical to ensure successful foundations. If proper and well-established procedures are employed, drilled shafts can be installed successfully in a wide variety of subsurface conditions with differing geometries and for a number of applications. The versatility of drilled shafts is evident when the constructability is considered in various subsurface conditions (O'Neill and Reese, 1999). In this work, focus will be given to sockets into soft Florida limestone that might be easily penetrated by a temporary casing.

The FHWA (2010) manual summarizes the most commonly used tools to excavate rocks. A flight auger specially designed for rock can be used to drill relatively soft rock (hard shale, sandstone, soft limestone, decomposed rock). Hard-surfaced, conical teeth, usually made of tungsten carbide, are used with the rock auger. Rock augers are often of the double-helix type. Three different rock augers are shown in Figure 2.18. The metal thickness in the flights is more substantial than that used in making augers for excavating soil. The geometry and pitch of the teeth are important details in the success of the excavation process, and the orientation of the teeth on a rock auger is usually designed to promote chipping of rock fragments. Rock augers can also be tapered.

Figure 2.18 Examples of rock augers (FHWA, 2010).

If augers are ineffective in excavating rock (for example, the rock is too hard), most contractors would next attempt to excavate the rock with a core barrel. Coring can be more effective in loading the individual cutting bits, thus increasing the pressure on these bits. Ideally, the tube cores into the rock until a discontinuity is reached and the core breaks off. The section of rock contained in the tube, or "core," is held in place by friction from the cuttings and is brought to the surface by simply lifting the core barrel. The simplest form of core barrel is a single, cylindrical steel tube with hard metal teeth at the bottom edge to cut into the rock, as illustrated in Figure 2.19. The chisel teeth shown at top left would be used in soft rock, while the conical points shown at top right would be used in somewhat harder material. The “button” teeth shown at the bottom are used to cut harder rock where the conical points are prone to breaking off. The oscillator/rotator casing is a type of core barrel which commonly employs the button teeth (FHWA, 2010).

Figure 2.19 Examples of single wall core barrels (FHWA, 2010).

If the rock is hard and a significant penetration into the rock is required, a double walled core barrel may be more effective, and can incorporate roller bits as well as teeth. Some examples are shown in Figure 2.20 (FHWA, 2010).

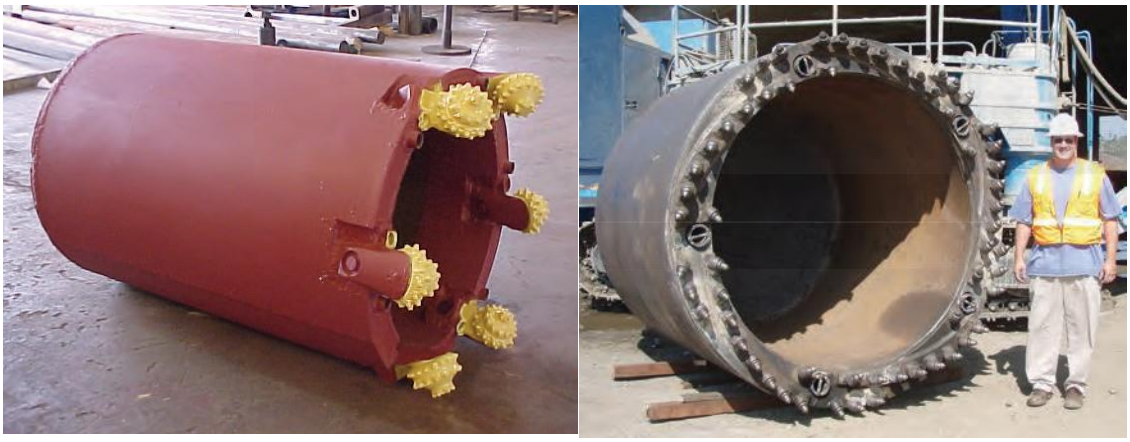

Figure 2.20 Examples of double wall core barrels (FHWA, 2010).

As described earlier on this report, drilled shafts may be constructed using temporary or permanent casing. However, the drilled shaft design methods, in general, are applicable only for computing the resistance of the uncased portions of the shaft, and do not take into account the borehole stabilization technique. FDOT (2015) and FDOT (2014) consider the portions of the shaft constructed with temporary casing will most likely have reduced side shear resistance versus constructing the same portion of the shaft using slurry or with no deepening of the cased portion into the rock, respectively. Confirming this assumption formed the primary objective of this study.

2.6 Summary of States Standard Specifications for Drilled Shafts Constructed with Temporary Casing

In the preparation of this report, a review of the drilled shafts standard specification of the 50 US states was performed. The summary of how each state transportation department recommends the construction of drilled shafts and rock sockets with temporary casings (if any recommendation) is presented below and in Tables 2.3 to 2.6.

Table 2.3 U.S. States that do not provide specifications for drilled shafts for primary structures.

US States	References
AK, AR, DE, ID, IN, MN, NH, ND, NY, TN, VT	AKDOT (2015), AHTD (2014), DELDOT (2001), ITD (2012), INDOT (2016), MNDOT (2014), NHDOT (2010), NDDOT (2014), NYSDOT (2008), TDOT (2015), Vermont DOT (2011).

Note that the State of New York only defines drilled shafts for overhead sign structures (NYSDOT, 2008).

Table 2.4 U.S. States that provide general specifications for drilled shafts, but not specific recommendations for the use of temporary casings.

US States	References
GA, MD, NE, OK, PA, RI, UT	GDOT SSP 524 (2013), MDOT (2008), NDOR (2014), ODOT (2009), PENNDOT (2008), Baxter et al. (2005), UDOT (2012)

Note that the State of Nevada does not allow construction of drilled shafts using temporary casing (NDOR, 2014).

Most of the states have very similar specifications for the construction of drilled shafts using temporary casings, with few variations on the wording. In general, it seems that there is more concern regarding the removal of the casing rather than with its installation. Essentially, as the casing is being withdrawn, the specifications usually recommend to maintain a 5-foot minimum head of fresh, fluid concrete in the casing (above the ground water table or hydrostatic line) so that all the fluid trapped behind the casing is displaced upward without contaminating the shaft concrete. The removal method shall prevent the intrusion of water, grout and soil into the

excavation, displacement of the reinforcing steel, and lifting of the concrete. Casing should not be pulled after the concrete begins to set. Casing that cannot be extracted during, or immediately after, the concrete placement operation may be cause for rejection of the shaft, or remedial measures have to be taken as approved. Some of the suggested remedial measures include removing shaft concrete and extending shaft deeper; providing replacement shaft; or providing straddle shafts to compensate for capacity loss.

Table 2.5 U.S. States that provide similar specifications for construction of drilled shafts using temporary casings, with no further details.

US States	References
AZ, CA, CO, CT, HI, LA, ME, MI, MT, NC, OH, OR, SC, SD, TX, VA, WA, WI, WY	ADOT (2008), CALTRANS (2010), CDOT (2011), ConnDOT (2005); *, HIDOT Section 511 (2013), DOTD (2006), MaineDOT (2014), MDOT (2012), MDT (2014), NCDOT (2012), Ohio DOT (2013), Oregon DOT (2015), SCDOT (2007), SDDOT (2015), TXDOT (2014), VDOT (2007), WSDOT (2014), WisDOT (2014); **, WYDOT (2010)

*http://www.ct.gov/dot/lib/dot/documents/dsoils/ConnDOTGuideDrilledShaftSpec.pdf
** wisconsindot.gov/dtsdManuals/strct/spec-provs/drldshft.doc

Some other states have more detailed specifications, especially regarding construction of rock sockets and its final roughness. The specifications of these states also include the same general statements summarized above. In general, these specifications also require that the Engineer inspect the samples and cores to determine the final depth of required excavation, overream sidewalls of drilled shaft within the rock socket to increase roughness (such as producing channels with approximate dimensions of 2 inch deep by 3 inch high at intervals of 1 foot (Iowa DOT). Not all the states specify these dimensions, but those listed on Table 2.6 require overreaming of the rock socket walls if the sidewall of the hole is determined by the Engineer to have either softened due to excavation methods or delays in excavation completion. Inspection of the sidewalls, sometimes using video technology, may be required.

Table 2.6 U.S. States that provide more detailed specifications for construction of rock sockets using temporary casings.

US States	References
AL, IL, IA, KS, KY, MA, MO, MS, NV, NJ, NM, WV,	ALDOT (2012), IDOT (2012), Iowa DOT (2012), KSDOT (2015), KYTC Special Note 11C (2012), MassDOT (2012), MDOT (2004), MODOT (2011), NDOT (2014), NJDOT (2007), NMDOT (2014), WVDOH (2010),

The State of Florida is the only state to have been found to recommend any increase in rock socket length due to deeper than expected temporary casing installations. Furthermore, FDOT (2014) also includes similar specifications as those states listed on Tables 2.5 and 2.6.

2.7 Construction Effects on Side Resistance of Rock Sockets – Case Studies

Casing installed into a predrilled hole may affect side resistance within the temporarily cased portion of the shaft if contaminants or debris or loosened soil are trapped behind the casing and are left between the concrete and native soil or rock. Contaminants can also become trapped if thick, heavy slurry is used and left in the annular space behind the casing. In addition, debris can fall into this annular space. Where temporary casing is installed into rock via a predrilled hole, it is likely that debris will collect in this space and a good concrete to rock bond will not be developed (FHWA, 2010).

Computing side shear resistances requires a keen knowledge of the effects of fundamental geotechnical and construction phenomenon and of the past performance of shafts in geologic formations similar to that for which the shaft is to be designed. The effects of construction on the behavior of individual shafts are still to be properly understood and quantified. Examples of these construction effects to be quantified are the installation method, lateral movements of casing during installation, borehole roughness, slump of fluid concrete, time required for excavation (stress relief), impact of the details of drilling slurry, and the effect of drilling tools and practices on development of rock smear (O'Neill, 2001).

2.7.1 Case Study: Influence of Side Walls Roughness (O'Neill, 2001)

Observations of load tests performed on drilled shafts in rock indicate that the side resistance depends upon the cohesive and frictional shear strength of the rock, the roughness of the borehole, the presence or absence of highly degraded, smeared rock at the interface, and the effects of seams and discontinuities in the rock. (O'Neill, 2001, O'Neill and Hassan, 1994, and Williams et al. 1980).

O'Neill (2001) reported a model in finite elements that simulated a typical, idealized interface in soft, cohesive rock, or intermediate geomaterial (earth material that is transitional from soil to hard rock, denoted as IGM) in which a sinusoidal roughness profile had been generated by the drilling tool. Figure 2.21 represents this typical, idealized surface. The analysis considered the elastic-plastic axisymmetric finite-element to investigate the side load-transfer mechanism of drilled shafts socketed into very hard clays/very soft rocks (Hassan and O'Neill, 1997).

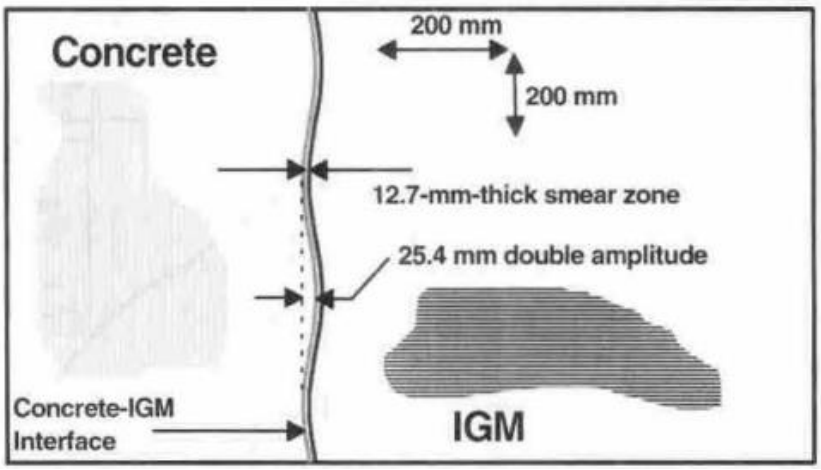

Figure 2.21 Sinusoidal roughness pattern, with potential smear zone at concrete-soft rock (IGM) interface (O'Neill, 2001, after Hassan and O'Neill, 1997).

In this model, two interface conditions were investigated: (1) no smeared IGM between the concrete and parent IGM; and (2) soft, smeared (wet, soil-like) IGM in the 12.7mm gap between the concrete and parent IGM. Four curves showing the unit side resistance (f) versus settlement for a socket 0.61 m diameter and 6.1 m long were analytically generated and presented (Figure 2.22), as well as the materials properties used on this analysis (O'Neill and Hassan, 1994, O'Neill, 2001). It is important to note that the process of constructing rock sockets with temporary casings may potentially lead to one of the three conditions: rough interface between concrete and IGM with no smeared zone, rough interface with smeared zone, and smooth surface (for instance, if the casing is extracted vertically with use of a vibratory hammer).

The calculated values of f_{max} for the unsmeared, rough sockets with the roughness profile shown on Figure 2.21 are about in proportion to the values of q_u for the parent geomaterial ("stiff" and "soft"). When the interface is smooth (no sinusoidal roughness pattern) and the geomaterial is "stiff," f_{max} is reduced to about one-third of the value for the rough interface in the stiff geomaterial. When the interface is rough, the geomaterial is stiff, and there is smeared geomaterial at the interface (as from reworked cuttings mixed with free water), the load-movement behavior is similar to that for the smooth interface in the stiff geomaterial, despite the fact that the thickness of the smear zone is only one-half that of the asperity height (O'Neill, 2001).

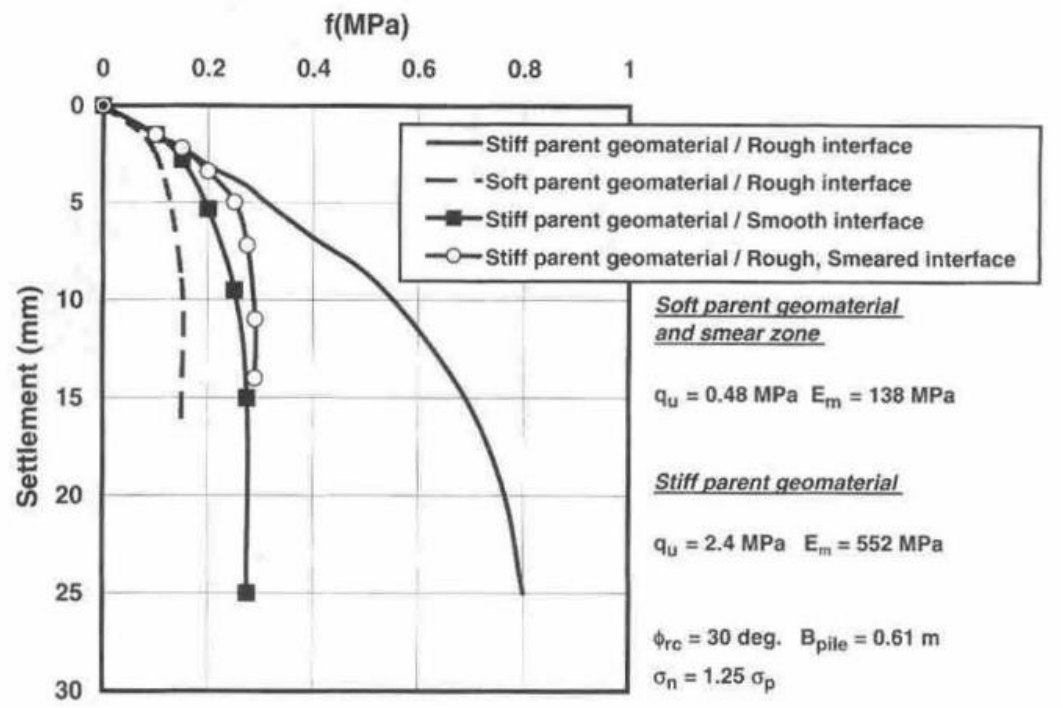

Figure 2.22 Predicted side resistance versus displacement relationships for rock sockets with different interface conditions (O'Neill and Hassan, 1994, O'Neill, 2001).

The undrained shear strength of 2.4MPa is equivalent to 350psi, which corresponds to a typical compressive strength of a Miami limestone with porosity of around 0.4, while the Young's modulus of 552MPa (80ksi) is smaller than a typical value for the Miami limestone (limestone data from Saxena, 1982).

This model indicates that interface dilation has a very strong effect on f_{max}, which, in sound, unsmeared rock, decreases dramatically as the radius of the socket increases, partially because radial strain in the rock due to dilation is inversely proportional to the socket diameter in an elastic system (O'Neill, 2001). Considering a sound, unsmeared rock with q_u of 3MPa, O'Neill (2001) reports a reduction in f_{max} from 0.72MPa to 0.30MPa when the socket diameter is increased from about 1 to 6.5ft (after Baycan 1996).

2.7.2 Case Study: Effect of Bond between Limestone Side Walls and Concrete (Law, 2002)

Two test shafts were built in downtown Jacksonville, Florida, during the construction of an office building, with the objective of investigating the changes in side resistance due to different construction procedures (Law, 2002).

The two test shafts were very similar in terms of design side shear and depths, but completely different in construction procedures. Figures 2.23 and 2.24 present, schematically, the two test

shafts. A 13ft thickness overburden layer overlaying a 16ft thickness variably cemented limestone layer, followed by a marl layer, comprised the site. The ground water table was near the surface. The drilled shaft tip was at a depth of 43ft. For design purposes, the overburden material resistance was disregarded, as well as the tip resistance in the marl. A 13 inch Osterberg cell was installed at a depth of 36ft in both shafts. The ultimate side shear was estimated to be between 4 and 20ksf for the limestone, and 5.8 to 8.0ksf for the marl (Law, 2002).

In the first test shaft, an outside surface temporary casing, with outer diameter of 42.5 inches, was installed with a vibratory hammer to the top of rock elevation, and an earth auger removed the spoil from inside this casing. Next, a 15ft long, 36.75 inch outside diameter core barrel cored the entire limestone layer at once. Using this procedure, the entire rock plug remained in the hole. Then, a telescopic casing, with outer diameter of 36 inches, was placed in the annular space excavated by the core barrel, and rotated into the marl formation. The rock plug and the marl were drilled with a rock auger, the borehole was cleaned and the concrete was poured by free fall. The temporary casings were extracted from outside to inside (Law, 2002).

In the second test shaft, the limestone was penetrated using a rock auger, which removed the inner rock from the borehole during the excavation. The temporary casings were extracted from the inside out.

The results of the load tests performed on the two test shafts (Figures 2.25 and 2.26, respectively), are significantly different. For the first test shaft, the upper portion of the shaft failed plastically when the O-cell applied load reached around 205kips. For the second test shaft, no signs of failure can be identified on the upper portion up to the maximum applied O-cell load of around 1,220kips.

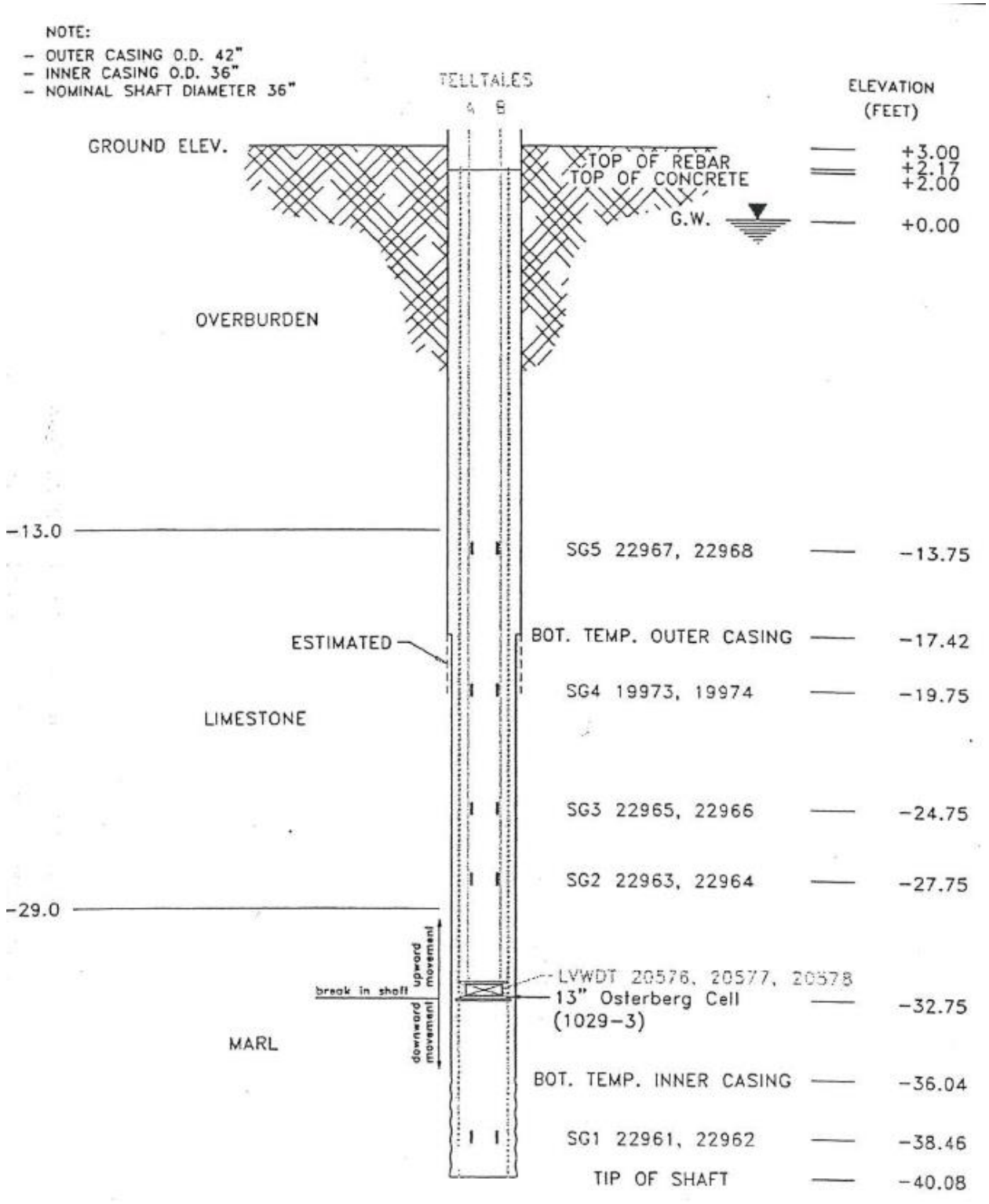

Figure 2.23 Schematic section of Test Shaft 1 (Law, 2002).

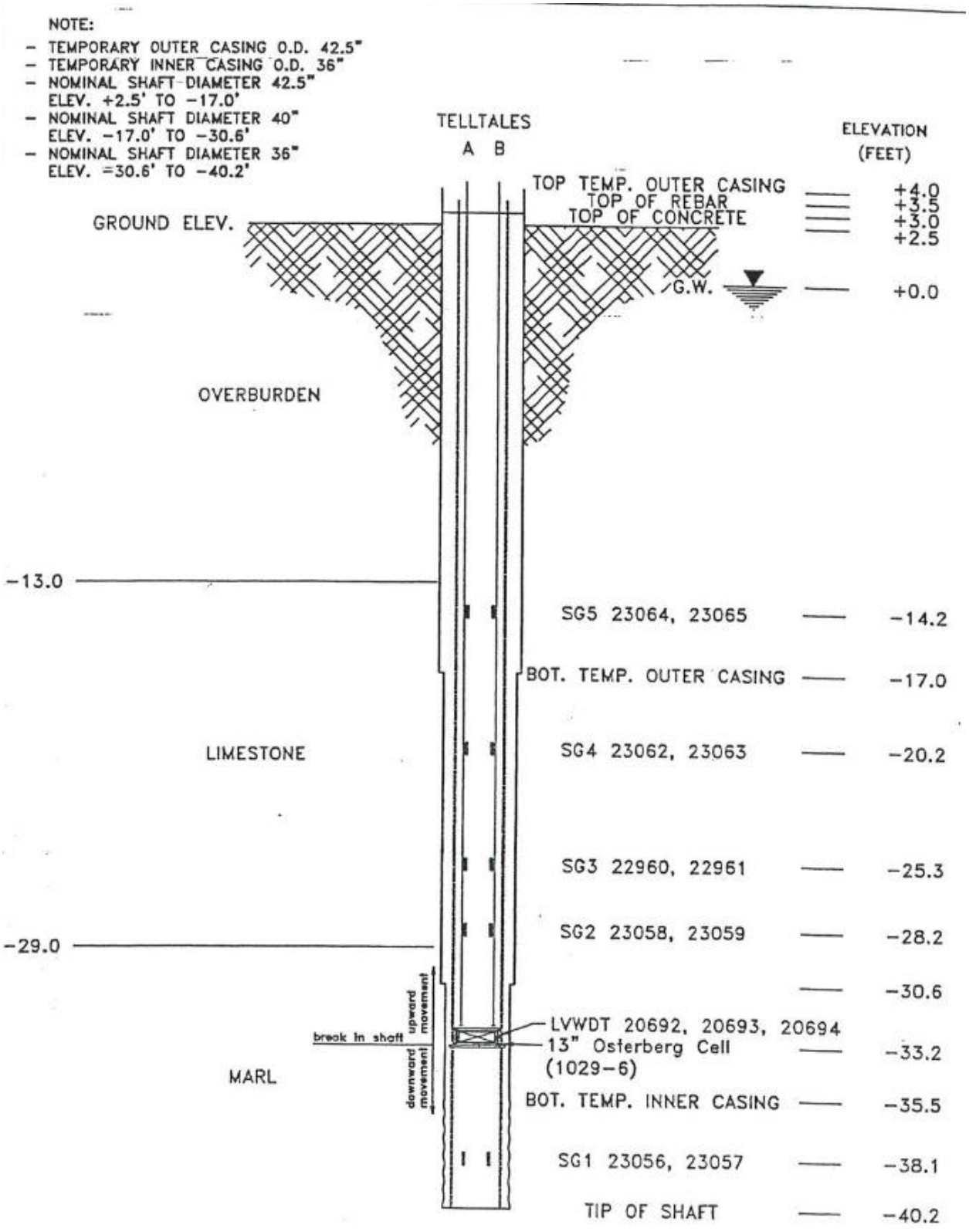

Figure 2.24 Schematic section of Test Shaft 2 (Law, 2002).

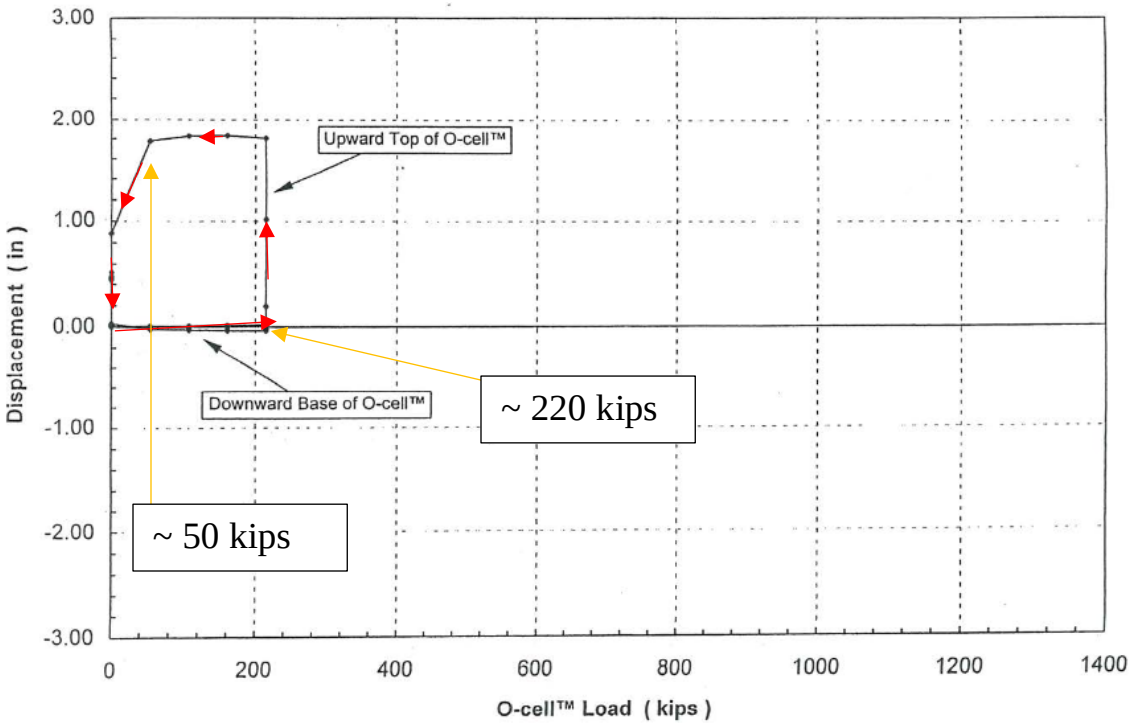

Figure 2.25 Load-displacement at top for test shaft 1. (Law, 2002)

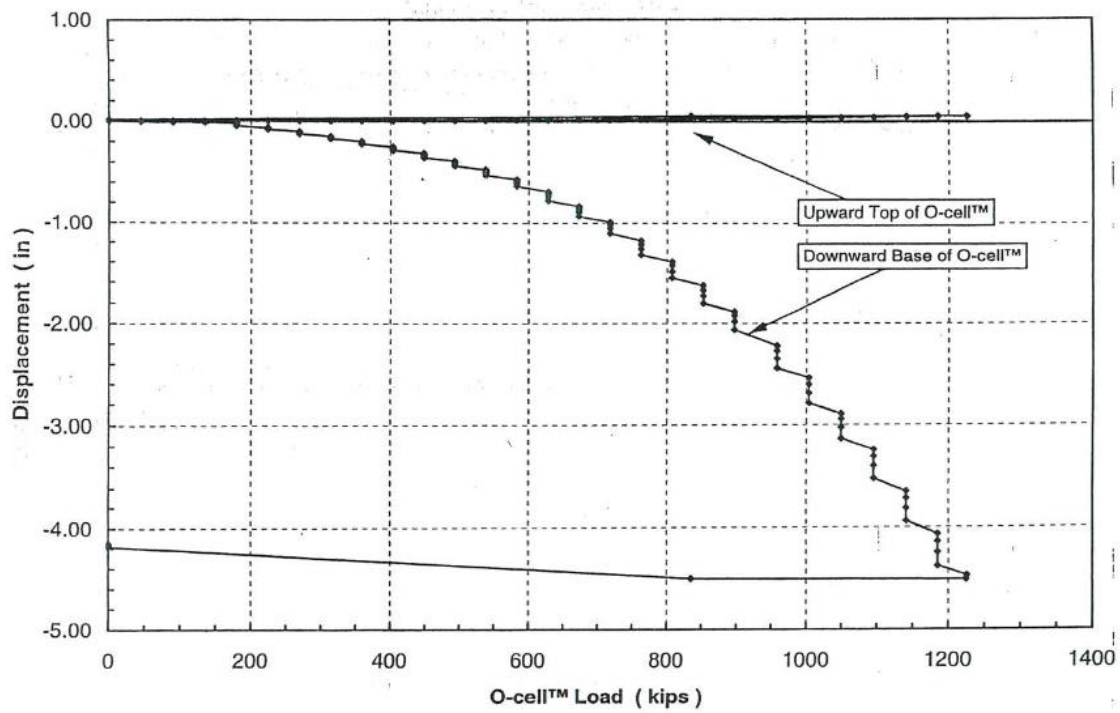

Figure 2.26 Load-displacement at top for test shaft 2 (Law, 2002).

Some of the technical factors that could have resulted in this difference may be the concrete slump by the time of the casings extraction (which means that the concrete could have already started to strengthen), the drilling methods, and the sequence of casings extraction. It is important to note that, after the failure of test shaft 1 and removal of the load, the displacement went back to zero, which means that the self-weight of the upper portion of the shaft, estimated at 45 kips, pushed it back down to its original position. Thus, there was no significant residual side resistance available in the upper portion of test shaft 1, which could be a result of a reduced zone of contact between the concrete and the excavation walls with no significant residual shear resistance, after the failure.

2.7.3 Case Study: Comparison between Temporary Casing, Bentonite and Polymer Slurries (Brown, 2002)

Brown (2002) reported research performed at the Auburn University National Geotechnical Experimentation Site, at Spring Villa, AL, in Piedmont geology comprised of silty soils formed by weathering of parent metamorphic rocks. Piedmont soils typically have high silt content, often classifying as ML-CL or ML-SM and frequently contain mica, feldspar, and other non-quartz minerals.

Ten 3 foot diameter and 36 foot deep drilled shafts were constructed, four of which using temporary casing, four using polymer slurries and two using bentonite slurry. In the cased shafts, the casing was a segmental double-walled heavy steel, with cutting teeth on the bottom, which made a hole a few millimeters larger than the outside diameter of the casing. The casing was advanced by rotating, then the soil inside was drilled out. Two of the cased ahead shafts were left opened overnight (with the casing in-place) and concrete was placed the next day. One shaft that was concreted within 1 hour (1CDef) and one that was left open overnight (24CDef) were constructed intentionally with a two soil inclusions, made using soil bags with dimensions of 2 foot height and cross sectional area between 10% and 20% of the shaft diameter. Concrete was placed by free fall into the dry holes, up to the top of excavation, then the casing was withdrawn by the rig, with a back and forth twisting motion through about 30° of rotation while pulling. (Brown, 2002).

Static axial compression load tests of all test shafts were conducted in a similar manner. The test shafts were loaded in compression by hydraulic jacking against a reaction frame, comprised of four CFA piles acting in tension, each at a radial distance of 15 foot from the test shaft. The load was applied in increments of approximately 200 to 300kN, using an electric pump to supply pressure to the jack. Each load increment was held for a period of 5min. Total testing time was generally around 1hr. An electronic data acquisition system (Megadac, from Optim Electronics) recorded data at 10 second intervals during the entire test. The measurements included load from a load cell, displacement from two linear potentiometers at the top of the test shaft, and up to 12 strain gauges within the test shaft (Brown, 2002). From the results shown in Figure 2.27, it is possible to infer that there is no significant difference between the four shafts constructed with

the temporary casing method, even if the borehole was concreted on the next day of the excavation.

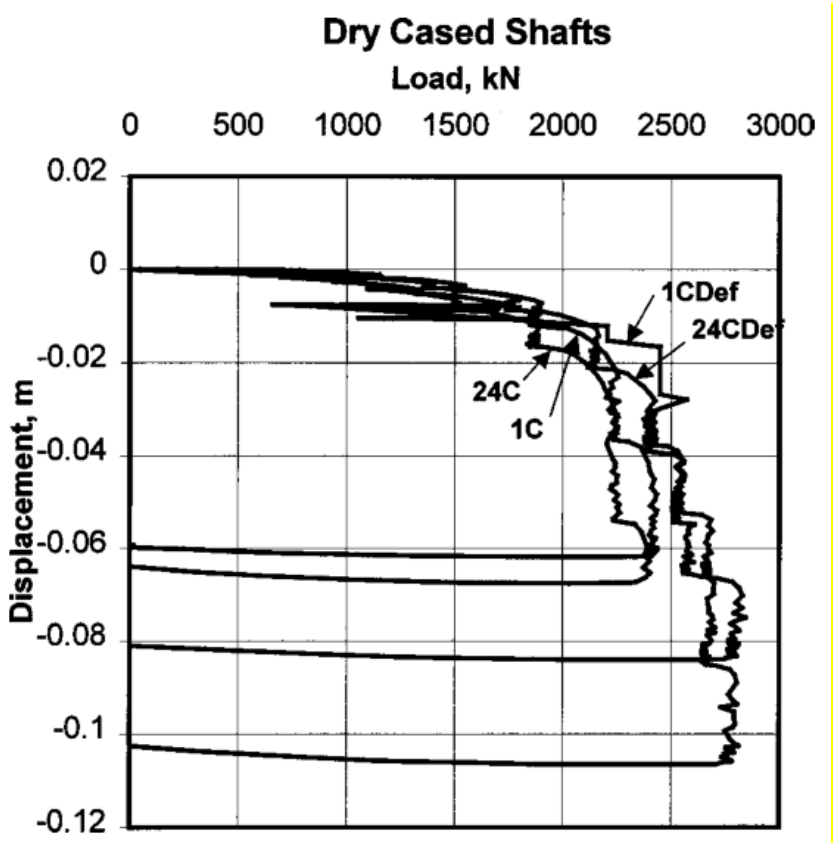

Figure 2.27 Load versus deflection results from load tests performed on the four cased shafts (Brown, 2002).

Figure 2.28 shows a comparison in the measured side shear between the cased shafts (CAD) with the other construction methods used. Among the other shafts, two were constructed with bentonite slurry, and four with polymer slurry (two with dry polymer ,DP and two with liquid polymer, LP). Also in Figure 2.28 is presented the measured side shear on the CFA reaction piles. It is possible to infer that the shafts have shown similar behavior up to 4 mm displacement (0.45% of the diameter). After that, despite the difference in side shear between the two different types of polymer used, the shafts constructed with temporary casing have shown larger displacements than the polymer-constructed shafts (100% more for 50kPa side shear), but they performed significantly better than the bentonite-constructed shafts.

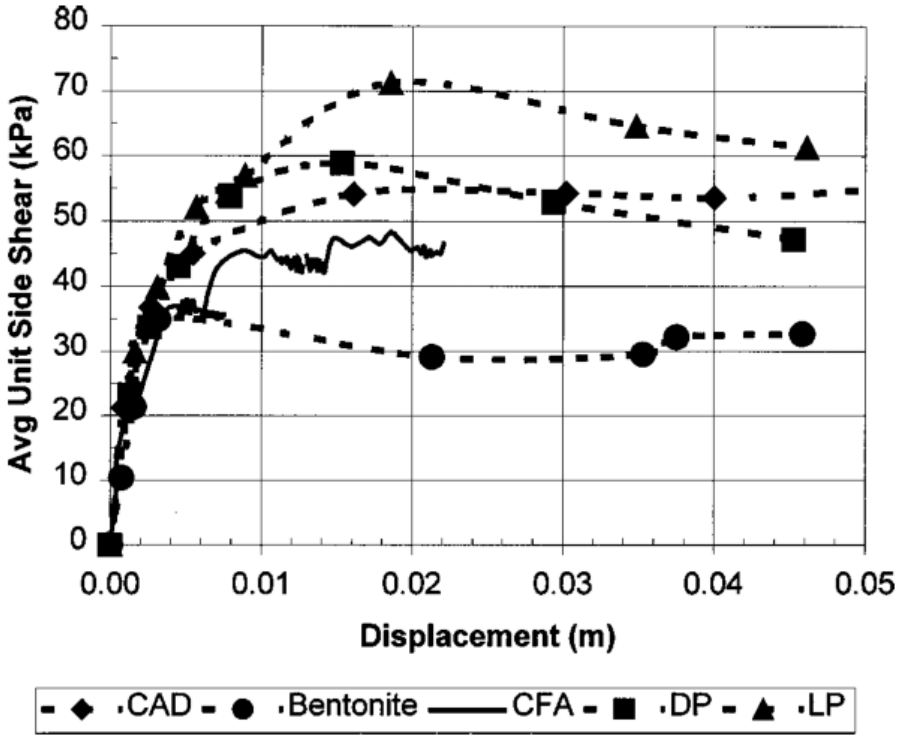

Figure 2.28 Measured side shear on the shafts constructed with different methods (Brown, 2002).

A few months after completion of testing, a backhoe was used to excavate to a depth of around 10 to 12ft on one of the temporary casing shafts. Soil disturbance and remolding was detected in the near field within about 5 to 15mm adjacent to the shaft concrete. The soil coloration and structure were sheared from the rotation and twisting of the casing during installation and extraction, leaving this remolded zone of soil at the soil/concrete interface. These results are not conclusive, but they give the insight that temporary casings, as a construction technique, do not necessarily reduce the side shear of drilled shafts in comparison with other methodologies.

2.7.4 Case Study: Comparison between Cased and Uncased Zones in the Florida's Limestone (Castelli and Fan, 2002)

Castelli and Fan (2002) presented the results of load tests conducted in two drilled shafts constructed with temporary casings into the limestone, during the replacement of the existing I-95 Fuller Warren Bridge over the St. Johns River in Jacksonville, Florida.

The bridge alignment is generally underlain by three formations, including overburden soils, limestone, and marl. The limestone was found to be porous, weakly-cemented to well-cemented (SPT N-values from less than 10 blows per foot to over 50/2 inches), having a thickness up to 20ft. The top of the limestone stratum was typically encountered at elevations -15 to -35ft, and contains interbedded seams of calcareous sand, silt, and clay, and is underlain by the marl (Hawthorne formation). Figure 2.29 illustrates the subsurface materials found on the bridge

alignment, and Table 2.7 summarizes the ranges of unconfined compression strength and SPT N values of the limestone, as well as the design side shear (Castelli and Fan, 2002) (using a factor of safety of 2). The ultimate side shear in limestone presented by Castelli and Fan (2002) was calculated based on McVay et al (1992), and also on Law (1995), using correlations between SPT N-values and the unconfined compressive strength of the limestone developed for the Fuller Warren Bridge site (Castelli and Fan, 2002).

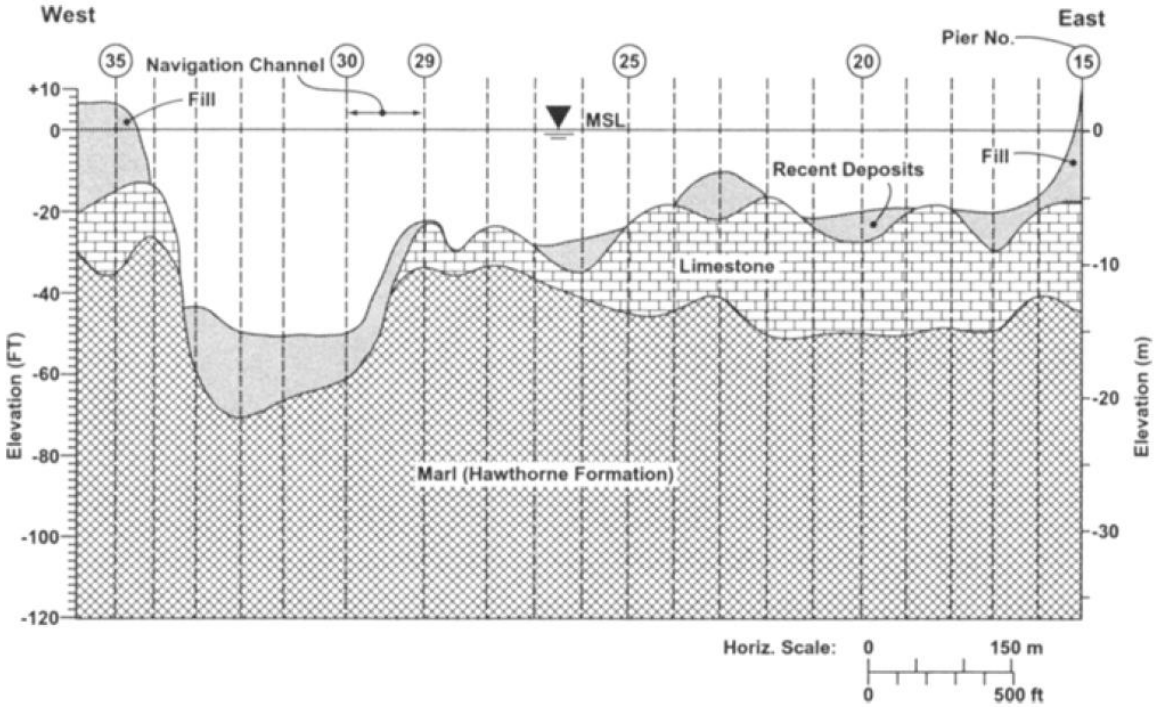

Figure 2.29 Subsurface profile at St. Johns River crossing (Castelli and Fan, 2002).

Table 2.7 Design side shear used for the limestone (Castelli and Fan, 2002).

Limestone Classification	Unconfined Compression Strength (ksf)	SPT N-Value	Design Side Shear (tsf)
Weakly Cemented	< 100	25 to 100	5
Cemented	100 to 250	100 to 50/2in	15
Well-Cemented	> 250	> 50/2in	45

For test shaft 1 (Figure 2.30), the design relied only on friction in the limestone to achieve their capacity. End bearing was not included due to the designer's concern that the larger displacements necessary to develop end bearing would be achieved only after bond failure along the sides of the shaft in the brittle limestone. The nominal shaft diameter was 36 inches. Test shaft 2 (Figure 2.31), was 48 inch diameter located on the west side of the river, where the

bearing strata consisted of an irregular thickness of limestone and the underlying marl, and was designed for end bearing and skin friction resistances (Castelli and Fan, 2002).

Both test shafts were constructed by driving a temporary casing into the limestone, and then drilling below the casing while maintaining a positive head of water to stabilize the hole. The bottom of the shaft excavation was cleaned using a submersible pump. To achieve the required O-Cell level at LT-1, a 6ft height of concrete was placed at the bottom of the hole before installing the reinforcing cage and O-Cell. Concrete was pumped through a slickline to the bottom of the O-Cell, and tremied until the concrete reached the shaft top level above the ground surface. The temporary casing was removed with a vibratory hammer immediately following completion of the concrete placement (Castelli and Fan, 2002). The results are presented in Table 2.8.

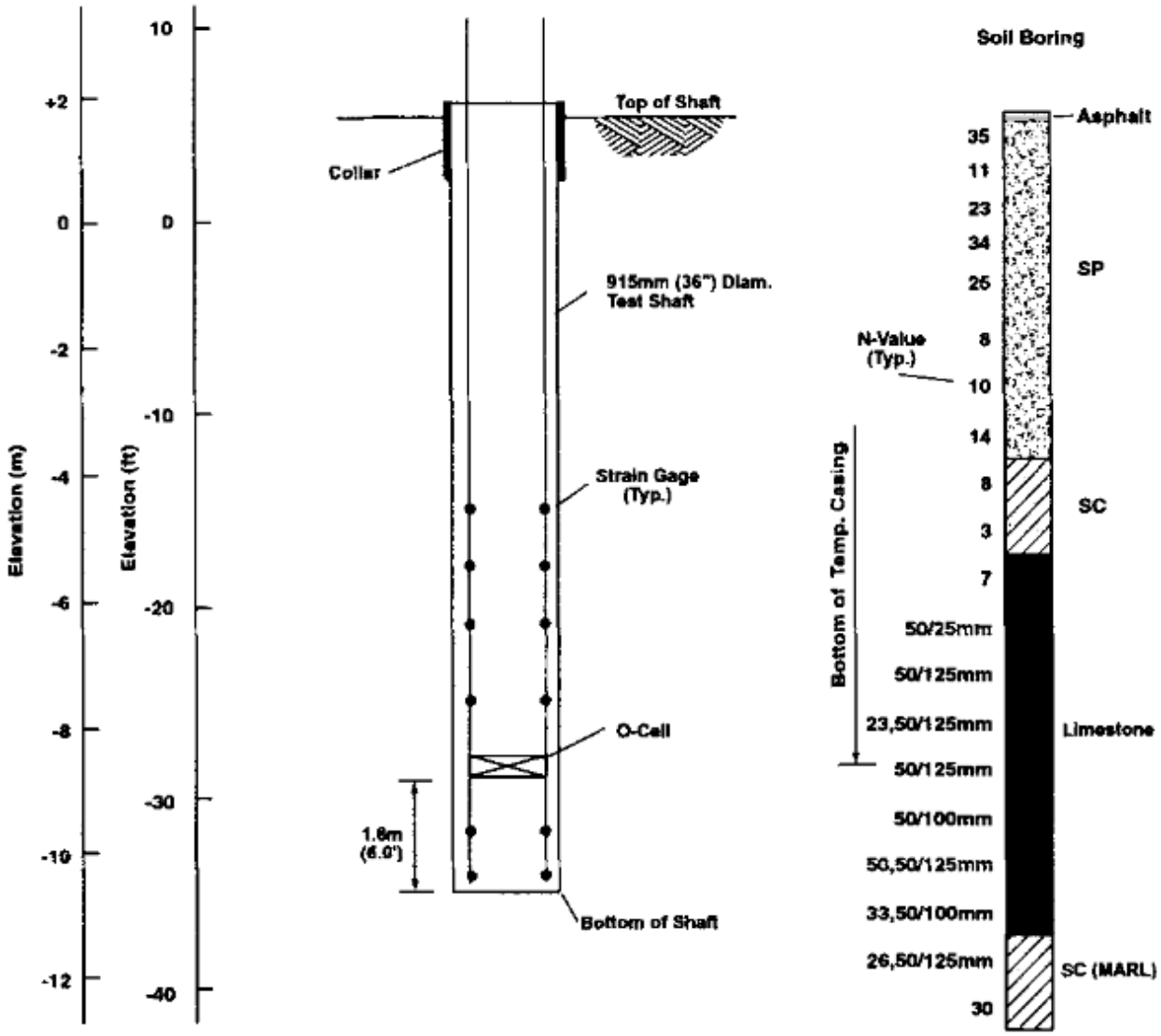

Figure 2.30 Details and Subsurface Conditions for Test Shaft 1 (Castelli and Fan, 2002).

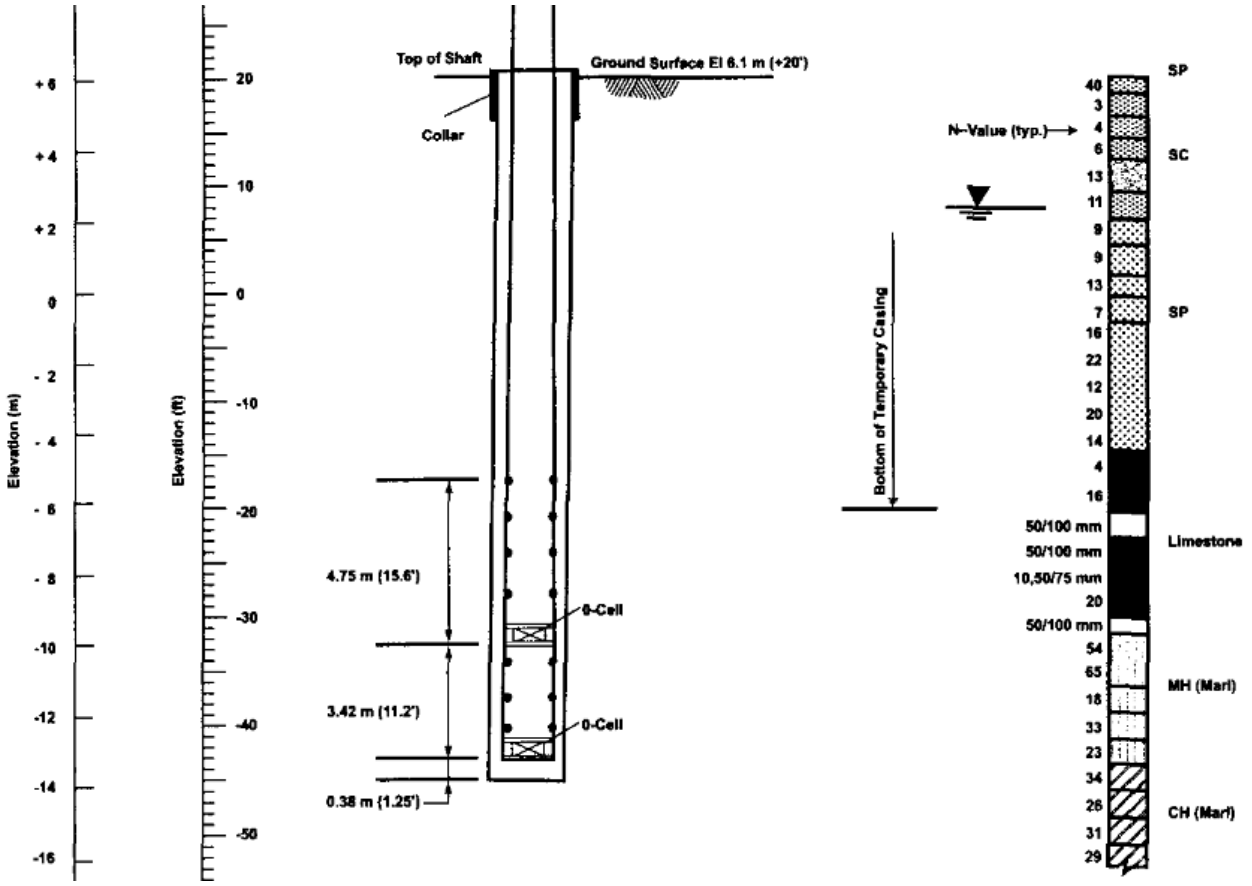

Figure 2.31 Details and Subsurface Conditions for Test Shaft 2 (Castelli and Fan, 2002).

Table 2.8 Summary of measured side friction in Limestone, from the load tests data (Castelli and Fan, 2002).

Test Shaft No	Shaft Diameter (inches)	Maximum O-cell load (tons)	Strain Gage Elevation (ft)	Limestone Classification and SPT N-Value	Mobilized Side Shear (tsf)	Upward Disp. (inches)
1	36	970	-18 to -21	Decomposed Limestone, N ≈ 7	0.5	0.94
			-21 to -25	Cemented Limestone, N ≈ 50/1in to 50/5in	8.2	
			-25 to -28		19.0	
			-29 to -34.3		5.6*	
2	48	1465	-17.7 to -21.7	Decomposed Limestone, N ≈ 16	2.1*	0.50
			-21.7 to -25.6	Cemented Limestone, N ≈ 50/3in	6.2*	
			-25.6 to -29.5	Cemented Limestone, N ≈ 50/3in	14.1*	
			-29.5 to -32.3	Weakly Cemented Limestone, N ≈ 20 to 50/4in	4.1*	

*Failure was not observed in these segments.

From Table 2.8, note that the temporary casing bottom elevation was -29ft on test shaft 1, and -20ft on test shaft 2. The mobilized side shear of the three upper monitored segments of shaft one may be assumed as the ultimate. According to (Castelli and Fan, 2002), the load test on shaft 2 did not reach failure, thus one should expect higher ultimate side shear in all of its segments.

Comparing the measured, mobilized side shear from the two test shafts presented, considering the cased and uncased portions, the limestone average SPT N-values, the shafts diameter, and the load-displacement results, it is unclear whether the temporary casing had any notable reduction on the side shear. However, it is interesting to note that the cased zones failed, and the uncased zones, did not. On the other hand, the upward movement to diameter ratio of test shaft 1 is 2.5 times this ratio of test shaft 2, and projections of how much more side resistance would develop on test shaft 2 are similarly unclear.

2.7.5 Case Study: IGM Calculated Ultimate Side Shear versus Measured using Temporary Casing (Hossain et al., 2007)

Hossain et al. (2007) presented a case study of drilled shaft load testing results conducted at the Clinical Research Center (CRC) located near the National Institutes of Health (NIH) campus in Bethesda, Maryland. The subgrade consisted of a thick layer of a residual, highly weathered, decomposed (disintegrated) rock, underlain by bedrock mainly consisting of gneiss and schist of the Wissahicken Formation within the Piedmont Physiographic Province (Figure 2.32). Disintegrated rocks were defined as residual earthen material with SPT N-values between 60 blows and 100 blows per 2 inches, and were considered to behave as an IGM.

The test shaft was constructed using telescopic casings with diameters of 48, 42, and 36 inches, withdrawn during the placement of the 5 ksi concrete placement, by the free fall method. The bottom of the drilled shaft excavation (63 foot deep into the ground) was cleaned and inspected prior to installation of the O-cell at the base of excavation. A series of strain gauges were installed in the test drilled shaft to measure the mobilized side shear during a quick load test. A schematic section of the instrumented test shaft at CRC facility project is shown in Figure 2.33 (Hossain et al., 2007). No further information regarding the construction of this drilled shaft was provided. The load-displacement curve due to the load applied by the O-cell is presented on Figure 2.34. The maximum net load applied to the base and shear section of the shaft was 368 tons. At this loading the measured downward movement was 0.48 inches, and the total upward movement was 1.98 inches, which was considered by the authors to approach the ultimate side shear capacity (Hossain et al., 2007), but it could have been a slightly higher.

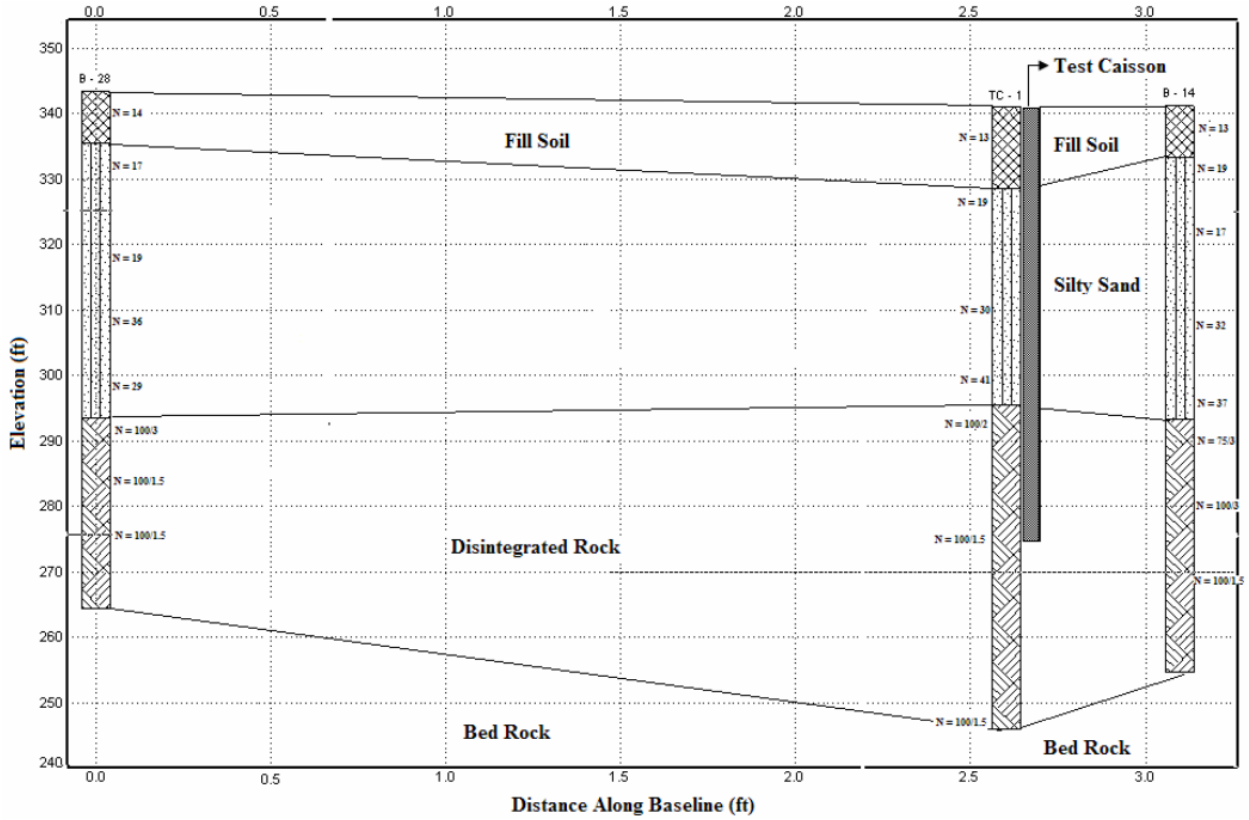

Figure 2.32 Generalized subsurface soil profile at the Clinical Research Center facility, Bethesda, Maryland Hossain et al. (2007).

The ultimate skin friction was predicted using the O'Neill and Reese (1999) method for IGM to be 541 tons. It is not certain if the use of temporary casing affected the side shear; however, the upward displacements reached 2 inches at a corresponding load of 368 tons, around 30% less than the calculated ultimate side shear for this shaft zone.

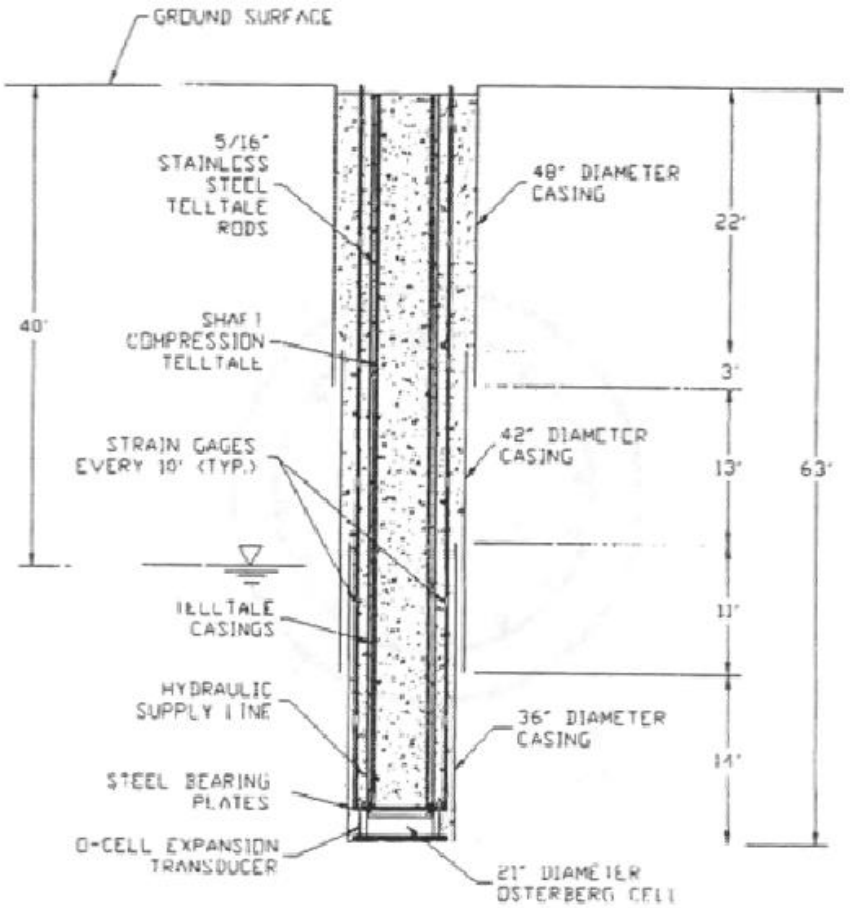

Figure 2.33 Scheme of the test shaft instrumented at CRC facility project (Hossain et al., 2007).

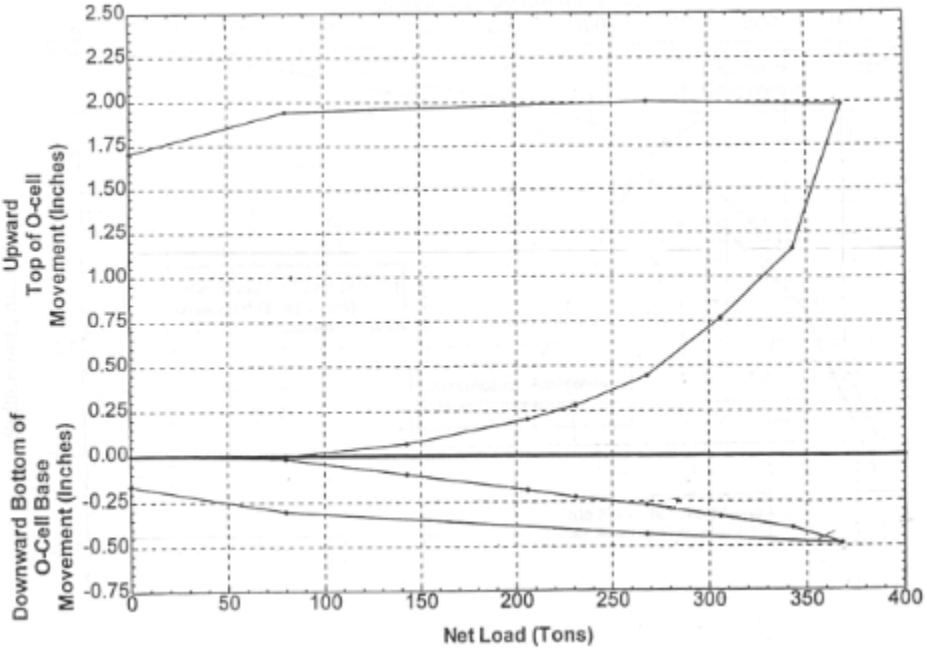

Figure 2.34 O-cell load – displacement curves from CRC facility project (Hossain et al., 2007).

2.7.6 Case Study: Effects of Stress Relaxation on Granular IGM (Seavey and Ashford, 2004)

Seavey and Ashford (2004) presented a final report to the California Department of Transportation with the objective to identify some issues that would require further research regarding how construction methods affect the axial capacity of drilled shaft, and one of the topics was construction with temporary casing. The authors cite a study presented by Reese et al. (1985), consisting of three test shafts constructed with temporary and/or permanent casing.

The subgrade consisted of a loose to firm sand/soft clay mixture for the top 20ft, soft to medium clay to 30ft, a very dense sand layer for the next 10ft, with SPT N-values around 175 (it is not clear why refusal was not noted). This dense sand layer was classified as an IGM and was underlain by a soft to medium silty clay, with an undrained cohesive strength, s_u = 0.4tsf.

The first shaft was 60ft long and 48 inch diameter, constructed with temporary casing to the depth of 52ft, and augering the soil from inside. The remaining length was excavated with slurry, but the type of slurry was not provided. As the concrete was poured, the casing was removed. This shaft was chosen to be the control shaft. The second shaft was constructed with a temporary 48 inch diameter casing that was driven to 50ft. The inner 36 inches were excavated with slurry, and a permanent 36 inch diameter casing was placed inside the first casing and the concrete poured. The third shaft used surface casing for the upper 10ft, and was excavated with the slurry method for the remaining depth with a permanent 36 inch casing placed down to 40ft (Reese et al., 1985), from Seavey and Ashford (2004).

Test shaft 1 showed the highest measured side shear among these three piles (Table 2.9). The side resistance dropped significantly when permanent casing was installed, especially on test shaft 2, where a combination of temporary and permanent casing was used in construction. In test shaft 2, upon removal of the outer temporary casing, the soil experienced a significant relaxation and possibly moved inward, indicating a void space between the pile and soil; thus, side resistance was expected to be low. The ultimate side shear was estimated between 2.1 and 2.8tsf for the IGM layer, using the procedure of O'Neill and Reese (1999), and limiting SPT-N value at 100. (Reese et al., 1985), from Seavey and Ashford (2004). From these results, it is possible to infer that constructing with temporary casing, and then extracting it, did not affect the side shear in comparison with the designed / calculated values. No information regarding how the casings were installed and extracted was presented.

Table 2.9 Calculated versus measured side shear (Reese et al., 1985), from Seavey and Ashford (2004).

	Test Shaft 1	Test Shaft 2	Test Shaft 3
Nominal Diameter (in)	48	36	36
Casing method	Temporary	Temporary + Permanent	Permanent (installed after excavation with slurry)
Calculated ultimate side shear (tsf)	2.1 to 2.8	2.1 to 2.8	2.1 to 2.8
Measured Side Shear (tsf)	2.3	0.5	1.5

2.8 Brief Introduction to Limestones

While the purpose of this research was to quantify the effects of temporary casing installation and extraction on the resulting side shear in the portions of the rock sockets used to embed and seal the casing, it seems important to present some basic geologic aspects and a summary of engineering properties of Florida limestone types. This information was used as reference for the laboratory tests setup regarding the preparation of the representative limestone samples.

According to Tucker (2003), limestones are classified as sedimentary rocks, composed of more than 50% calcium carbonate ($CaCO_3$). Dolomites, which are also reported to be found in Florida, are sedimentary rocks composed of more than 50% Magnesium calcium carbonate – $CaMg(CO_3)_2$.

Three components constitute the majority of limestones: carbonate grains, lime mud / micrite and cemented (usually calcite spar, also fibrous calcite). Bioclasts (skeletal grains, including shells, or fossils), ooids, peloids and intraclasts are the principal grains in limestones. Many limestones consist of sand-sized carbonate grains, but some limestones are more similar to mudrocks, being fine-grained and composed of lithified lime mud. Some limestones are formed by the growth of carbonate skeletons (reef limestones) or through trapping and binding of sediment by microbial mats (stromatolites and microbial laminites). In some limestones, originally aragonitic fossils and ooids have been dissolved out, creating a structure with holes (moulds), as illustrated in Figure 2.35 (Tucker 2003).

For the purposes of this study is was deemed reasonable to replicate some of the Florida limestones in laboratory by combining the aggregates (quartz sand, ooids, peloids, and other structural properties) with chemical reactions as shown below, or casting composite cemented soil. The calcium oxide, which can be purchased from construction retailers, reacts chemically with water and results in calcium hydroxide (which can also be sourced at the same stores). The produced calcium hydroxide reacts with carbon dioxide and produces the calcium carbonate.

Alternatively, cemented soils can be used to obtain samples with higher levels of resistance and with a shorter curing time. The study of these materials was extensively reviewed for possible use as a simulated limestone.

$$CaO + H_2O \rightarrow Ca(OH)_2 + heat \qquad eq.2.11$$

$$Ca(OH)_2 + CO_2 \rightarrow CaCO_3 + H_2O + heat \qquad eq.2.12$$

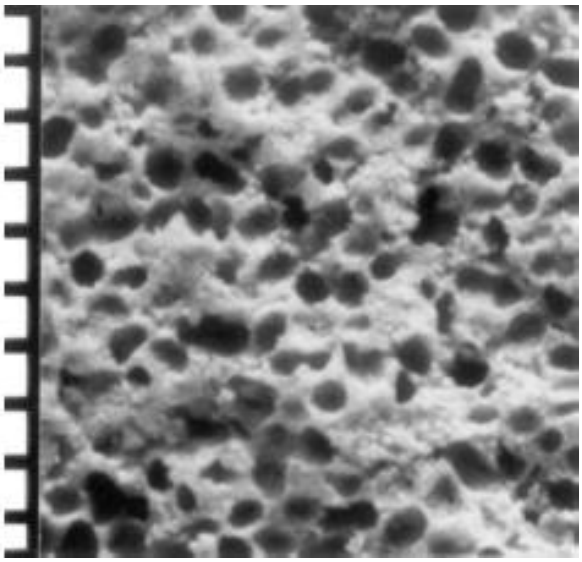

Figure 2.35 Detail of an oolitic limestone, where ooids have been dissolved out; millimetric scale, Permian, N. E., England (Tucker 2003).

2.8.1 Florida Limestones

Scott (2001) noted, in some locations, limestone is found at relatively shallow depths, or even exposed in the State of Florida. Figures 2.36 and 2.37 show two geological cross sections of the State of Florida. Hudyma and Hiltunen (2014) also discussed this variability.

The initial work to develop the FDOT limestone/rock socket design procedure was conducted by McVay et al. (1992). Therein, fragmentation of a concrete plug in a block of limestone during small scale pull out tests occurred, instead of slipping along the concrete-limestone interface. In order to perform an accurate core run scale assessment using the FDOT procedure, Hudyma and Hiltunen (2014) considered the importance of having at least one indirect tension specimen and one unconfined compression specimen from each run. The core run must have sufficient recovery and rock quality designation to then produce viable specimens for each test. However, recovering rock cores that are suitable for obtaining the unconfined compression and the splitting tensile strength depends again on the insitu, undisturbed limestone properties, but also on the coring method.

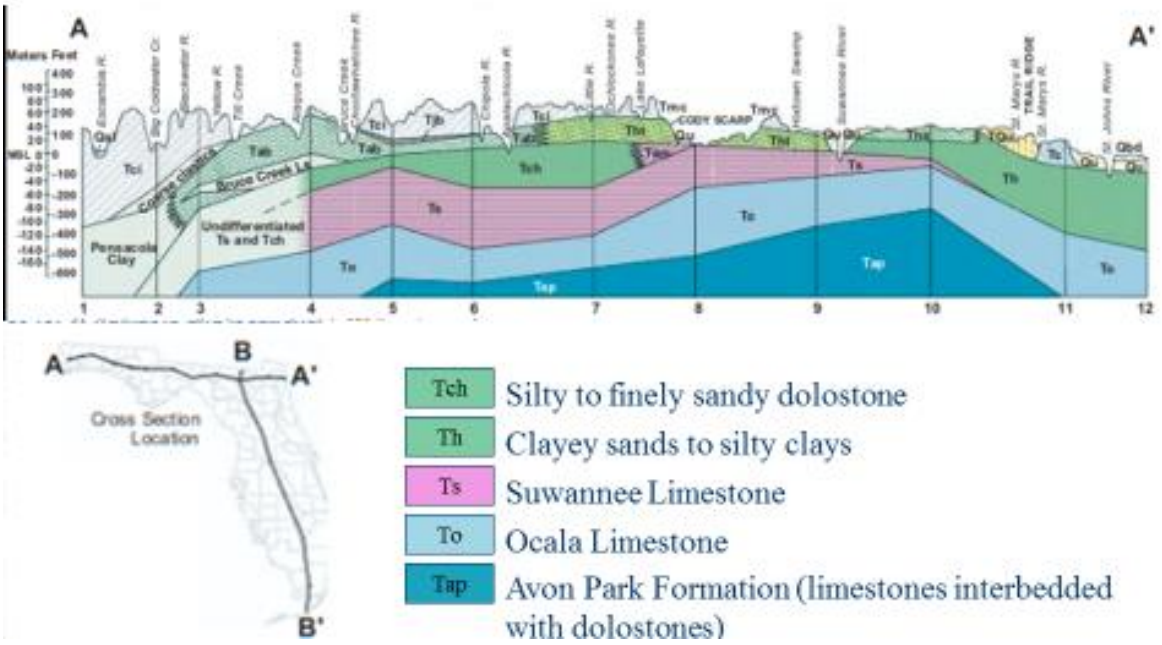

Figure 2.36 Geology of Florida, cross Section A-A' (Scott et. al, 2001).

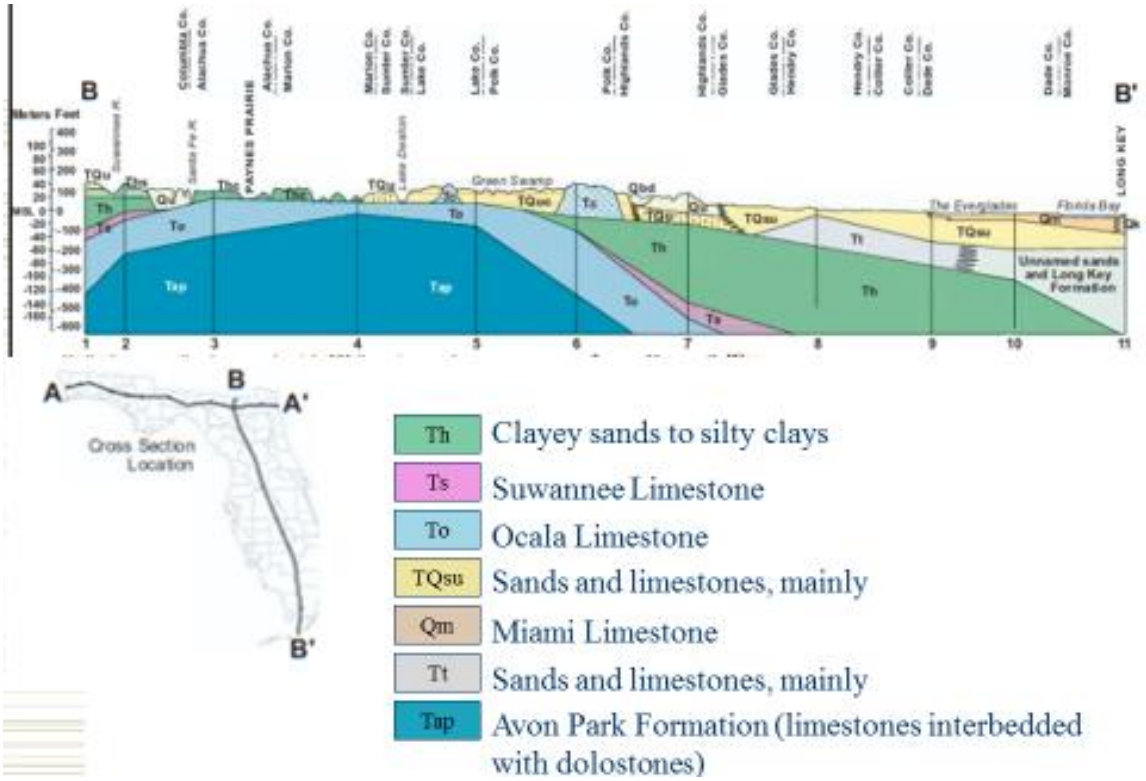

Figure 2.37 Geology of Florida, cross Section B-B' (Scott et. al, 2001).

Saxena (1982) and Prieto-Portar (1982) summarized the geotechnical properties of some of the young calcareous rocks of southern Florida, covering the Miami, Key Largo and Fort Thompson limestones down to 98ft from surface. Figures 2.38 and 2.39 present pictures of a porous oolitic

limestone (which is comparable to some samples of the Miami limestone), and a sample of the Fort Thompson limestone (Prieto-Portar 1982). It is important to note that not only the resistance properties of the limestone samples should be considered in the development of the simulated limestone for lab testing, but also its shape and structure, which can also affect the final side shear as well.

The Miami Limestone again was noted to occur at or near the surface by Scott (2001) and Saxena (1982) in southeastern peninsular Florida from Palm Beach County to Dade and Monroe Counties, and has a maximum thickness of about 39ft (Saxena 1982). It forms the Atlantic Coastal Ridge and extends beneath the Everglades where it is commonly covered by thin organic and freshwater sediments. The Miami Limestone occurs on the mainland and in the southern Florida Keys from Big Pine Key to the Marquesas Keys. From Big Pine Key to the mainland, the Miami Limestone is replaced by the Key Largo Limestone. To the north, in Palm Beach County, the Miami Limestone grades laterally northward into the Anastasia Formation (Scott 2001). For the purposes of this study, only weaker limestone formations or IGMs where a casing can be embedded were identified as useful.

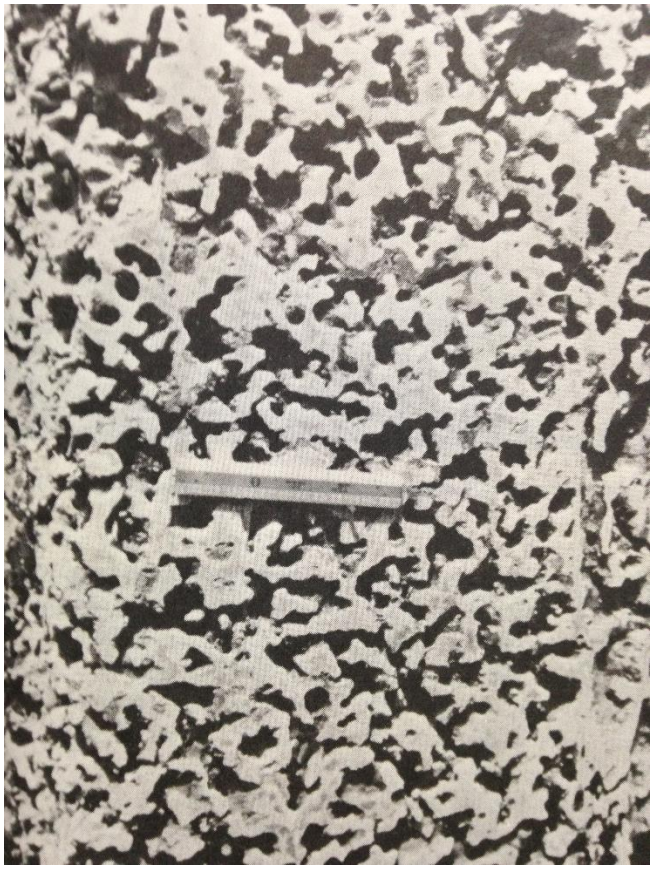

Figure 2.38 Porous oolitic limestone (Prieto-Portar 1982).

Figure 2.39 Fort Thompson limestone (Prieto-Portar 1982).

2.8.1.1 Geotechnical Properties of Southern Florida Limestone

The Miami Limestone formation was reported by GEOSOL (2014), at the Tamiami Canal Historic Swing Bridge Replacement project site, to be the upper rock formation at this site. It was described as soft to moderately hard and very porous, with SPT N-values ranging from 5 to 53 blows per foot. The statistical average was 19 blows per foot. The unconfined compressive strength was admitted as 2.5tsf, and the total unit weight was 115pcf, based on the SPT results (GEOSOL 2014).

Saxena (1982) presented a collection of calcareous rock engineering properties in southern Florida, close to Miami FL, at depths up to 98ft. In south Miami-Dade County, the rocks encountered within this depth are part of the Miami limestone, usually followed by the Key Largo limestone and Fort Thompson limestone. Figure 2.40 presents the unconfined compressive strength (UCS) results for the three limestone formations reported in Saxena (1982), and the typical UCS ranges as reported by Prieto-Portar (1982), where auger-cast foundation elements were constructed in the Metropolitan Dade County's Rapid Rail Transit System project. It is clear that there is a relationship between UCS and porosity.

Frizzi and Meyer (2000) presented ranges of limestone unconfined compression strength in Miami-Dade County, Florida, collected during the subsurface investigations for the Metropolitan Dade County's Rapid Rail Transit System (Prieto-Portar 1982). The types of tests and its results were not provided by both Frizzi and Meyer (2000) and Prieto-Portar (1982). Information about the Key Largo limestone was not provided as well. These ranges were considered the typical UCS values along the zones where auger-cast piles and footings were typically constructed in Miami-Dade County. Frizzi and Meyer (2000) suggested that the UCS in the Miami limestone ranged from 90psi to 265psi, and in the Fort Thompson limestone, from 395psi to 615psi in this zone, based on the work of Prieto-Portar (1982). These ranges seem to be in agreement with the values reported by Saxena (1982) for the Miami and Fort Thompson limestone, as represented in Figure 2.40. This also seems to be in agreement with the typical unconfined compressive

strengths where temporary casings are successfully used in drilled shaft construction socketed into Florida limestone.

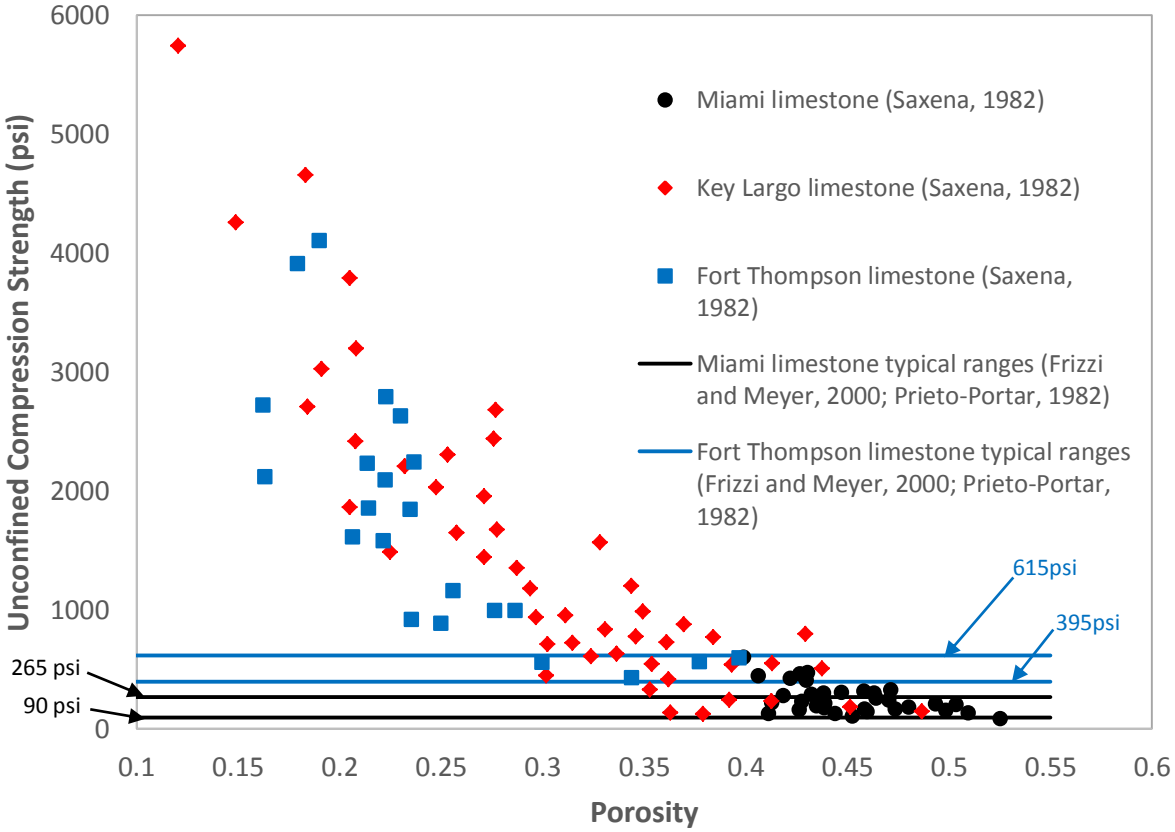

Figure 2.40 UCS vs porosity of southern Florida limestone (data from Saxena 1982; Frizzi and Meyer 2000).

It is clear that the Miami limestone, which is closer to the surface, or even exposed, has a higher porosity, with a slight trend to be more compact at increasing depths. The Key Largo and Fort Thompson limestone formations exhibited highly variable compressive strengths. The relationship between the UCS and dry density was not available in Saxena (1982); instead, data relating the elastic modulus with the dry density is presented (Figure 2.41). The dry density exhibits an inverse relationship with the porosity, and it might be said that, in general, the elastic modulus has a direct relationship with the UCS. Therefore, it would be expected that higher dry densities show a trend of increasing the UCS. This same trend was verified by trial mixes targeting the development of simulated limestones for lab scale testing (discussed in Chapter 3).

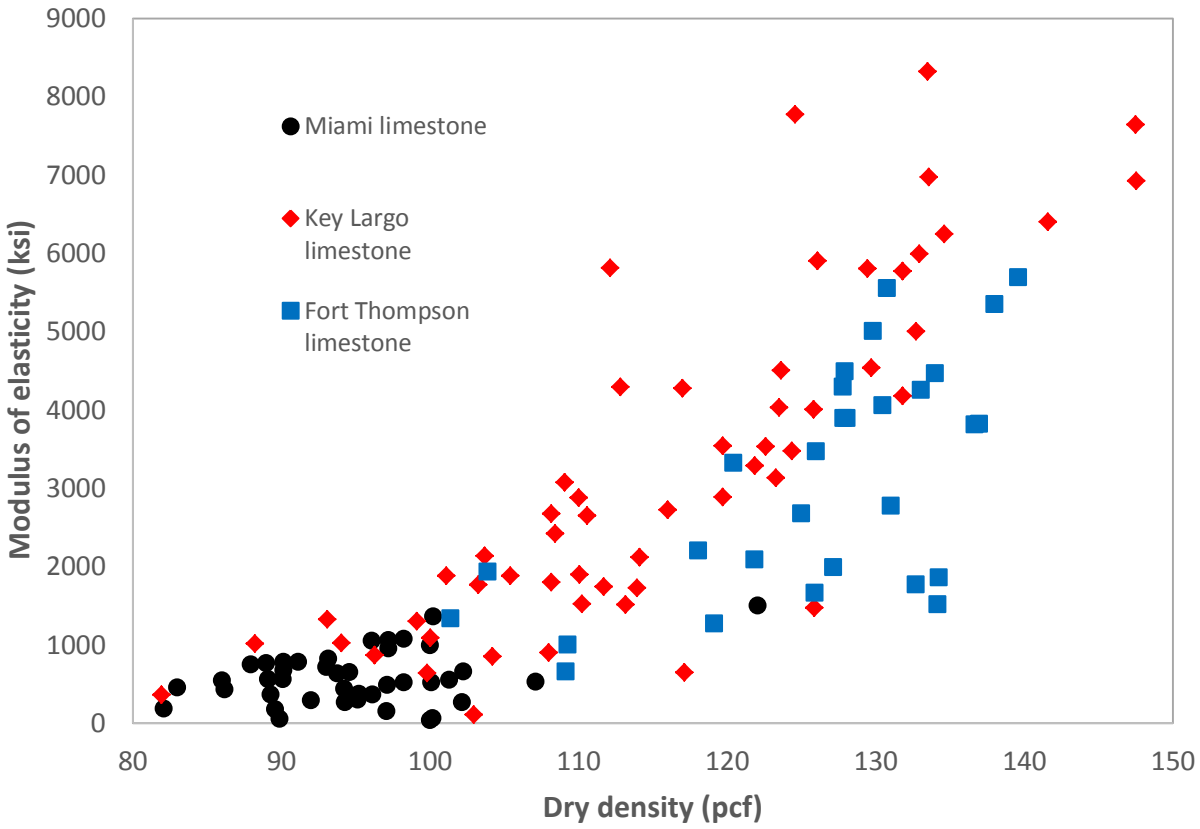

Figure 2.41 Elastic modulus vs dry density of southern Florida limestone (data from Saxena 1982).

It is also notable that the relationship between dry density and elastic modulus (or, indirectly, to unconfined compression strength) is highly variable. Consequently, it would be inaccurate to assume that deeper limestone is stronger, especially when comparing data from the Key Largo and Fort Thompson limestone formations. This is also supported by Figures 2.40 and 2.41.

Kulhawy (1986) presented a summary of several correlations for estimating the soil properties as related to foundation engineering. Relationships between the SPT-N and the unconfined compression strength for cohesive soils, proposed by Terzaghi and Peck (1967) and Djoenaidi (1985), are presented in Table 2.10 and Figure 2.42, respectively. These studies are in agreement with the overall trend of increasing UCS values with SPT-N blow counts.

Table 2.10 Variation of UCS with SPT-N (Terzaghi and Peck 1967).

SPT-N	0-2	2-4	4-8	8-15	15-30	>30
S_u (psi)	< 1.74	1.74 – 3.47	3.47 – 6.95	6.95 – 13.9	13.9 – 27.8	> 27.8

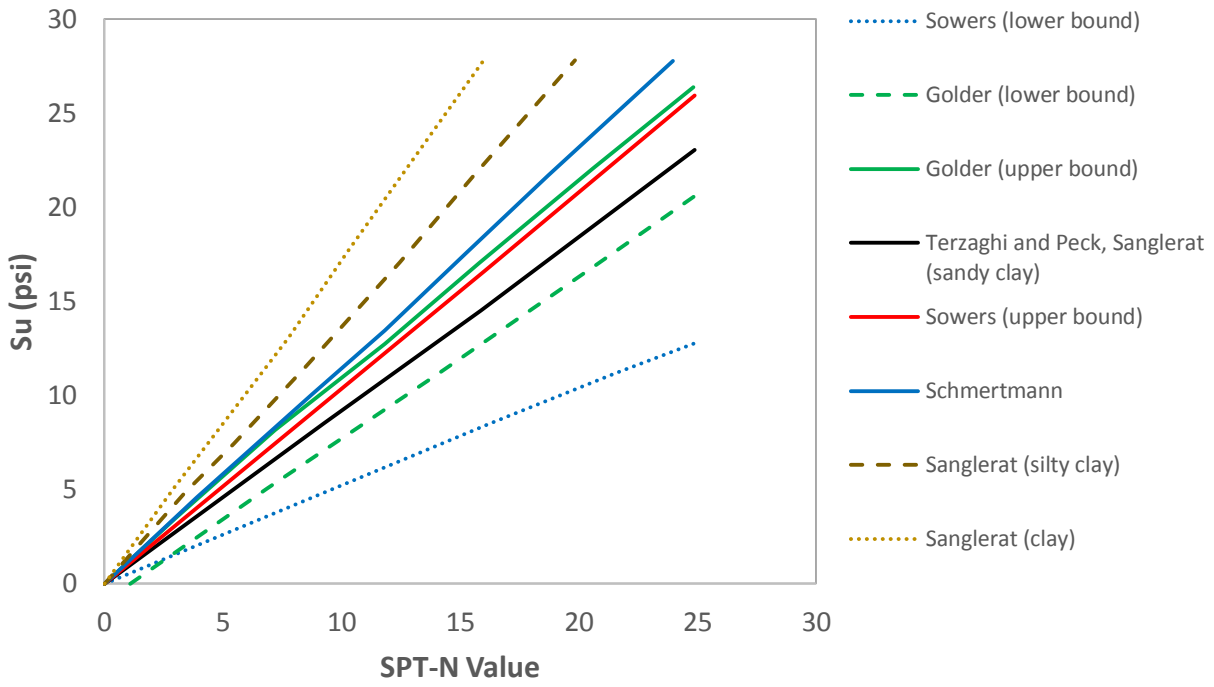

Figure 2.42 Relationships between SPT-N and Su (data from Djoenaidi 1985).

Based on the work proposed by Terzaghi and Peck (1967), as shown in Table 2.10 and Figure 2.42, Kulhawy (1986) suggested that using equation 2.12 would provide a convenient approximation:

$$Su \approx 0.87N \quad (psi) \qquad eqn\ 2.12$$

Where N is the SPT blow counts. Based on equation 2.12, Table 2.11 presents values of SPT-N versus unconfined compression strengths extrapolated beyond that cited by Djoenaidi (1985).

Table 2.11 Extrapolated values of SPT-N vs Su (psi) (Djoenaidi 1985; Kulhawy 1986; Schmertmann 1975).

SPT-N	30	50	50/10in	50/7in	50/5in	50/2in	50/1in
S_u 0.87N	26	43	52	74	104	261	522
S_u 1.06N	32	53	66	91	127	318	636

If the Schmertmann (1975) relationship (Figure 2.42) is considered, then S_u would be approximately equal to 1.06 times the SPT-N blow count (also in psi). In this case, the maximum practical S_u value would be about 636psi. No further details about the references were provided by Kulhawy (1986).

Based on the presented works and on the case studies analyzed so far, it seems that 600psi would be the practical upper limit of unconfined compression strength where casings might be routinely installed and extracted (i.e. blow counts in Table 2.11 were noted from cited limestone studies).

Kulhawy (1986) noted that the relationship proposed on equation 2.12 is highly variable and imprecise. Regardless, its purpose is to serve as a guideline for early design stages. From Figure 2.42, it seems that Terzaghi and Peck's (1967) suggested relationship (expressed by equation 2.12) could be considered the lower bound limit (using the same term as proposed by Reese and O'Neill, 1988) for sandy clays, including hard clays, in terms of unconfined compression strength. Blow counts of about 50/2in seem to be the upper limit in case histories reporting the use of temporary casing into Florida limestone formations.

Frizzi and Meyer (2000) reported typical ranges of SPT-N blow counts for the Miami and Fort Thompson limestone formations. Table 2.12 shows the ranges of SPT-N values, unconfined compression strength, and unit side shear for the two analyzed limestone formations (Miami and Fort Thompson) along with the respective ranges of depth. The S_u (i.e. UCS/2) ranges are also shown in Figure 2.40.

Table 2.12 Typical relationships in Miami and Fort Thompson Limestone (Frizzi and Meyer 2000).

Limestone Formation	Typical Depths (ft)	SPT-N Typical Ranges	S_u Typical Ranges (psi)	f_s Typical Ranges (ksf)
Miami	0 to 25	15 to 30	90 to 265	2.7 to 12
Fort Thompson	10 to >100	>50	395 to 615	12 to 25

Frizzi and Meyer (2000) also reported that auger-cast pile penetration into very hard zones was limited to between 5ft and 10ft, although these zones were not defined from a geotechnical / practical standpoint. One might infer that the harder limestones to which Frizzi and Meyer (2000) referred are those with SPT-N blow counts above 50 (per foot), but casings were shown to be installed in rock socket construction through materials with SPT-N of up to 50 per 2in (considering case studies in Florida limestone). Based on this type of information, the initial proposed ranges of unconfined compression strength for the simulated limestone beds (Chapter 3) targeted UCS values from about 70psi to 600psi. This range matched those cases presented by Frizzi and Meyer and others.

The FDOT / McVay et al. (1992) design method for rock sockets into Florida limestone (FDOT 2015) was supported by 14 case studies, located in 5 different regions of the state of Florida (1 in the Florida Keys, 4 in bigger Miami, 4 in Tampa Bay, 1 in Gainesville, and 4 in Jacksonville). The use of casings (permanent or temporary) was not considered in the basis of this design method, therefore construction effects were not incorporated.

A total of 1,404 unconfined compression tests, 922 splitting tensile tests and 60 load tests (7 under compression and 53 pull-out tests) comprised the database for this method which are summarized in Table 2.13.

Table 2.13 Table 3.4. Lab and field tests setup (data from McVay et al. 1992).

Site in FL	# of UCS tests	# of splitting tensile tests	Load test orientation and scale			
			Orientation		Scale	
			Compression	Pull-out	Small	Full
Florida Keys	45	0	0	37	37	0
Metro Dade	200	200	0	2	2	0
	1,100	700	0	5	5	0
Miami	4	0	0	3	3	0
Ft. Lauderdale	3	6	0	3	3	0
Clearwater	5	5	0	1	1	0
	5	4	0	1	1	0
Tampa	2	4	1	0	0	1
	5	0	1	0	0	1
Gainesville	4	3	0	1	1	0
Jacksonville	3	0	1	0	NR	NR
	13	0	1	0	NR	NR
	10	0	1	0	NR	NR
	5	0	2	0	NR	NR

*NR = not reported in McVay et al. (1992).

The description of how and at what depth the load tests were performed is not clear. It is evident that the majority of the UCS tests and splitting tensile tests were performed in the Miami region. The reason for the enormous amount of laboratory tests (representing about 95% of the total) was the design and construction of the Miami Metrorail System rapid transit project in the early 1980's, as reported by Prieto-Portar (1982), mostly socketed in the Miami limestone formation.

The values of unconfined compression strengths, corresponding SPT-N values, and the limestone formations, as reported by McVay et al. (1992), are summarized in Table 2.14. No relationships with density and porosity were provided.

Table 2.14 Summary of UCS vs SPT-N Values (data from McVay et al. 1992).

Site in FL	UCS (psi)	SPT-N average value or range	Limestone Formation
Florida Keys	1,027	Not available	Key Largo
Metro Dade	541	50 to 123	Miami
	375	NR	NR
Miami	736	NR	Fort Thompson
Ft. Lauderdale	161	25	Miami
Clearwater	1,416	50/2in	Tampa

	1,166	50/4in	Tampa
Tampa	333	60	Tampa
	659	50/5in	NR
Gainesville	382	38	Hawthorne
Jacksonville	972	30 to 80	NR
	639	130/6in	NR
	250	30	NR
	521	108	NR

NR = not reported in McVay et al. (1992).

It seems that temporary casings are not usually installed through thick layers of limestone with SPT-N blow counts of 50 or higher, but isolated lenses of up to 50/2in have been reported; this type of variability is the exact type of circumstances that plague unpredictable casing installation lengths/depths. These results again suggest the upper unconfined strength limit to be between 300psi and 600psi.

Sarno et al. (2010) cited the relevance of the limestone surface texture for engineering purposes. Figure 2.43 illustrates different surface textures in rock cores. This type of information is equally important in when manufacturing simulated limestone for lab scale tests.

Figure 2.43 Different limestone surface textures (Sarno et al. 2010).

Finally, piles extracted from Tampa Bay that had penetrated into the limestone were scrutinized for limestone texture. These piles originally supported the 1950s era Gandy Bridge, later deemed the Friendship Trails Bridge, which spanned from Tampa to St. Petersburg. Piles were either

pulled or cutoff at the mudline during the 2015 demolition of the bridge. As part of a separate study, pile used to assess the performance of FRP repairs were extracted and delivered to USF for examination. The piles were encrusted with the surrounding limestone that failed rather than shearing at the pile / limestone interface. This material was deemed suitable as the target strength and texture for the simulated limestone as piles could penetrate the material similar to casing installation. Figure 2.44 illustrates the texture of limestone that adhered on the sides of extracted piles from the Gandy Bridge in Tampa, as part of an on-going research program.

Figure 2.44 Figure 3.5. Limestone adhered to piles extracted from Gandy Bridge / Friendship Trail over Tampa Bay.

2.9 Chapter Summary

Many of the different construction practices for rock sockets using temporary casings may have significant effects on the shaft side shear performance and at present are not explicitly included in the latest design manuals (e.g. FHWA, 2010 or AASHTO, 2012, FDOT 2014). Recall that some of these variables include construction equipment, vibrated or oscillated casing installation, concrete slump at the time of casing extraction, etc. Side shear capacity in the Florida limestone is simply computed based on rock parameters, such as unconfined compression strength and splitting tensile strength, or correlations with SPT-N blow counts.

It seems reasonable that each type of casing installation and / or extraction, and the other applicable construction variables, can also lead to differences in side shear. Knowing how different types of construction of rock sockets using temporary casings changes the side shear is the primary goal of this research project.

Chapter Three: Small Scale Testing

3.1 Overview

A total of 29 small scale rock sockets (nominally 4.6in to 4.8in diameter and 18in long) were constructed. The sockets were excavated into different simulated limestone materials, using different casing installation and extraction procedures. Among these sockets, 11 were selected to be inspection holes (control specimens), in which the casings were extracted before concrete placement and the open excavation was cleaned out and inspected prior to concreting. The intent of the control specimens was to set a baseline for comparisons between temporarily cased and uncased construction conditions.

All sockets were pull-out tested with tension loads applied on sleeved anchor bars, which extended to a bearing plate on the bottom of the excavation, subjecting the socket concrete to compression. After extraction, the dimensions of the sockets were determined from the observable failure surface.

3.2 Simulated Limestone Material

The search for representative simulated limestone materials was a challenge involving over 200 unconfined compression test specimens prepared from 29 different mixes. All mixes were cast using varying ratios of sand, coquina shells, calcium hydroxide, cement and water. The simulated limestone mixes targeted strengths between 100psi and 600psi. Similarly, texture and porosity needed to replicate the porous structure typical of natural Florida limestone. Figure 3.1 shows side-by-side images of field (left) and the simulated limestone samples (right). Details addressing the simulated limestone development and the unconfined compressive strength test results are presented in Hagerman (2017).

Figure 3.1 Field retrieved limestone cores (left); core from simulated limestone bed and simulated limestone cylinder specimen (right).

Upon identifying a suitable simulated limestone, larger scale samples were prepared in large diameter beds. The simulated limestone beds were 42in in diameter and 23in tall, cast inside circular steel formworks, which remained in place until the subsequent pullout tests and

extractions were completed. A steel reinforcing cage consisting of 6 vertical #3 bars, 23in long and 4 - #3 stirrups 38in in diameter was installed to provide confinement during load testing and to prevent bed cracking from an adjacent test.

A 1 cubic yard mobile mixer was used for mixing the materials and dispensing into the steel formworks (Figure 3.2). When the fresh limestone reached a height of 6in inside the formwork, 6in diameter plastic disks were placed at the corresponding plan view socket positions to debond the bottom of the cored rock socket excavations without causing needless damage to the parent limestone beds (Figure 3.3). After the bed casting was completed centering rods were installed in the fresh limestone at the same position as the plastic disks to serve as drilling guides and to prevent the core barrel from walking across the surface of the simulated limestone. Cylinders of the limestone bed material were also prepared at the time of casting for unconfined compression tests and visual inspection (Figure 3.4).

Figure 3.2 Casting of simulated limestone bed.

Figure 3.3 Debonding plastic disks (left) and centering rods (right).

Figure 3.4 Preparation of cylinders from limestone bed material.

3.3 Shafts Construction

Each bed provided adequate room to cast five rock socket specimens without interfering with the adjacent specimen. Figure 3.5 illustrates the sockets layout used on the 6 simulated limestone beds. One of the beds (B3) had 4 rock sockets instead of the desired 5 because one of the holes was lost during the bed preparation. For all casing installation / construction methods, an aluminum tripod with an overhead hoist was used to support the casing installation equipment. Table 3.1 lists the different construction procedures used on the 29 rock sockets. The bed ID numbers refer to the chronological order of construction which did not correspond to any trend in UCS values.

Three different procedures for casing installation and extraction were used: driven (DR), rotated with fine cutting teeth (FT), and rotated with coarse cutting teeth (CT). Figure 3.6 shows the

casing components including extensions, coring bits, coring head, and pipe wrenches used for assembling and disassembling the casings. The control casing types for each bed were varied to provide different comparison combinations (DR-C, FT-C and CT-C, Table 4.1). Figure 3.7 shows details of the coring bits used on this research program.

A driven control was constructed on all beds along with a rotated option (except bed 3). The control specimens provided baseline capacity measurements for comparison with the temporary casing methods commonly used and similar to field practice. The construction methods are further described in this Chapter.

Figure 3.5 Rock socket construction layout on each simulated limestone bed.

Table 3.1 Types of construction used on the rock socket specimens.

Bed UCS (psi)	Bed ID Number	Construction Method				
		A	B	C	D	E
64.8	4	CT	FT	FT-C	DR	DR-C
163.4	5	CT	FT	DR	DR-C	CT-C
487.4	3	CT	FT	DR-C	DR	None
502.8	1	CT	FT	FT-C	DR	DR-C
685.6	6	CT	FT	FT-C	DR	DR-C
885.0	2	CT	FT	DR	DR-C	CT-C

Figure 3.6 Casing cutting tips, drive shoe, casing extensions and drill rod couplers.

Figure 3.7 Fine-tooth (left), coarse-tooth (center) and driving shoe (right).

3.3.1 Rock Socket Excavation

The rock socket specimens were constructed between 7 and 21 days after the beds were cast. Before starting the excavation, the gap between the top of the simulated limestone and the formwork edges (1in to 2in) was flooded with water (Figure 3.8). All excavation and concreting was performed via the wet method, simulating common field conditions. All inspected, control excavations were flooded again before concrete casting.

Figure 3.8 Top of simulated limestone beds flooded with water and being pre-cored.

The driven casing specimens (both temporary casing and control) were cast and removed first in all beds. The purpose was to prevent disturbances caused by vibration and consequent consolidation of other sockets in the same bed. Rotated temporary specimens were cast next, and finally, the control sockets with no casing were cast.

3.3.1.1 Driven Casing Sockets

A pilot hole was cored prior to driven casing installation to prevent excessive stress development and global cracking of the beds. A coring machine was positioned on the corresponding socket positions and a 16in long, 4in diameter, coring bit was attached (Figure 3.9). The resulting pilot holes were smaller than the driving shoe outer diameter (4.6in) thereby producing the desired crumbled / pulverized material outside the driven casing.

A standard SPT safety hammer, attached to a rope, overhead pulley system and cathead motor was used to drive and extract the casing. The fragments that remained inside the installed casings

were flushed out with the use of an air vacuum (Figure 3.10) before concrete placement or casing extraction (temporary driven casing or driven control specimens, respectively).

A cathead motor was used to lift the hammer and provide just enough drop energy to advance the casing. Increasing drop heights were required as the embedment depth increased (Figure 3.9). For extraction, the same setup was used, but the blows were applied upward with smaller strokes to avoid damaging the just-cast specimen and the bed.

Figure 3.9 Pre-drilling (left) and driving the casing (right).

Figure 3.10 Airlift vacuum used to clean up fragments from inside the installed casings.

3.3.1.2 Coarse-Tooth and Fine-Tooth Rotated Casing Sockets

The construction procedure for the rotated fine and coarse-tooth casings was the same. The assembled coring bit with the 2ft extension attached to the coring head were lifted and positioned with support of the overhead hoist. The coring assembly was attached to a gas-powered rotary reduction gear box and continuously flushed with water to prevent the cutting from binding the casing. After the casing reached the desired depth, an internal carbide-tipped drill bit was used to break up material that could not be extracted as a core (Figure 3.11). This procedure was eventually necessary on the driven casing specimens as well, whenever the pre-coring procedure was not able to remove the core to the desired full depth of the rock socket.

The vertical alignment was checked before and during coring. After concrete placement, the casings were extracted by slowly rotating it with 2 pipe wrenches while applying upward force small enough to keep the casings coming up without causing damages to the beds and the shafts.

Figure 3.11 Rotatory casing installation (left) and drill bit (right).

During the installation of the rotated casings, part of the crumbled material that would normally form outside the casing was flushed out from the annulus space between the outside of the casings and the intact bed material. This normally would not occur in field applications where circulation is not used during rotated casing installation. The material flushed out of the annulus was reintroduced before concreting and subsequent casing extraction to more closely simulate the debris left in the annulus during field operations (Figure 3.12).

3.3.1.3 Control Specimens

Two rock sockets on each bed were selected to be control specimens (except on bed 3, which had only 1 control). These holes were flushed out before and after casing extraction, removing all remaining smeared and crushed rock fragments, and drained for inspection. On the majority of these inspection holes, high-resolution pictures were taken using a Model DSC1600A (from General Tools & Instruments, LLC) and the excavated diameter was measured (Figure 3.13). The obtained high-resolution pictures are presented in Hagerman (2017).

Figure 3.12 Cuttings replacement on the outer perimeter of the casings.

Figure 3.13 Example of high-resolution pictures taken on the control holes.

The rotated controls were extracted the same way as the temporary rotated specimens, but before concreting. The driven control casing also was extracted using the same method as on the driven temporary sockets, also before concreting. So, all control excavations were completed and inspected prior to commencing any excavation operations with temporary casing.

3.3.2 Concrete Placement

The shaft concrete was actually mortar mixed in a 1 ft^3 mixer and designed to have a compressive strength of 10ksi. In order to achieve this strength and keep the fresh concrete with slump near 10in, a superplasticizer additive was introduced after mixing the cement with sand

and water (w/c ratio = 0.34). Details about mix design and compressive strength are presented in Hagerman (2017).

A 3in diameter tremie pipe with a hopper attached at the top, capped at the tip, was pushed to the bottom of the sockets. The hopper was large enough such that it could hold all shaft mix volume necessary to cast the entire shaft. The fresh concrete (mortar) was poured from the mixer into 5 gallon buckets and poured in the hopper (Figure 3.14). Next, the tremie was slowly raised to expel/displace water in the excavation leaving the fresh concrete in the holes. No drilling slurry was used.

A 1in diameter anchor rod was either inserted inside the tremie and concreted into place or inserted after concreting while the mortar was still fluid. A circular 1/2in thick base plate was bolted to the bottom of the rod which had a diameter of either 2.5in (when inside tremie, Figure 3.15) or 4in (when inserted last). The change was required when stronger beds developed higher than anticipated pullout forces. The tension force in the rod acted at the base of the rock socket which would cause only compression stress in the concrete during the pullout (actually push up) tests.

A debonding plastic sleeve, 8in long and adjustable to the socket diameter, was inserted at the top of the fresh concrete to prevent undesired side shear to develop too close to the surface, that could damage other sockets nearby (Figure 3.16). Figure 3.17 shows several beds cast and ready for load testing.

Figure 3.14 Filling tremie and hopper while casting rock sockets.

Figure 3.15 Anchor rod placed in tremie before concreting.

Figure 3.16 Debonding plastic sleeves on top 8in of the sockets.

Figure 3.17 Rock socket specimens after concreting (left), ready for load testing (right).

3.4 Pull-Out Load Tests

The pullout tests were performed 7 days after concreting of the shafts, on all beds. Cylinders made from the corresponding simulated limestone materials and the shaft concrete were broken the same day of the pullout tests to provide the shaft and bed UCS strength. The reaction system was setup directly on the surface of the simulated limestone beds using steel blocks with dimensions of 6in x 3in x 3in, preventing stress concentration and its undesired affects. These blocks were placed just outside of the concreted shaft area to prevent unquantifiable influences on the results.

A 1in steel plate with a 1.25in diameter hole on the center was carefully placed on the steel blocks. The all thread steel bars passed through the hole and extended to a height tall enough to permit installing a load cell and hydraulic jack. Pieces of lead shims were placed as necessary to keep the steel blocks leveled on the bed surface, preventing misalignment during the pullout tests. Figure 3.18 shows load testing in progress.

Figure 3.18 Pull-out load test in progress.

Depending on the expected load carrying capacity of the sockets, the pullout load was applied by either a 30ton or a 60ton capacity jack. A manually operated pump provided the hydraulic pressure, and the load readings were monitored by load cells with capacities of 30 or 50ton, installed just above the jack. A 1.5in stroke displacement transducer was used to track displacement and all data was recorded by a MEGADAC data acquisition system.

After all specimens in a given bed were pulled upward 1.5 in, each specimen was fully extracted and its bonded zone was measured to compute shear stress that developed on the observable failure surface. Figure 3.19 shows examples of the fully removed rock socket samples. Table 3.2 shows the shaft bonded dimensions considered in the side shear calculations, which effectively contributed to the load-carrying capacity. Complete details about the testing procedures, equipment and extracted shafts can be found in Hagerman (2017) and Caliari de Lima et al. (2017).

Figure 3.19 Extracted sockets from bed 5 (left), bed 1 (center) and bed 4 (right).

3.5 Test Results

The load versus displacement data from each pull out test was plotted by bed ID denoted by the UCS strength (Figure 3.20). The graphs are arranged by increasing UCS strength (top left to bottom right). Tables 3.3 and 3.4 list the maximum load and corresponding displacement, respectively, for each pullout test.

Table 3.2 Measured dimensions of the extracted sockets.

Bed UCS (psi) and ID Number	Socket Construction Method	Socket ID	Bonded Diameter (in)	Bonded Length (in)	Bonded Surface Area (ft^2)
64.8 (B4)	DR	D	5.06	14.06	1.55
	CT	A	6.11	16.00	2.13
	FT	B	6.31	14.88	2.05
	DR-C	E	5.85	16.00	2.04
	FT-C	C	5.92	15.63	2.02
163.4 (B5)	DR	C	4.83	9.62	1.01
	CT	A	5.19	16.34	1.85
	FT	B	5.16	8.46	0.95
	DR-C	D	5.14	9.17	1.03
	CT-C	E	5.75	9.14	1.15
487.4 (B3)	DR	D	4.73	11.70	1.21
	CT	A	4.89	12.80	1.37
	FT	B	4.93	11.00	1.18
	DR-C	C	4.81	13.75	1.44
502.8 (B1)	DR	D	4.68	14.07	1.44
	CT	A	4.92	8.02	0.86
	FT	B	4.81	8.61	0.90
	DR-C	E	4.81	9.48	1.00
	FT-C	C	5.09	7.53	0.84
685.6 (B6)	DR	D	4.70	8.13	0.83
	CT	A	5.04	9.54	1.05
	FT	B	4.86	9.26	0.98
	DR-C	E	4.61	9.14	0.92
	FT-C	C	4.89	9.18	0.98
885.0 (B2)	DR	C	4.64	9.56	0.97
	CT	A	4.93	8.25	0.89
	FT	B	4.80	8.69	0.91
	DR-C	D	4.73	9.13	0.94
	CT-C	E	4.93	8.03	0.86

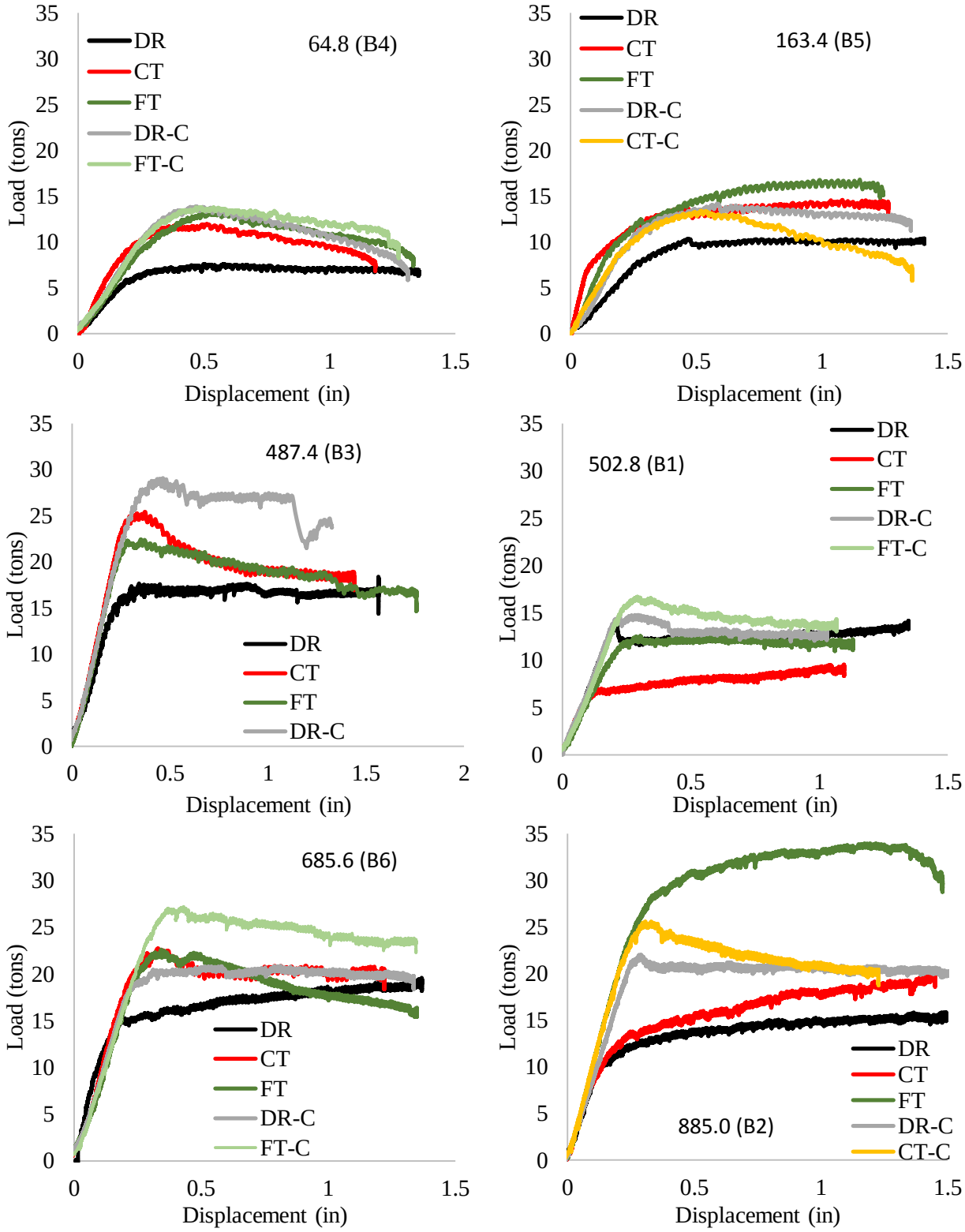

Figure 3.20 Load vs displacement for all sockets.

Table 3.3 Maximum load for all sockets.

Bed UCS (psi)	Bed ID	Peak Load (tons)					
		DR	CT	FT	DR-C	CT-C	FT-C
64.8	B4	7.49	11.70	13.15	13.62	-	13.79
163.4	B5	10.30	13.74	15.23	14.00	13.28	-
487.4	B3	16.16	25.40	21.91	28.57	-	-
502.8	B1	13.53	6.94	12.43	14.55	-	16.51
685.6	B6	15.11	22.38	22.47	20.34	-	26.81
885.0	B2	10.72	13.70	28.13	21.88	25.23	-

Table 3.4 Displacement at peak load for all sockets.

Bed UCS (psi)	Bed ID	Upward Displacement at Maximum Load (in)					
		DR	CT	FT	DR-C	CT-C	FT-C
64.8	B4	0.52	0.39	0.61	0.48	-	0.49
163.4	B5	0.48	0.47	0.58	0.59	0.54	-
487.4	B3	0.34	0.37	0.31	0.44	-	-
502.8	B1	0.21	0.15	0.31	0.30	-	0.29
685.6	B6	0.21	0.34	0.35	0.32	-	0.39
885.0	B2	0.16	0.25	0.33	0.28	0.31	-

In general, a trend of increasing pullout load was noted for higher UCS. However, given the variations in socket dimensions (Table 3.5) this can be misleading. Figure 3.21 presents the same results in terms of side shear stress and displacement determined by dividing the pullout load by the surface area of the sockets. Table 3.5 presents the maximum side shear resistance for all sockets, computed at the displacements shown on Table 3.4.

From Figure 3.21 and Table 3.5, the true side shear relationship to the geomaterial strength becomes clear, as considered in design methods. Figure 3.22 shows the same results in terms of normalized side shear (relative to the bed UCS) versus displacement.

Further observations may also be made after analyzing Figures 3.21 and 3.22. In all beds, the driven temporary sockets (DR) exhibited lower strength than the corresponding control sockets (DR-C). The DR and CT sockets showed the lowest side shear resistance among the construction methods investigated, whereas the fine-tooth rotated sockets (FT) exhibited the highest side shear values when considering the temporary casing sockets only. The control sockets consistently showed higher side shear resistance as well, comparable to the temporary casing specimens. Table 3.6 shows the summary of maximum normalized side shear. These ratios were obtaining by dividing the maximum side shear by the bed unconfined compressive strength, both in tons per square foot (tsf).

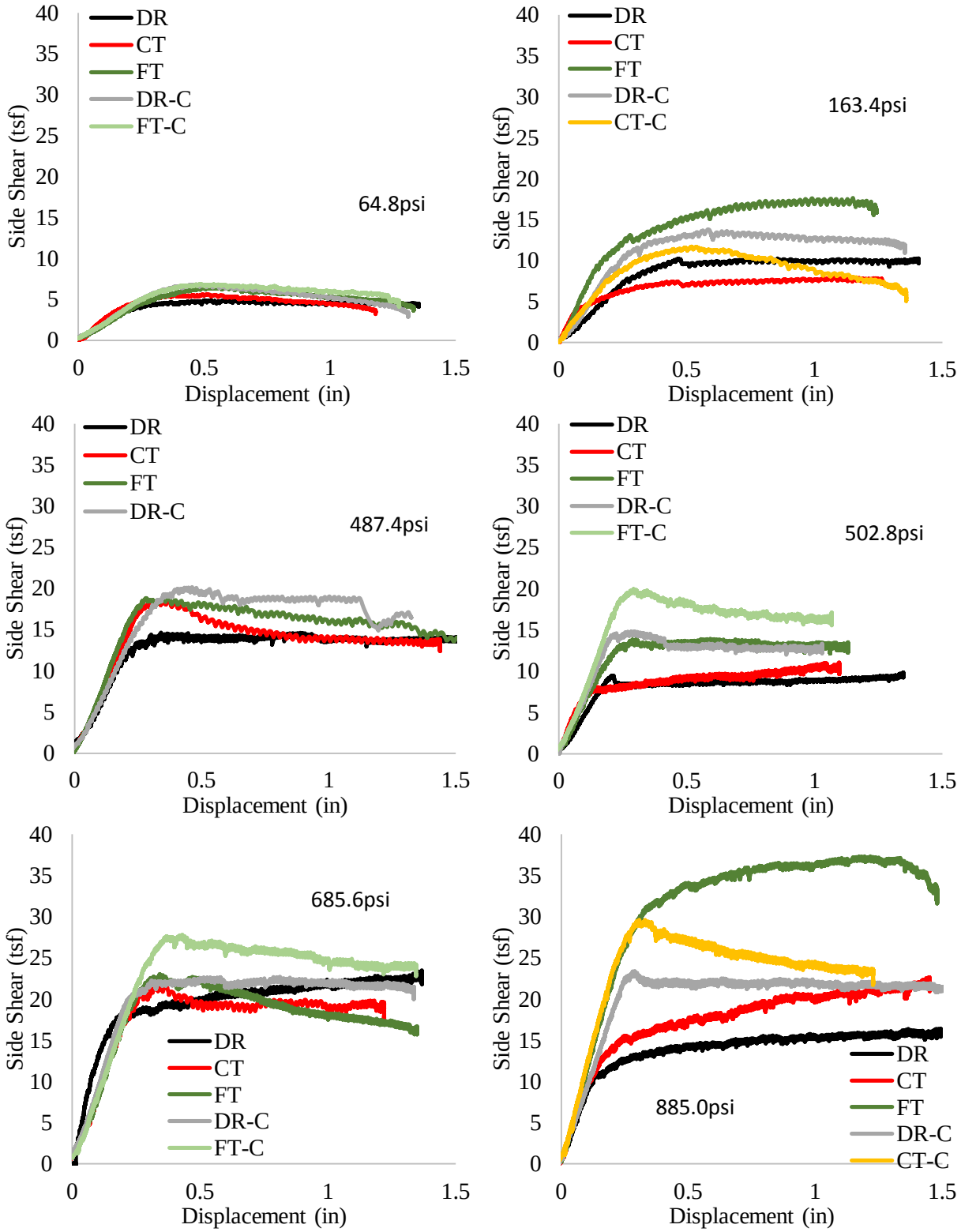

Figure 3.21 Side shear resistance vs displacement for all sockets.

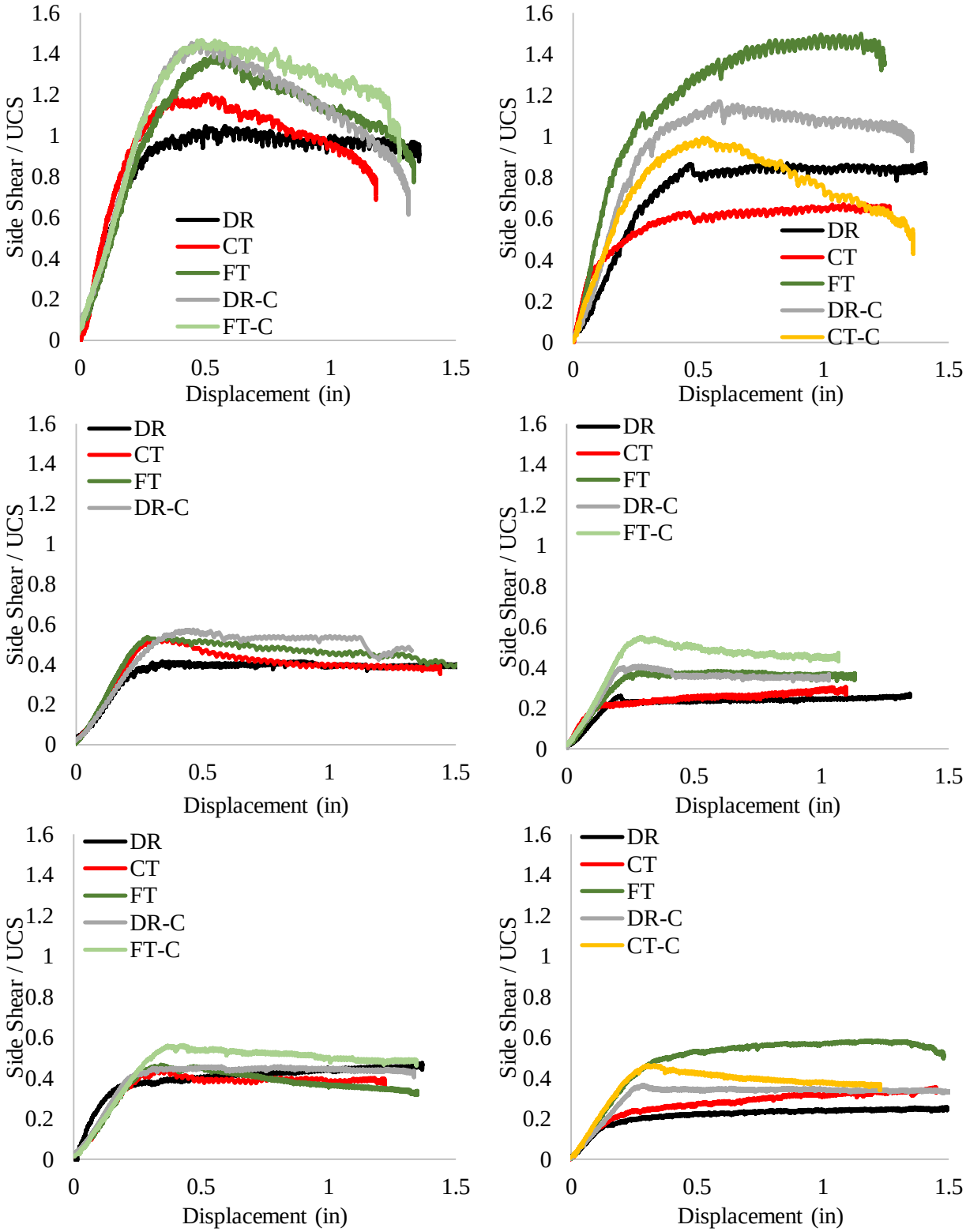

Figure 3.22 Normalized side shear resistance (by bed UCS) vs displacement.

Table 3.5 Maximum side shear strength for all sockets.

Bed UCS (psi)	Bed ID	Maximum Side Shear (tsf)					
		DR	CT	FT	DR-C	CT-C	FT-C
64.8	B4	4.82	5.49	6.43	6.67	-	6.84
163.4	B5	10.16	7.44	15.99	13.60	11.59	-
487.4	B3	13.40	18.59	18.51	19.81	-	-
502.8	B1	9.42	8.05	13.76	14.62	-	19.74
685.6	B6	18.11	21.34	22.89	22.12	-	27.40
885.0	B2	11.08	15.43	30.89	23.21	29.20	-

Table 3.6 Maximum normalized side shear.

Bed UCS (psi)	Bed ID	Maximum Normalized Side Shear (Side Shear / UCS Ratio)					
		DR	CT	FT	DR-C	CT-C	FT-C
64.8	B4	1.03	1.18	1.38	1.43	-	1.47
163.4	B5	0.86	0.63	1.36	1.16	0.99	-
487.4	B3	0.38	0.53	0.53	0.56	-	-
502.8	B1	0.26	0.22	0.38	0.40	-	0.55
685.6	B6	0.37	0.43	0.46	0.45	-	0.56
885.0	B2	0.17	0.24	0.48	0.36	0.46	-

Table 3.7 shows the ultimate side shear ratios between the temporary casing and the control sockets, using the values shown on Table 3.4. Figure 3.23 shows the side shear ratios versus displacement.

Table 3.7 Side shear ratios between temporary and respective control casings.

Casing Type	Bed UCS (psi) and ID	Peak Displacement (in)	Ultimate Stress Ratio	Average Peak Stress Ratio
Driven (DR)	64.8 (B4)	0.52	0.72	0.68
	163.4 (B5)	0.48	0.75	
	487.4 (B3)	0.34	0.68	
	502.8 (B1)	0.21	0.64	
	685.6 (B6)	0.21	0.82	
	885.0 (B2)	0.16	0.48	
Coarse-Tooth Rotated (CT)	163.4 (B5)	0.47	0.64	0.59
	885.0 (B2)	0.25	0.53	
Fine-Tooth Rotated (FT)	64.8 (B4)	0.61	0.94	0.82
	502.8 (B1)	0.31	0.70	
	685.6 (B6)	0.35	0.84	

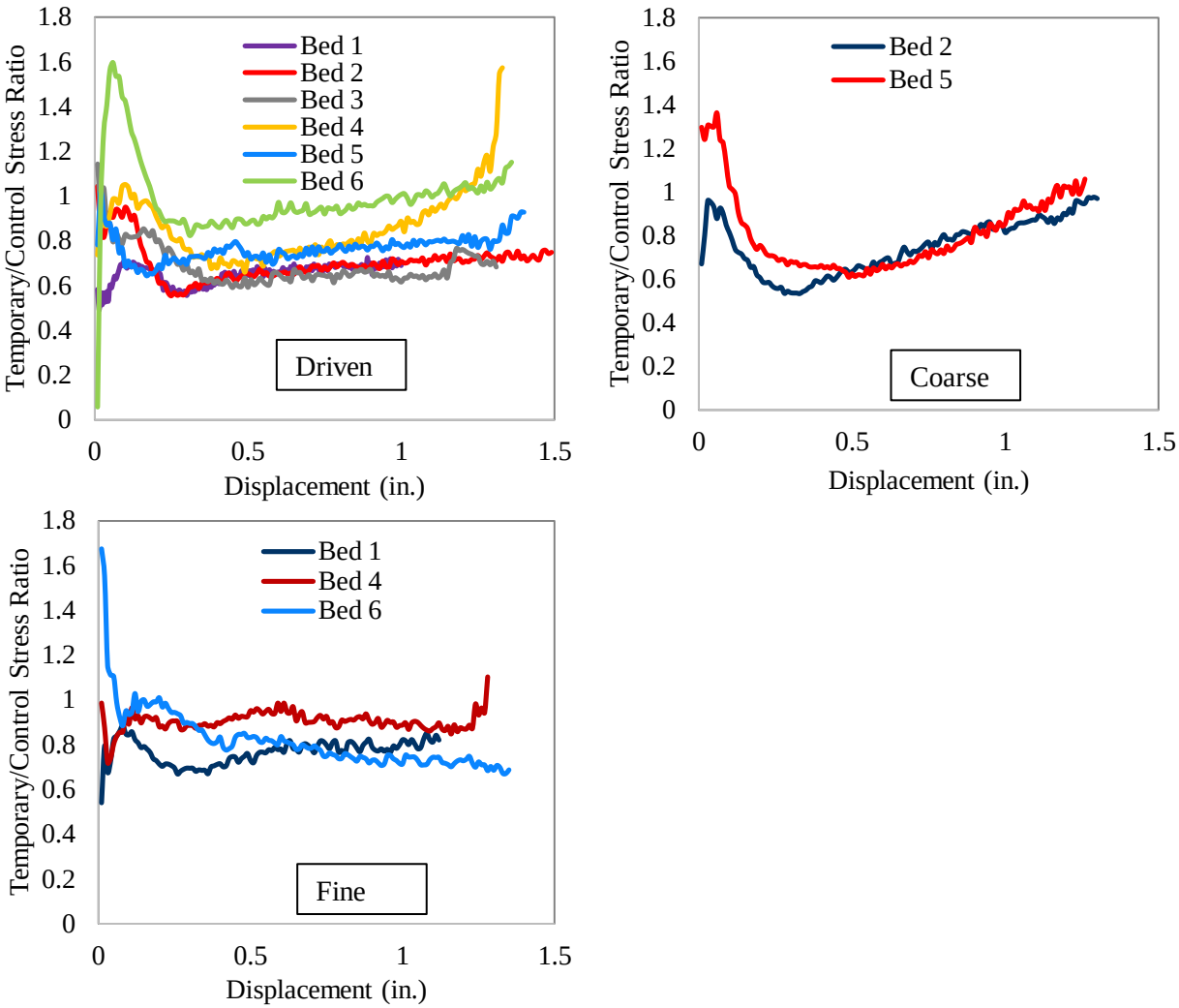

Figure 3.23 Temporary / control side shear ratio vs displacement.

3.6 Chapter Summary

Six simulated limestone beds were cast where the unconfined compressive strength ranged from 65 to 885psi which bounded the anticipated strengths through which a temporary casing made be driven and seated. In each bed 5 rock socket specimens were cast using different cased or uncased conditions to assess the effects of construction method and sequencing on side shear capacity. When comparing the three temporary casing installation/extraction methods to similarly constructed shafts where casing was extracted to concreting, side shear values were observed to decrease to 0.6 of the uncased controls. The disturbance to the limestone around the casing from the casing installation and/or the debris that became entrapped behind the casing in the annular cavity around the casing appeared to be the primary mode of capacity reduction. One casing installation method using a fine-toothed rotated casing which had a smaller annulus showed little to no change. Therein, little to no disturbance to the limestone resulted from the installation and a thinner zone for debris entrapment is thought to have made the difference.

Chapter Four: Full Scale Testing

The primary goal of this task was to cast full size specimens and verify some of the findings of previous lab and small scale efforts. In summary, lab scale work investigated various mixes of cement, slacked lime, sand, coquina and oyster shells in search of a simulated limestone that could be replicated and where the strength could be tailored to meet the study goals. Small scale tests involved casting simulated limestone beds in which drilled shaft rock-sockets were cast and tested using different temporary casing installation and extraction methodologies. The temporary driven casing option (commonly used in Florida) was found to have the most effect on side shear. Therefore, the driven casing installation method was used to cast specimens that were subsequently load tested, again, to confirm the smaller scale findings.

4.1 Site Selection

In previous studies, the USF foundation research group cast full scale shaft specimens in the Tampa Bay area in close proximity to the university campus. However, this site (at R. W. Harris, Inc. offices in Clearwater) does not have a representative limestone that meets the criteria set forth by this study; the rock should be relatively weak through which casing may be inadvertently driven deeper than planned as a temporary means of stabilizing an excavation. Further, limestone on the west coast of Florida is typically relatively deep and in this case deeper than 50ft. This would both increase the cost of creating test shafts and the size of the testing apparatus required. Therefore this phase of the research was performed in the Miami area where limestone is very near the ground surface.

Preliminary estimates of load testing equipment needs were based on rock-socket capacity alone. Table 4.1 shows acceptable rock socket dimensions based on limiting the capacity to half the maximum USF rapid load test device capabilities. Alternately, static load testing using a pull-out frame was also entertained with an upper limit of 600k.

Table 4.1 Possible testable shaft dimensions based on a 500kip limit1.

Shaft Diam	Socket Length	Insitu Unit Side Shear		
(ft)	(ft)	4(ksf)	8(ksf)	12(ksf)
2	4	101	201	302
3	4	151	302	452
4	4	201	402	603
2	6	151	302	452
3	6	226	452	679
4	6	302	603	905
2	8	201	402	603
3	8	302	603	905
4	8	402	804	1206

[1] Greyed-out configurations were ruled out.

After discussions with R.W. Harris, Inc. personnel, a similarly accessible site in Miami was suggested that fit the needs of the study where limestone is nearer to the ground surface.

4.2 Site Exploration

A portion of the R.W. Harris, Inc. Miami equipment yard was set aside for the study use and where borings were performed around the perimeter of the area. Figures 4.1 and 4.2 show the locator map and boring layouts, respectively. All four borings were conducted in a relatively small area using Standard Penetration testing and from which split spoon and core samples were recovered.

Figure 4.1 Locator map for the Miami test site.

Figure 4.2 Plan view of R.W. Harris yard in Northeast Miami, Hialeah area.

Subsurface conditions within the upper 10ft contained, sand, limestone and weathered limestone in varied layering orders. Figures 4.3 and 4.4 show the boring soil profiles. These profiles showed the SW corner to be the most conducive to the study needs where weathered limestone was found within the upper 10ft. Although deeper samples of competent limestone produced cores that could be tested, Boring SW-3 could only be classified by visual inspection and SPT blow counts. No cores were retrieve that could be tested in compression or splitting tension.

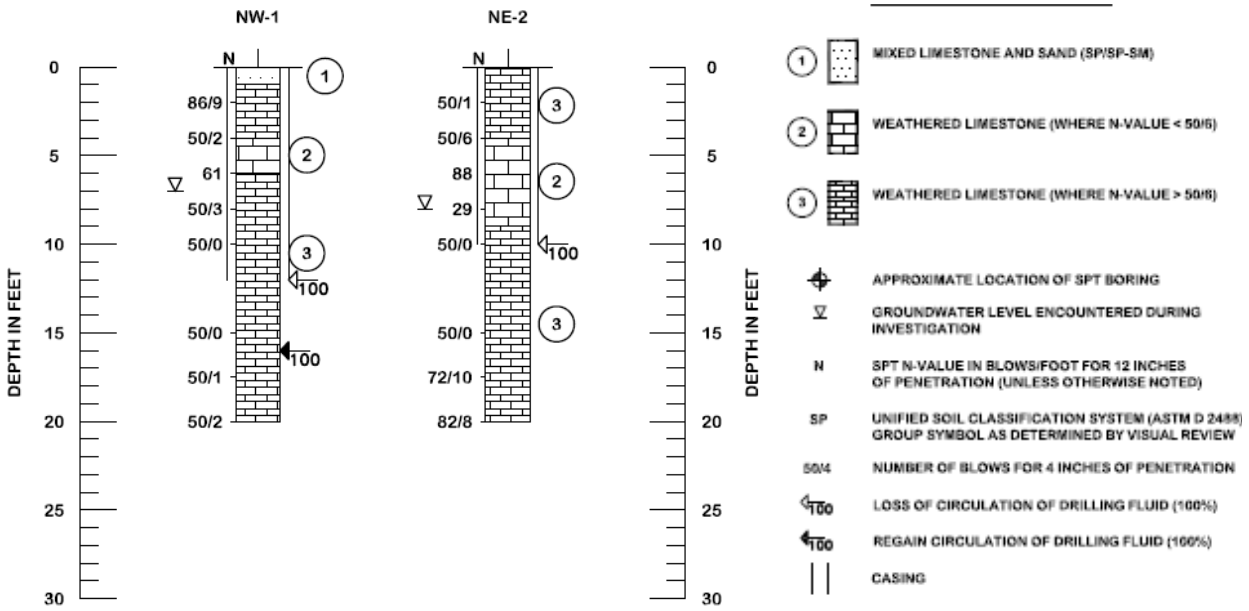

Figure 4.3 Soil profile from the NW and NE borings (Tierra, 2017).

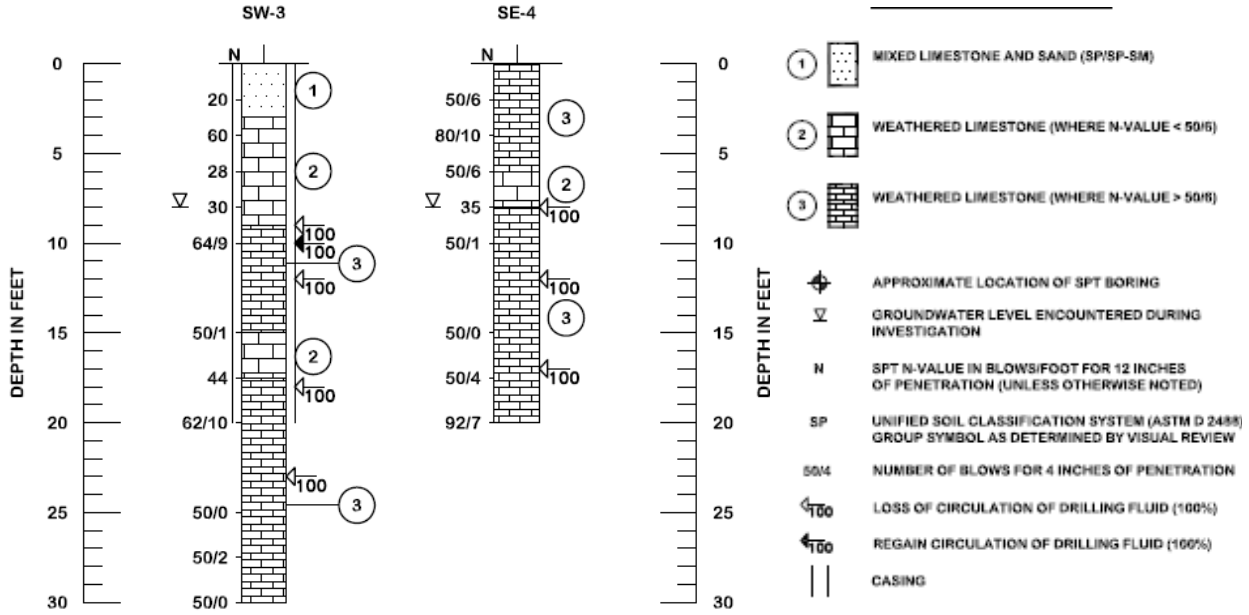

Figure 4.4 Soil profile from the SW and SE borings (Tierra, 2017).

4.3 Estimated Rock Socket Capacity

Each boring was evaluated for the estimated side shear capacity using the AASHTO, FHWA and the FDOT methods. Table 4.2 shows the range of unit side shear and nominal pull-out force for each boring and capacity estimation method. Capacity was estimated based on a 8ft depth/length of shaft and 36in nominal diameter.

Table 4.2 Estimated pullout capacity.

BOREHOLE	Nominal f_{max} (tsf)				Design max pull-out load (ton)			
	AASHTO (2012)	FHWA (2010) - Low	FHWA (2010) - high	FDOT (2016)	AASHTO (2012)	FHWA (2010) - Low	FHWA (2010) - high	FDOT (2016)
1	1.52	1.47	2.33	0.81	143	139	220	77
2	1.33	1.29	2.05	0.63	126	122	194	59
3	1.27	1.24	1.96	0.57	120	116	185	54
4	1.58	1.53	2.43	0.88	149	144	229	83

4.4 Construction Preparations

Two shafts were planned for construction: one with temporary driven casing that would be removed after concreting, and another constructed exactly the same way with temporary casing but where the casing would be removed prior to clean out, cage placement and concreting.

Two identical cages were constructed with four 1-3/8in diameter full length high strength threaded bars from Williams Form Engineering Corp. Each bar was bolted to a 1/2in thick base plate to increase anchor bar pullout resistance (from the concrete). The bars were oriented to be on opposite sides of the cage to facilitate clearance around the reaction beam with an approximate flange width of 16in (Figure 4.5).

At the top of each cage, the anchor bars were similarly bolted to a spacer plate to maintain the bar alignment for subsequent coupling to the pull out apparatus. Figure 4.6 shows the plates being cutout. Figures 4.7 and 4.8 show the cage components and assembly, respectively.

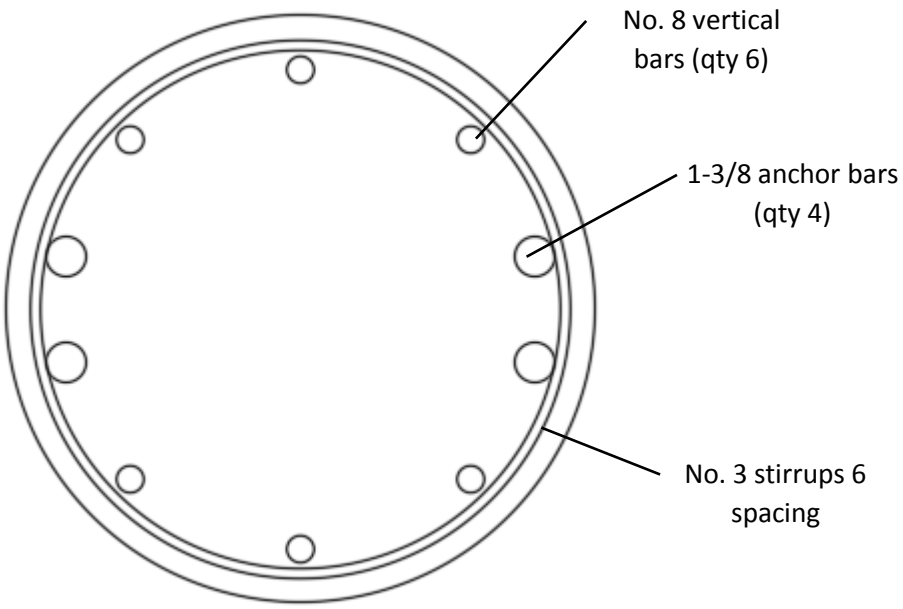

Figure 4.5 Reinforcing cage layout for pull out cages.

Figure 4.6 Base plates (left) and upper spacer plates (right) being cut out.

Figure 4.7 Cage components.

The cage was first assembled by bolting the anchor bars to base plate and upper spacer plate with a nut on top and bottom of the plates, stirrups were attached on a 6in spacing, and No. 8 main bars were added to fill out the cage between the anchor bars again with a 6in spacing between vertical bars (Figure 4.8).

Figure 4.8 Cage assembly.

4.5 Shaft Construction

For both shafts an under-sized rock auger (21in diameter) was drilled to a depth of 8ft through the weathered limestone and a 24in OD casing was driven to the same depth. The temporary casing shaft was then cleaned out, cage placed, concrete poured and casing extracted. For the uncased control shaft, the casing was removed, the bottom was cleaned out, the cage was placed and concrete was poured. At the time of excavation, the water table was approximately 3ft below the ground surface and concrete was tremie placed with a pump truck. Figures 4.9 – 4.14 show the entire construction process.

Figure 4.9 Rock auger and casing used to excavate both shafts.

Figure 4.10 Both shafts after excavation and casing advancement.

Figure 4.11 Casing extraction and clean out of uncased control shaft.

Figure 4.12 Cage installation: control shaft (left) and temporary cased shaft (right).

Figure 4.13 Concreting: control shaft (left) and temporary cased shaft (right).

Concrete was slump tested (8.5 in) and compression testing cylinders were prepared. The temporary cased shaft was concreted first and the casing was left in place while the control shaft was concreted (about 10 min).

The 8.5in slump was used to comply with acceptable fresh concrete properties at the time of placement (7 to 10in). The reinforcing cages, although not needed for the purposes of pullout testing, were included to provide the tightest permissible cage spacing and thereby provide some level of concrete flow obstruction; this can be especially problematic after the concrete has been allowed to sit for some amount of time and where the thixotropic properties start to resist flow at the time of casing extraction. It is not uncommon for extended concrete set times over several hours that cause slump to fall appreciably below the as-placed slump to a point that concrete would not flow as well during casing extraction. Present specifications allow for the concrete slump of the already placed concrete to fall as low as 5in during the pour and subsequent casing extraction. Recall, Chapter 2 showed even when within this limit, a significant reduction in side shear can result. As a result, the tested conditions represent ideal middle of the specification limits conditions and not worst case (i.e. as-placed slump 7in and long wait time that allows slump to fall to 5in before casing extraction). Figure 4.14 shows the final stages of concreting both shafts. While the temporary casing was being extracted, concrete was continuously added such that a sufficient concrete volume would be present to fully displace any fluid in the annulus around the casing.

Figure 4.14 Concreting: over-pouring control shaft (top left); filling temporary casing with extra concrete (top right and bottom left) and after casing extraction (bottom right).

4.6 Load Testing

Based on the estimated capacity of the rock sockets, a load testing assembly was designed that could provide three times the ultimate capacity and be integrated into the anchor rod configuration (16in clear spacing, Figure 4.5).

The loading assembly incorporated a 14ft long, W36x288 beam supported on either side of the test shafts on crane mates and steel plates. As the anchor bars that were stubbed out of the shaft were not perfectly plumb, the beam was positioned such that the centerline of the beam in both the lateral and longitudinal direction was directly above the center of the anchor bar pattern at the top of the shaft (not where the bars terminated 18in above ground). This is important as the process of loading the rods can cause the reaction beam to become unstable if permitted to be loaded on an incline. With the beam centered and leveled in both directions, a load cell (300 ton capacity) was centered on the beam and a 13in stroke hydraulic jack (300 ton capacity) was centered on the load cell. The load cell was equipped with a hemispherical ball joint at the top which was in turn bolted to a 1-1/8 in thick 16in x 16in plate. Two additional 2 in thick plates 18 in x 24 in were match drilled to accommodate the 1-3/8in anchor rods in the pre-designated anchor rod pattern / configuration (Figure 4.15).

Figure 4.15 Two 18in x 24in x 2in thick plates match drilled as top load transfer beam.

All equipment was prepped at the USF campus, loaded on an equipment trailer and taken to the Miami test site (Figure 4.16). The W36x288 beam complete with welded web stiffeners and bearing plates was supplied courtesy of Hayward Baker's Tampa, FL office. Figures 4.17 and 4.18 show the test system being setup.

Figure 4.16 All load testing equipment loaded out for Miami test site.

Figure 4.17 Load test setup.

Figure 4.18 Completed loading system with reference beam.

Load was applied in 20 kip intervals (approximately 1/10th the anticipated highest load) and each interval was held for 2 minutes to confirm no creep. For both shaft specimens, the anticipated design load was under predicted by about two-fold, so the load steps resulted in closer to 20 steps (not 10). Figure 4.19 shows the load versus time data for both shaft specimens and demonstrates the steps and holds. Figure 4.20 shows the load vs displacement response for the two specimens.

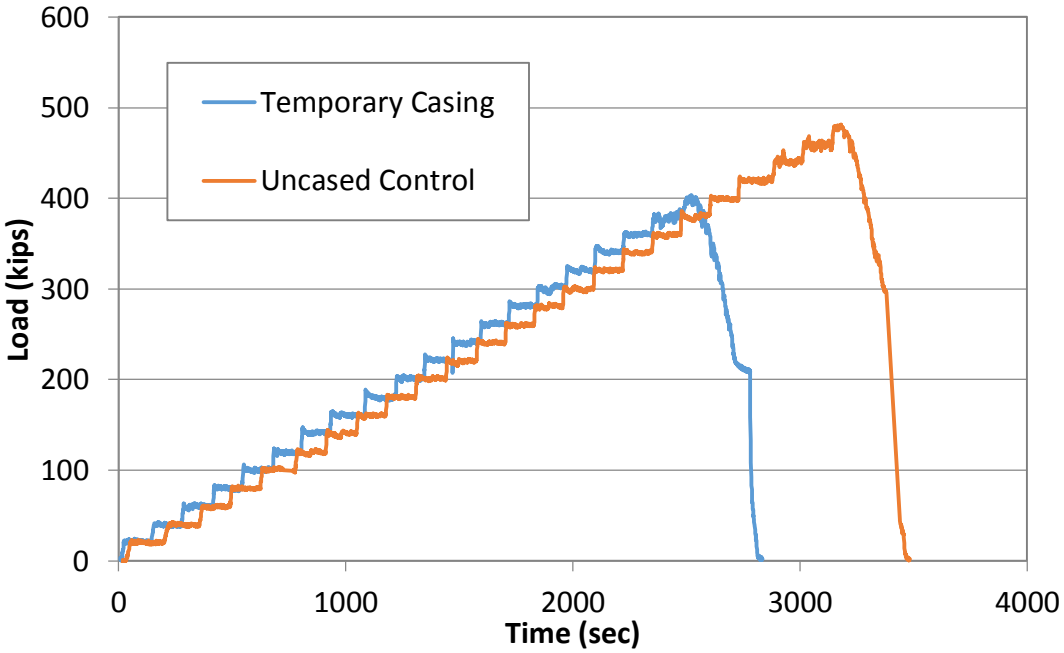

Figure 4.19 Load trace showing uniform loads for the two shaft specimens.

The control shaft exhibited a linear load versus displacement response up to a load of 420 kips and approximately 0.14in of upward movement. The increased rate of loading occurred upon arriving at that load step. The temporary casing shaft showed almost the same linear response but only developed 374 kips at approximately 0.11in of upward movement. This occurred while increasing load to the 380 kip load step which was not achieved without active hydraulic fluid flow (falling load during holds) or until far more displacement was imposed. Some strain softening was also noted for the temporary casing shaft whereas the control shaft continued to gain strength with the additional of four more load steps.

Beyond the point of initial shear failure (420 and 374kips for the control and temporary casing specimens, respectively), both shafts could not hold the load without increased displacement rate. Ultimate capacity of the control and temporary casing specimens was 400 and 480kips, respectively. This translates to 83% of the control, uncased capacity for the temporary casing shaft. Figure 4.21 shows the displacement rate vs applied load.

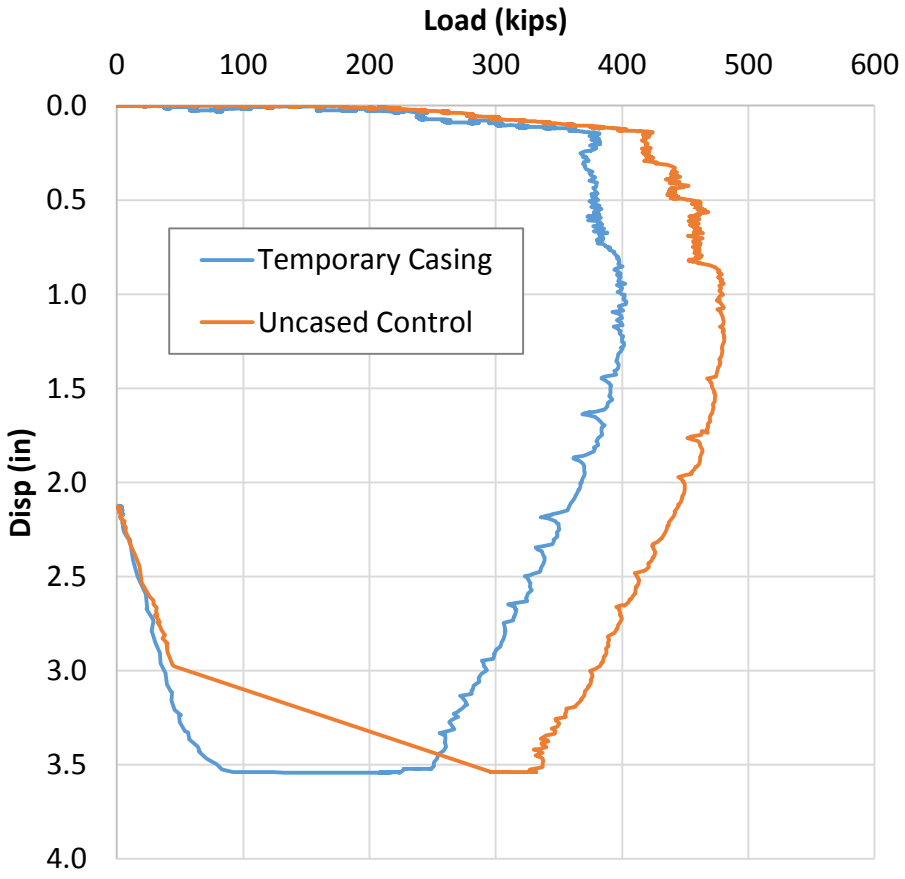

Figure 4.20 Comparative load test results for temporarily cased and uncased conditions.

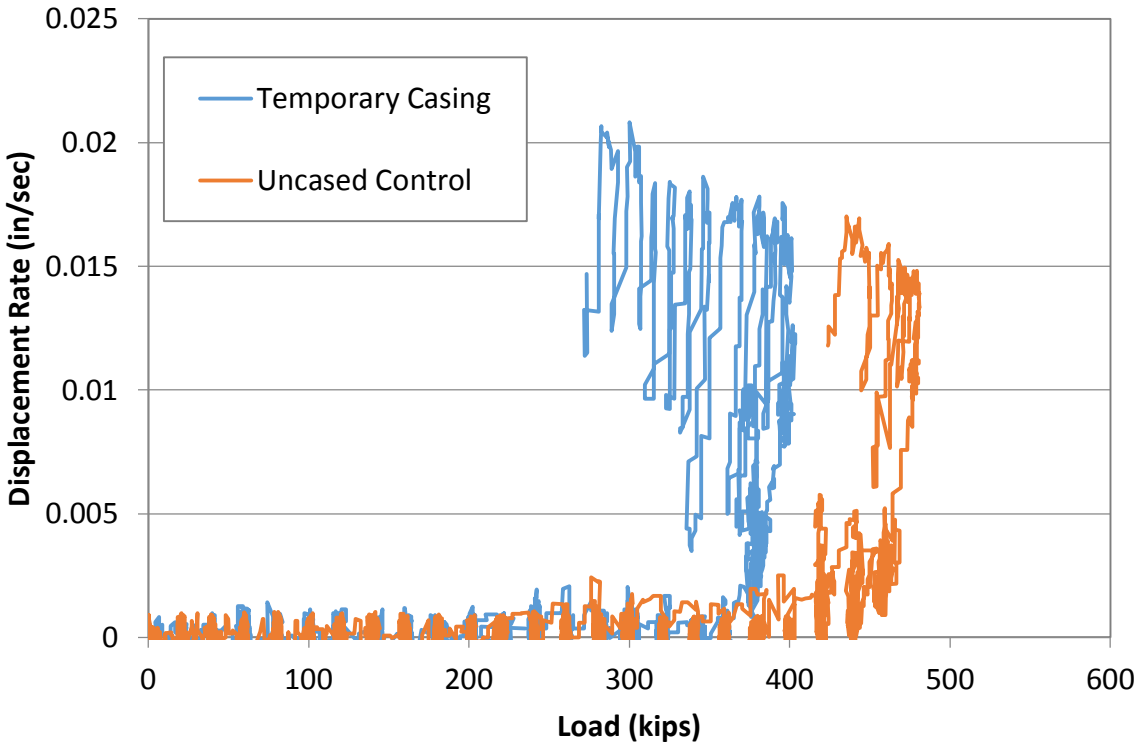

Figure 4.21 Displacement rate vs load.

4.7 Chapter Summary

Full scale pullout tests were performed on rock socketed shaft specimens cast in near-surface limestone. SPT blow counts for the material were in the range of 60 which fit the criteria set for marginal strength limestone where casing advancement may or may not actually be needed. The concrete slump was in the middle of the specified range between 7 and 10in. Specimens were cast where the cage congestion was at the tightest permissible 6in clear spacing. The concrete set time was low (10-15min) when compared to the amount of time a casing might be left in place with fresh concrete prior to extraction (several hours). Nevertheless, the temporary cased drilled shaft developed only 83% of the uncased counterpart, even under the ideal conditions described.

Chapter Five: Discussions and Conclusion

5.1 Overview

Present design methods for side shear resistance of drilled shafts in soils and rock were derived and/or verified from full scale case studies, but do not make any distinctions for a wide range of construction techniques. Instead, the design parameters encompass all excavation procedures, and therefore the resulting calculated side shear is solely dependent on the soil type regardless of whether slurry, temporary casing or dry construction is used.

This study investigated the effects of temporary casing on the resulting side shear in rock sockets. To this end, different procedures to install and extract temporary casings in limestone were examined on both small and large scales (Chapter 3 and 4, respectively).

5.2 Small Scale Testing

In this portion of the study, twenty nine small scale rock socketed drilled shafts were constructed in simulated limestone beds where the unconfined compressive strength of the beds ranged from 64.8psi to 885psi. All sockets were pull-out tested for quantification of side shear resistance. All construction and testing was performed at the outdoor Engineering Research Compound, at the University of South Florida. The range of unconfined compressive strengths of the simulated limestone beds targeted typical Florida limestone formations and the strength values that might be encountered in the field where temporary casings are likely to be used. Figure 5.1 shows one of the six beds curing in preparation for the pull-out tests.

The side shear resistance of each specimen was divided by the unconfined compressive strength of each simulated limestone bed as one means of comparison. Figure 5.2 shows a comparison between the measured side shear resistance for the 29 specimens and four design methods (discussed in Chapter 2). The design methods include: (1) that recommended by FDOT (2017a), based on McVay et al. (1992), with percent recovery equal to 48.5% (based on an example shown on FDOT 2017a), (2 and 3) from Brown et al. (2010), with C coefficient of 0.63 (lower) and 1.00 (upper), and (4) from Horvath and Kenney (1979), in which C = 0.65. Recovery refers to that proportion (length) of a small diameter cored limestone samples that was recovered relative to the total cored length.

A practical UCS strength threshold was also defined based on discussions with contractors that noted that limestone with SPT blow counts of 60 or higher form sufficient resistance for embedment and where casings are not likely to inadvertently penetrate too deeply. This threshold was translated to an UCS value of approximately 330psi. Figure 5.3 shows the resistance bias corresponding to the four methods used where the bias is the ratio of measured to predicted capacity.

Figure 5.1 Rock socketed specimens being prepared for pull-out tests.

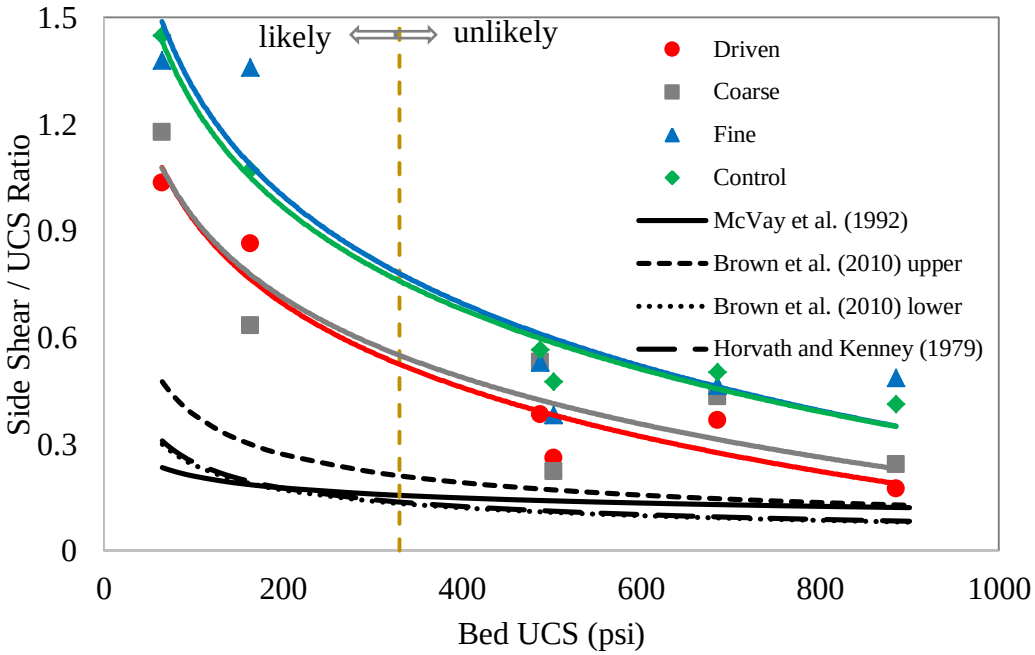

Figure 5.2 Design and measured side shear / UCS ratio vs simulated limestone beds UCS.

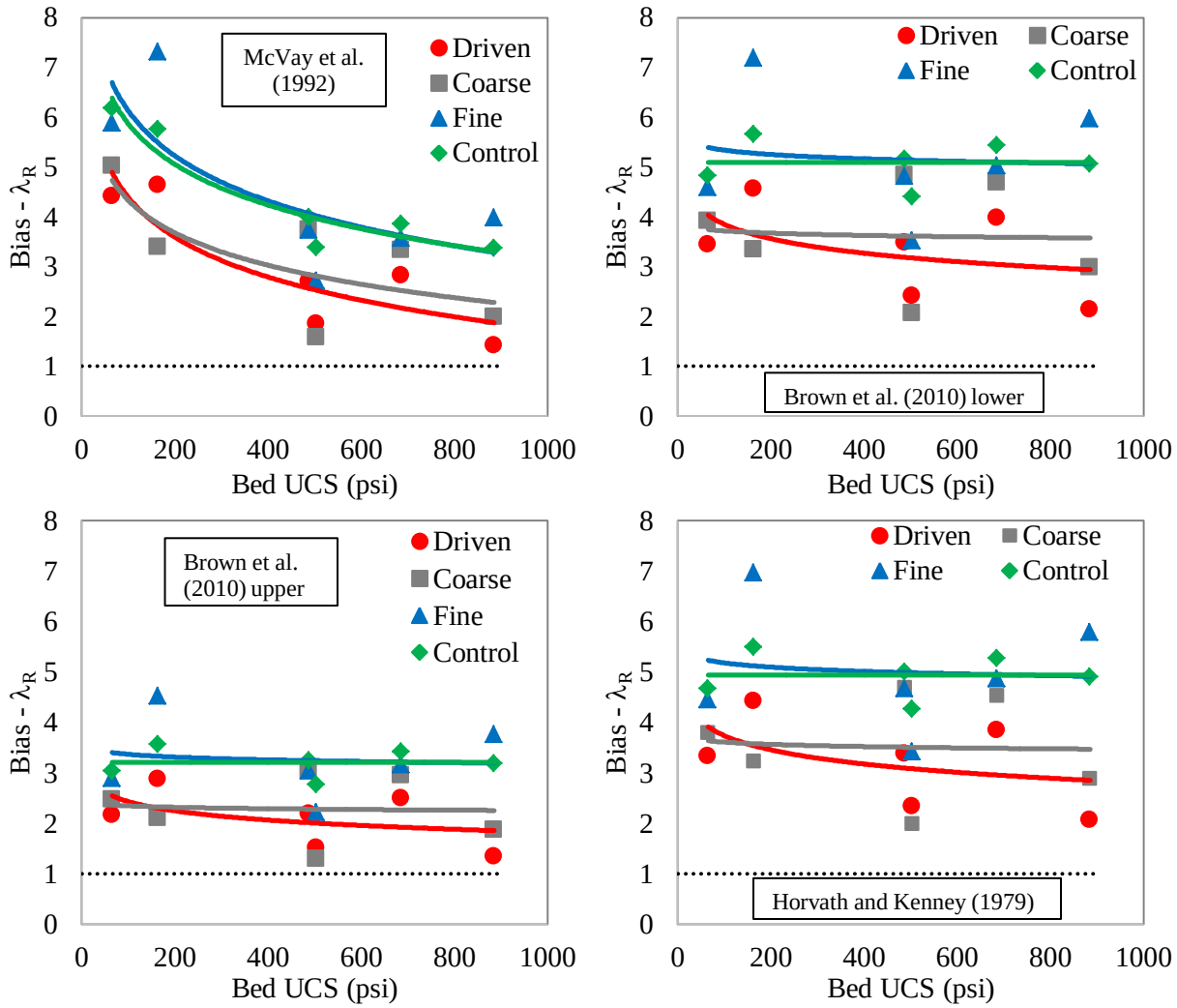

Figure 5.3 Resistance bias factor based on four design methods.

The resistance bias in the temporary casing showed construction procedure dependency. However, all resistance bias values were larger than 1.0 indicating that all construction procedures exceeded the anticipated strength. One installation method, the fine-tooth rotated temporary casing sockets, exhibited side shear values that could be considered comparable with the control sockets (i.e. no adverse effects). The driven temporary casing developed the lowest side shear values, but relatively close to the coarse-tooth rotated casing installation method. Because the fragments cannot be practically removed from around the casing, the concrete could not bond as well to the parent simulated limestone.

5.3 Large Scale Testing

One pair of large scale rock socketed shaft specimens was tested to failure to complement the small scale testing program. Both specimens were constructed identically such that the two shafts would have the same dimensions and amount of damage to the near-field excavation walls. However, one had the casing removed and the excavation cleaned out before concreting (control shaft). For the other specimen, the casing was left in-place, excavation bottom was cleaned out,

cage placed and concreted before the casing was extracted. Under the ideal conditions of no slump loss and highly fluid concrete, the temporary cased shaft still developed only 83% of the adjacent uncased shaft capacity. Both test shafts developed 2 to 2.5 times the expected ultimate design capacity.

While the construction targeted identical side shear surface area dimensions, it could be argued the control shaft should not have been exposed to the casing installation damage which would not normally occur when the casing embedment is terminated above the rock socket. This may have caused an un-conservatively higher cased/uncased strength ratio. Small scale tests showed that driven inspection holes (controls) performed poorer than rotated casing controls that were not subjected to the driving damage.

5.4 Conclusions

Combining the small scale and full scale test results, similar trends can be seen as a function of pullout displacement. Figure 5.4 shows the temporary to uncased capacity ratios for both the full scale and small scale testing. The small scale data represents an average of those shafts cased with the coarse tooth, fine tooth, and driven casing types. This was only computed for those shafts that had both a cased and uncased specimen in a given simulated limestone bed and includes all limestone strengths. The full scale ratio is simply the ratio of the resulting loads from the two shafts as a function of displacement where both were assumed to have identical bond areas. The dashed line shows the present specification in the form of a 50% rock socket bond reduction. Again, the full scale ratio may be artificially high if casing installation caused peripheral damage to the control shaft.

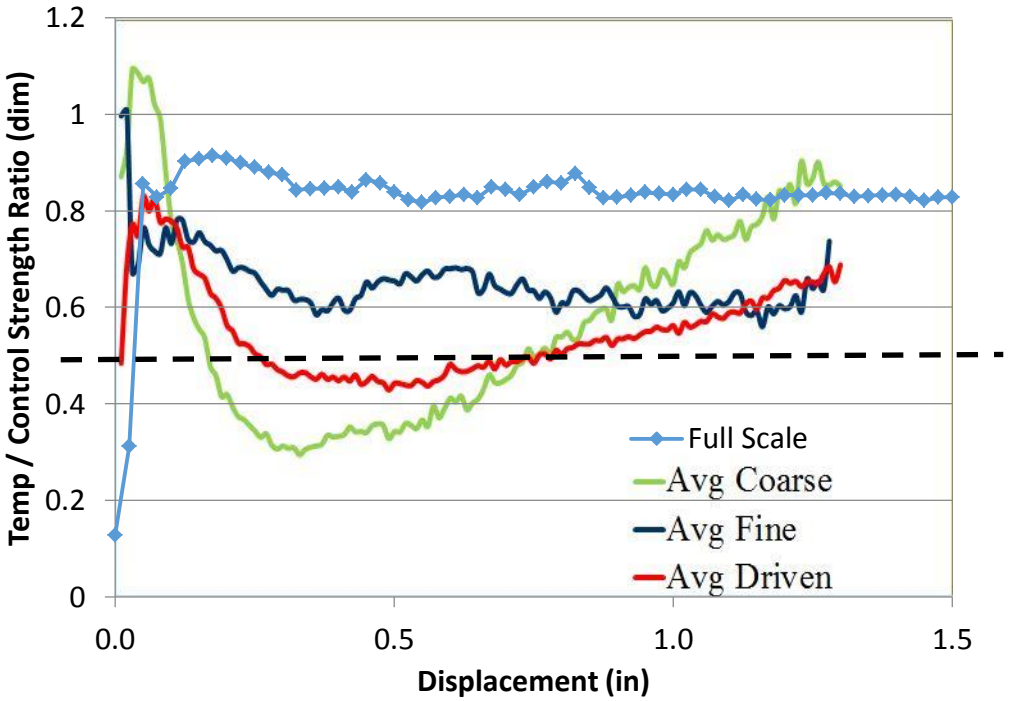

Figure 5.4 Strength ratio of temporary cased to uncased shaft capacities.

When comparing the results of all tests to the 50% specified reduction (0.5 side shear stress ratio) where temporary casing is within the design rock socket, the average ultimate stress ratio for all tested installation methods (from small scale and full scale) is shown to be above this limit (Table 5.1).

Table 5.1 Small and full scale stress ratios.

Test Series	Casing Type	Ultimate Stress Ratio	Avg Stress Ratio
Small Scale	Driven	0.67	0.72
		0.70	
		0.65	
		0.69	
		0.75	
		0.86	
	Fine	0.69	0.82
		0.95	
		0.81	
	Coarse	0.75	0.65
		0.56	
Full Scale	Drilled and Driven	0.84	0.84

The causes for deeper than expected casing installation can be broken into four categories:

1. Top of rock is not where the closest boring located it and therefore boring logs do not reflect the actual field conditions. With proper inspection this condition should be detected and the overall rock socket depth would necessarily be lowered,
2. When reviewing casing installation case studies (Chapter 2), casing was found to be terminated in material that was less than 50 blow count all the way up to 50/2in. Therefore, in many cases the contractor may have intentionally or inadvertently extended the casing depth beyond the anticipated/target depth.
3. The top of rock is technically where the borings located it (i.e. distinct change in material type), but the strength or composition is not suitable/sufficient to seat or seal the casing.
4. Strength may be acceptable and similar to boring prediction, but the formation is too porous and does not seal the casing.

While often not necessary, the casing can be driven through extremely hard material which was tested in the small scale testing with a wide range of limestone strengths; the full scale tests

could not practically test the same range of strengths. To this end, the large scale tests targeted what was thought to be the most likely scenario ($N \leq 60$). Small scale tests showed a higher reduction in side shear relative to the unconfined compression strength for stronger parent limestone (Figure 5.2). This is thought to be a by-product of larger voids / higher roughness in the weaker material that promotes better bond even when debris from outside the casing is present.

The evaluation of temporary casing used in rock socketed drilled shafts in simulated limestone showed construction procedures can lead to different side shear and hence an adjusted resistance factors could be considered. Based on the results of this study, the present FDOT specification requiring extending the socket depth by 50% of the unplanned additional embedment depth in Florida limestone formations is reasonable.

References

ASF – Applied Foundation Engineering, Inc. (2009). Final Report of Axial Load Testing, Orange Line Metrorail Project, Miami FL.

AASHTO (2012). AASHTO LRFD "Bridge Design Specifications", Customary U.S. Units. ISBN: 978-1-56051-523-4, Publication Code: LRFDUS-6.

ASTM (2013). "Annual Book of ASTM Standards, Vol. 04.08 Soil and Rock (1)," ASTM International, 100 Barr Harbor Drive, West Conshohocken, PA.

FHWA (2010). "Drilled Shafts: Construction Procedures and LRFD Design Methods," NHI Course No. 132014, FHWA-NHI-10-016, FHWA GEC 010, U.S. Department of Transportation, Federal Highway Administration.

FDOT (2017a). "Standard Specifications for Road and Bridge Construction". State of Florida Derpartment of Transportation.

FDOT (2017b). "Soils and Foundation Handbook." State Materials Office, Gainesville, Florida.

Horvath, R. G., and Kenney, T. C. (1979). "Shaft Resistance of Rock-Socketed Drilled Piers," in Proceedings, Symposium on Deep Foundations (Fuller, ed.), ASCE, Atlanta, October, pp. 182 – 214.

Kulhawy, F. H. (1986). Notes on Estimation of Soil Properties for Foundation Engineering (draft), Cornell University, March 1986.

Kulhawy, F.H., Prakoso, W.A., and Akbas, S.O. (2005). "Evaluation of Capacity of Rock Foundation Sockets," Alaska Rocks 2005, Proceedings, 40th U.S. Symposium on Rock Mechanics, G. Chen, S. Huang, W. Zhou and J. Tinucci, Editors, American Rock Mechanics Association, Anchorage, AK, 8p.

Law Engineering and Environmental Services, Inc. (2002). "Interoffice Memorandum: Side Shear Loss Attributed to Rock Coring During Drilled Shaft Construction." Jacksonville, Florida.

McVay, M., Townsend, F., and Williams, R. (1992). "Design of Socketed Drilled Shafts in Limestone." Journal of Geotechnical Engineering, 118(10), 1626–1637.

NRC (1995). "Probabilistic Methods in Geotechnical Engineering." National Research Council, Washington, D.C., 84p.

O'Neill, M. W., and Reese, L. C. (1999). Drilled Shafts: Construction Procedures and Design Methods. DTFH6 1-96-2-0005, Report Number FHWA-IF-99-025.

O'Neill, M. W., (2001). "Side Resistance In Piles and Drilled Shafts." Journal of Geotechnical and Geoenvironmental Engineering, 127(1), 3–16. 34th Terzaghi Lecture.

Prieto-Portar, L. A. (1982). "Elastic and Strength Parameters of Calcareous Rocks of Dade County, Florida." In: Symposium of Geotechnical Properties, Behavior, and Performance of Calcareous Soils, ASTM Special Technical Publication 777, Ft. Lauderdale, Florida, pp 359-381.

Reese, L. C., and O'Neill, M. W. (1988a). "Drilled Shafts: Construction Procedures and Design Methods". US Department of Transportation, FHWA, Office of Implementation, McLean, Virginia.

Sarno, A., Farah, R., Hudyma, N., and Hiltunen, D. (2010) Relationships between Compression Wave Velocity and Unconfined Compression Strength for Weathered Florida Limestone. GeoFlorida 2010: pp. 950-959. doi: 10.1061/41095(365)94

Saxena, S. K. (1982). “Geotechnical Properties of Calcareous Rocks of Southern Florida.” In: Symposium of Geotechnical Properties, Behavior, and Performance of Calcareous Soils, ASTM Special Technical Publication 777, Ft. Lauderdale, Florida, pp 340-358.

Schmertmann, J. H. (1975). “Measurement of In-Situ Shear Strength”. Proceedings, Special Conference on In-Situ Measurements of Soil properties. ASCE, Vol. 2, Raleigh, NC, pp. 57-138 (closure 175-179).

Scott, T. M. (2001). “Florida Geological Survey.” Open-File Report 80, Tallahassee, Florida, ISSN 1058-1391.

Terzaghi, K. and Peck, R. B (1967). “Soil Mechanics in Engineering Practice”, 2nd Ed., John Willey and Sons, Inc, New York, NY, 729p.

TRB (2005). “Calibration to Determine Load and Resistance Factors for Geotechnical and Structural Design.” Transportation Research Board, Circular No E-C079, September 2005, Washington, D.C., 93p.

Castelli, R. J., and Fan, K. (2002). “O-Cell Test Results for Drilled Shafts in Marl and Limestone.” Deep Foundations 2002: pp. 807-823. doi: 10.1061/40601(256)57.